EFFECTS OF IONIC STRENGTH AND PORE WATER VELOCITY ON CADMIUM MOBILITY THROUGH CONTAMINATED SOIL IN MAE SOT DISTRICT, TAK PROVINCE

Miss Athiya Waleeittikul

A Thesis Submitted in Partial Fulfillment of the Requirements
for the Degree of Master of Science Program in Hazardous Substance and Environmental Management
(Interdisciplinary Program)
Graduate School
Chulalongkorn University
Academic Year 2016

ผลของความเข้มข้นไอออนและความเร็วการไหลต่อการเคลื่อนตัวแคดเมียม ผ่านดินปนเปื้อน อำเภอแม่สอด จังหวัดตาก

นางสาวอธิญาณ์ วลีอิทธิกุล

วิทยานิพนธ์นี้เป็นส่วนหนึ่งของการศึกษาตามหลักสูตรปริญญาวิทยาศาสตรมหาบัณฑิต
สาขาวิชาการจัดการสารอันตรายและสิ่งแวดล้อม (สหสาขาวิชา)
บัณฑิตวิทยาลัย จุฬาลงกรณ์มหาวิทยาลัย
ปีการศึกษา 2559

Thesis Title	EFFECTS OF IONIC STRENGTH AND PORE WATER VELOCITY ON CADMIUM MOBILITY THROUGH CONTAMINATED SOIL IN MAE SOT DISTRICT, TAK PROVINCE
By	Miss Athiya Waleeittikul
Field of Study	Hazardous Substance and Environmental Management
Thesis Advisor	Associate Professor Srilert Chotpantarat, Ph.D.
Thesis Co-Advisor	Professor Say Kee Ong, Ph.D.

Accepted by the Graduate School, Chulalongkorn University in Partial Fulfillment of the Requirements for the Master's Degree

.....Dean of the Graduate School
(Associate Professor Sunait Chutintaranond, Ph.D.)

THESIS COMMITTEE

.....Chairman
(Assistant Professor Chantra Tongcumpou, Ph.D.)
.....Thesis Advisor
(Associate Professor Srilert Chotpantarat, Ph.D.)
.....Thesis Co-Advisor
(Professor Say Kee Ong, Ph.D.)
.....Examiner
(Pichet Chaiwiwatworakul, Ph.D.)
.....External Examiner
(Pensiri Akkajit, Ph.D.)

อธิญาณ์ วลีอิทธิกุล : ผลของความเข้มข้นไอออนและความเร็วการไหลต่อการเคลื่อนตัวแคดเมียมผ่านดินปนเปื้อน อำเภอแม่สอด จังหวัดตาก (EFFECTS OF IONIC STRENGTH AND PORE WATER VELOCITY ON CADMIUM MOBILITY THROUGH CONTAMINATED SOIL IN MAE SOT DISTRICT, TAK PROVINCE) อ.ที่ปรึกษาวิทยานิพนธ์หลัก: รศ. ดร.ศรีเลิศ โชติพันธรัตน์, อ.ที่ปรึกษาวิทยานิพนธ์ร่วม: ศ. ดร.Say Kee Ong, 95 หน้า.

เนื่องจากได้มีการรายงานการปนเปื้อนของสารแคดเมียมบริเวณพื้นที่เกษตรกรรมของห้วยแม่ตาวและห้วยแม่กุ อำเภอแม่สอด จังหวัดตาก และสารแคดเมียมนั้นเป็นพิษต่อร่างกายของมนุษย์เป็นอย่างมาก จึงมีความจำเป็นอย่างยิ่งที่จะต้องมีการศึกษาระดับความเข้มข้นของแคดเมียมในดินและกลไกการเคลื่อนที่ของแคดเมียมในดิน งานวิจัยนี้มีวัตถุประสงค์เพื่อศึกษาผลกระทบของความเข้มข้นไอออนและความเร็วการไหลต่อการเคลื่อนตัวของแคดเมียมในดินปนเปื้อน โดยมีการทดลองแบ่งออกเป็นสามส่วน ได้แก่ 1. การวิเคราะห์ปริมาณแคดเมียมที่ปนเปื้อนในดินและคุณสมบัติของดินที่เลือกในการทดลอง 2. การทดลองการดูดซับและคายตัวแบบแบทช์ และ 3. การทดลองคอลัมน์

ปริมาณของแคดเมียมในตัวอย่างดินจากบริเวณห้วยแม่ตาวและห้วยแม่กุมีค่าอยู่ในช่วง 0.71-0.62 มก./กก. โดยบางตัวอย่างนั้นมีค่าสูงกว่าค่ามาตรฐานแคดเมียมในดินของสหภาพยุโรป (3 มก./กก.) ตัวอย่างดินที่เลือกในการทดลองพิจารณาจากปริมาณแคดเมียมที่ปนเปื้อนและค่าการนำชลศาสตร์ โดยดินที่เลือกนั้นเป็นดินร่วนปนทราย มีปริมาณแคดเมียม 26.5 มก./กก. และค่าการนำชลศาสตร์ 9.14 ซม./ชม.

ในการทดลองแบทช์และการทดลองคอลัมน์พบความสัมพันธ์แบบตรงกันข้ามระหว่างค่าสัมประสิทธิ์การดูดซับ (K_d, K_l , K_f) กับค่าความเข้มข้นไอออนที่เพิ่มขึ้น ขณะที่การคายตัวนั้นสูงขึ้นเมื่อความเข้มข้นไอออนสูงขึ้น สำหรับการทดลองแบทช์ ฟรุนดลิชไอโซเทอม เป็นไอโซเทอมการดูดซับที่อธิบายการดูดซับของแคดเมียมได้ดีที่สุด โดยมีค่า R^2>0.93 สำหรับการทดลองแบบคอลัมน์ พบว่าค่าการกระจายตัวอยู่ที่ 1.73 ซม.และค่าการกระจายตัวไม่ขึ้นกับความเร็วการไหล อย่างไรก็ตามจากการทดลองคอลัมน์พบว่าแลงเมียร์ไอโซเทอมแบบไม่สมดุล (Langmuir non-equilibrium model) อธิบายกราฟเบรคทรูจ์ (Breakthrough Curve) จากการทดลองคอลัมน์ทั้งหมดได้ดีที่สุด (R^2> 0.95 และ RMSE < 0.05) โดยมีค่า K_L 0.09-4.03 ลิตร/กรัม ความเข้มข้นไอออนส่งผลอย่างยิ่งต่อการดูดซับของแคดเมียมโดยเฉพาะช่วงความเข้มข้นไอออน 10-100 มิลลิโมลาร์ จากผลการทดลองคอลัมน์ ค่าความเข้มข้นไอออนที่สูงขึ้นส่งผลให้ค่า f และ α เพิ่มขึ้น เพราะการแข่งขันในการดูดซับระหว่างไอออนของแคดเมียมและแคลเซียม ค่าเพคเล็ต ที่ใกล้เคียง 1 แสดงว่าการทดลองคอลัมน์นั้นประกอบทั้งกระบวนการแพร่กระจาย (Diffusion) และ การนำ (Advection) โดยผลของความเร็วการไหลที่เพิ่มขึ้นนั้นทำให้ค่า K_L และ f ลดลง ขณะที่ค่า α เพิ่มขึ้น ซึ่งเป็นผลมาจากการกระบวนการดูดซับแบบกำหนดอัตรา (rate limited sorption) ที่เกิดในคอลัมน์

สาขาวิชา การจัดการสารอันตรายและสิ่งแวดล้อม ลายมือชื่อนิสิต .....

ปีการศึกษา 2559 ลายมือชื่อ อ.ที่ปรึกษาหลัก .....

ลายมือชื่อ อ.ที่ปรึกษาร่วม .....

5787550220 : MAJOR HAZARDOUS SUBSTANCE AND ENVIRONMENTAL MANAGEMENT
KEYWORDS: CADMIUM / CONTAMINANT TRANSPORT / COLUMN EXPERIMENT / TAK PROVINCE / IONIC STRENTH / PORE WATER VELOCITY

ATHIYA WALEEITTIKUL: EFFECTS OF IONIC STRENGTH AND PORE WATER VELOCITY ON CADMIUM MOBILITY THROUGH CONTAMINATED SOIL IN MAE SOT DISTRICT, TAK PROVINCE. ADVISOR: ASSOC. PROF. SRILERT CHOTPANTARAT, Ph.D., CO-ADVISOR: PROF. SAY KEE ONG, Ph.D., 95 pp.

Contamination of cadmium (Cd) was reported to be found at agricultural areas nearby Mae Tao and Mae Ku creek in the Mae Sot District, Tak Province, Thailand. Cadmium is an extremely toxic substance and harmful to human health. Therefore, Cd levels in soils and mechanisms of Cd movement into soils are needed to be investigated systematically. The objective of this research was to investigate the effects of ionic strength (IS) and pore water velocity on the Cd movement through contaminated soil. There were three laboratory parts in this study as follows: 1) analysis of Cd contaminated in soils and properties of the selected soil, 2) batch sorption-desorption experiments, and 3) column experiments. The concentrations of Cd in soils collected from Mae Tao and Mae Ku creek were in the ranges of 0.71-62.04 mg/kg, some of them are higher than the European Union Maximum Permissible level (3 mg/kg). Based on hydraulic conductivity and level of contaminated Cd in soils, the contaminated agricultural soil was selected for further experiments, which is a sandy loam soil with 26.5 mg/kg Cd and hydraulic conductivity of 9.14 cm/h.

Both batch adsorption experiments and column experiments showed inverse relationship between sorption coefficients (K_d, K_L, K_f) with increasing of IS, whereas desorption experiments revealed higher concentrations of desorbed Cd with increasing IS. For batch experiments, the Freundlich isotherm is the best adsorption isotherm, explaining Cd adsorption (R^2 >0.93). Regardless of pore water velocity, the dispersivity (λ) of low and high flow columns was approx.1.73 cm. However, the Langmuir non-equilibrium model (or two site sorption model) is well-fitted with observed BTCs from column experiments (R^2>0.95, RMSE<0.05) with K_L ranging from 0.09-4.03 l/g. Ionic strength appeared to significantly affect Cd sorption and transport in a range of IS from 10-100 mM. According to modeling results of column tests, higher IS resulted in increasing f and α, because the competition between Cd^{2+} and Ca^{2+}. Peclet numbers showed that both diffusion and advection process is dominated in the column experiments. Based on pore water velocity effect, K_L and f is inversely related with pore water velocity, while α is positively related with pore water velocity, which is responsible for the rate-limited process.

Field of Study:	Hazardous Substance and Environmental Management	Student's Signature .....
		Advisor's Signature .....
Academic Year:	2016	Co-Advisor's Signature .....

ACKNOWLEDGEMENTS

I would like to express my appreciation to my thesis advisor, Associate Professor Dr.Srilert Chotpantarat, who always kindly gives me useful advice during all these years. I also would like to express my gratitude to my co-advisor, Professor Dr.Say Kee Ong. for his kindness and support throughout this research. And I am gratefully thanks my thesis committees, Assistant Professor Dr.Chantra Tongcumpou, Dr.Pichet Chaiwiwatworakul, and Dr.Pensiri Akkajit. for the suggestions and comments.

I also would like to express our sincere thanks to the 90th Anniversary of the Chulalongkorn University Fund, Ratchadaphiseksomphot Endowment Fund, the Grant for International Research Integration: Chula Research Scholar, Ratchadaphiseksomphot Endowment Fund (GCURS-59-06-79-01), the Office of Higher Education Commission (OHEC) and the S&T Postgraduate Education and Research Development Office (PERDO) for the financial support of the Research Program and thanks the Ratchadaphiseksomphot Endowment Fund, Chulalongkorn University for the Research Unit.

Furthermore, I gratefully thank Mr. Narongsak Rachukan and Ms.Salinthip Wipatawit for help and support during field work. Ms. Chantana Intim and Ms. Chanunya Permchati are gratefully acknowledge for teaching, consulting, and helping during the laboratory work at Center of Excellent on Hazardous substance management. Lastly, this research won't be able to success without the kindly support from my family and friends.

CONTENTS

Page
THAI ABSTRACT iv
ENGLISH ABSTRACT v
ACKNOWLEDGEMENTS vi
CONTENTS vii
LIST OF TABLES ix
LIST OF FIGURES xi
CHAPTER1 1
1.1Rationale 1
1.2 Hypothesis 4
1.3 Objective 4
1.4 Scope of Study 4
CHAPTER2 5
2.1 Cadmium and its effect to human health 5
2.2 Cadmium contaminated in soil 6
2.3 General information of the study area 6
2.4 Solute transport through soil 10
2.5 Adsorption and desorption of Cd on soils 12
2.6 Factors controlling sorption and desorption of Cd 12
2.7 Ionic Strength (IS) 16
2.8 Cd Speciation in the environment 17
2.9 Batch Experiment 18
2.10 Column Experiment 18
2.11 Flow Interruption 19
CHAPTER3 20
3.1 Data Preparation and Field Observation 20
3.2 Soil preparation and analysis 21
3.3 Batch Experiments 23
3.4 Column experiments 24

Page

3.5 Data Analysis and Interpretation 25
CHAPTER4 32
4.1 Soil Sampling and Soil Selection 32
4.2 Soils and Selected soil properties 33
4.3 Batch sorption and desorption experiments 37
4.4 Column Experiments: Experimantal data and modelings 40
CHAPTER 5 56
5.1 Conclusion 56
5.2 Recommendations 58
REFERENCES lx
APPENDICIES 65
Appendix A 66
Appendix B 68
Appendix C 71
Appendix D 76
Appendix E 95
VITA xcviii

LIST OF TABLES

Page

CHAPTER3

Table 3.1: Data types and sources of data.....20

Table 3.2: Soil properties and analytical method.....23

CHAPTER4

Table 4.1: Summary of properties of the soil samples collected from agricultural areas nearby Mae Tao and Mae Ku creeks 33

Table 4.2: Chemical composition of the selected soil 36

Table 4.3: Parameters of Linear, Langmuir and Freundlich Isotherms for Cd on the selected soil form Mae Tao.....39

Table 4.4: Percentage of Cd adsorption and desorption of the selected soil for IS 1, 10 and 100 mM at pH 7.0 40

Table 4.5: Properties of the packed soil columns in the column experiments.....40

Table 4.6: Estimated parameters from CXTFIT program for tracer experiments, fitted by CDE and T-R models 42

Table 4.7: Parameters of Cd transport through various IS and pore water velocities as fitted by the Langmuir TSM model.....51

APPENDIX A

Table A-1: Data of all soil samples collected from agricultural area near Mae Tao and Mae Ku creeks.....**Error! Bookmark not defined.**

APPENDIX B

Table B-1: Experimental and fitted data of Cd amount adsorbed on the soil at IS 1mM, 10 mM and 100 mM.....**Error! Bookmark not defined.**

Table B-2: Experimental data of Cd adsorption and desorption on the soil at IS 1mM, 10 mM and 100 mM.....**Error! Bookmark not defined.**

APPENDIX C

Table C-1: Experimental and Fitted data of Column1 (Tracer transport with low pore water velocity) .....**Error! Bookmark not defined.**

Table C-2: Experimental and Fitted data of Column2 (Tracer transport with high pore water velocity) .....**Error! Bookmark not defined.**

APPENDIX D

Table D-1: Experimental and Fitted data of Column3 (Cd transport with low pore water velocity, IS 100 mM) ..... **Error! Bookmark not defined.**

Table D-2: Experimental and Fitted data of Column4 (Cd transport with low pore water velocity, IS 10 mM) ..... **Error! Bookmark not defined.**

Table D-3: Experimental and Fitted data of Column5 (Cd transport with low pore water velocity, IS 1 mM) ..... **Error! Bookmark not defined.**

Table D-4: Experimental and Fitted data of Column6 (Cd transport with high pore water velocity, IS 100 mM) ..... **Error! Bookmark not defined.**

Table D-5: Experimental and Fitted data of Column7 (Cd transport with high pore water velocity, IS 10 mM) ..... **Error! Bookmark not defined.**

Table D-6: Experimental and Fitted data of Column8 (Cd transport with high pore water velocity, IS 1 mM) ..... **Error! Bookmark not defined.**

APPENDIX E

Table E-1: Fitted parameter for Freundlich Equilibrium model . **Error! Bookmark not defined.**

Table E-2: Fitted parameter for Freundlch TSM model ..... **Error! Bookmark not defined.**

Table E-3: Fitted parameter for Langmuir Equilibrium model .. **Error! Bookmark not defined.**

LIST OF FIGURES

Page

CHAPTER 2
Figure 2.1: Cd speciation in fresh water system with air having a CO2 fugacity 370 µbar and ionic strength of 1.5 mM (Powell et al., 2011) 17

Figure 2.2: Cd speciation in saline water system with air having a CO_2 fugacity 316 µbar and ionic strength of 670 mM (Powell et al., 2011) 18

CHAPTER 3
Figure 3.1: Schematic figure of saturated soil column 24

CHAPTER 4
Figure 4.1: Soil sampling points around Mae Tao and Mae Ku creeks with 3 classes of Cd level in soils from low (green dots), medium (yellow dots), and high (red dots) 32

Figure 4.2: Relationship between Cd and Zn content in soils from Mae Tao and Mae Ku creeks 33

Figure 4.3: Point of zero charge of the selected soil 35

Figure 4.4: X-Ray diffraction pattern of the selected soil from Mae Tao area 36

Figure 4.5: Observed and fitted data of Cd adsorption on the selected soil from Mae Tao area at IS 1 mM(a), 10 mM (b), and100 mM (c) 38

Figure 4.6: Desorbed Cd on the selected soil as compared to adsorbed Cd on the selected soil for IS 1, 10 and 100 mM at pH 7.0 39

Figure 4.7: Observed data and fitted data by CDE and T-R models of bromide at low PV of Column no.1 41

Figure 4.8: Observed data and fitted data of bromide by CDE and T-R models of bromide at high PV of Column no.2 41

Figure 4.9: (a) Observed data of Column 3 and (b) fitted curves from different models of Column no.3 under low pore water velocity (2.0 cm/h) and high IS (100 mM) 44

Figure 4.10: (a) Observed data and (b) fitted curves from different models of Column no.4 under low pore water velocity (2.0 cm/h) and medium IS (10 mM) 45

Figure 4.11: (a) Observed data and (b) Fitted curves from different models of Column no.5 under low pore water velocity (2.0 cm/h) and low IS (1 mM) 47

Figure 4.12: (a) Observed data and (b) Fitted curves from different models of Column no.6 under high pore water velocity (9.0 cm/h) and high IS (100 mM) 48

Figure 4.13: (a) Observed data and (b) Fitted curves from different models of Column no.7 under high pore water velocity (9.0 cm/h) and medium IS (10 mM) 49

Figure 4.14: (a) Observed data and (b) Fitted curves from different models of Column no.8 under high pore water velocity (9.0 cm/h) and low IS (1 mM) 50

Figure 4.15: Effect of IS on Cd transport for (a) low pore water velocity columns and (b) high pore water velocity columns.....52

Figure 4.16: Effect of pore water velocity on Cd transport for IS 100 mM (a), 10 mM (b) and 1 mM (c) 55

CHAPTER1

INTRODUCTION

1.1Rationale

Cadmium (Cd) is one of well-known hazardous substances. It is found associated with zinc (Zn), copper (Cu), and lead (Pb) ores. Contamination of Cd in the environment can cause by natural source, and human activities such as mining activity, industrial activity and application of fertilizer (Järup, 2003). Cadmium will accumulate in human who exposed to, and consequently cause lethal effect such as renal disease and Itai-Itai disease (WHO, 2010). Therefore, it is vital to control and investigate Cd level in the environment as well as mechanisms of Cd migration.

One of the area in Thailand reported to be contaminated by Cd is located in Mae Sot district, Tak province, where International Water Management Institute (IWMI) found the high level of Cd in rice grain and agricultural soil in 1998. Concentrations of Cd in soil from paddy field in the study site ranged from 0.5-284 mg/kg, which extremely higher than European Union Maximum Permissible of 1.0-3.0 mg/kg, depending on soil pH (Simmons et al., 2005). Source of contaminants come from Padang zinc deposit, which is a secondary zinc ore deposit containing Cd and Pb as solid-solution or inclusion in hemimorphite (Pollution Control Department, 2010). These metals (Zn, Cd, and Pb), binding with suspended sediments, were transported downstream along Mae Tao and Mae Ku creek. In addition, rice cultivation in the study area has mainly used irrigation water from Mae Tao and Mae Ku creeks; therefore, suspended sediments were deposited in the paddy field and brought metals, especially Cd, contaminated in paddy soil and rice (Simmons et al., 2005).

This information led to many follow-up investigations on the Cd, Zn and related metals contaminated in this area. Akkajit and Tongcumpou (2010) studied fractionation of related metals in soils using BCR sequential extraction, and found out that Cd is most bioavailable compared to other metals (Zn, Pb, Mn, etc.), since Cd is mainly in the exchangeable fraction (BCR1). The fractionation of Cd was also studied by

Kosolsaksakul et al. (2014) and the result showed high proportion of exchangeable fraction (BCR1) of Cd in BCR sequential extraction in all range of contaminated soil (classified into low-, medium-, and high contaminated soils). For fractionation using Tessier sequential extraction, distinguished between easily exchangeable form and weak-acid soluble (or carbonate-binding) form, it showed that carbonate-bound fraction was higher in high contaminated soils, while the exchangeable form was the main fraction for medium contaminated soils. Both studies showed ability of Cd leaching into environment as well as plant can then uptake Cd through food chain. In contrast, study of Watcharamai and Saenton (2013) investigated leach ability of heavy metals in 39 agricultural soils in various pHs (4, 7, and 10) and ionic strengths (0.1, 0.01 M), and found that metal leached commonly less than 1% of total metal concentration, incomparable with fractionation studied of Akkajit and Tongcumpou (2010), and Kosolsaksakul et al. (2014). Another finding was that leaching behavior of metals from agricultural contaminated soils in this area was obviously influenced by pH and ionic strength of the solution, and the chemical reaction was reached equilibrium within 1 day.

Even though there were many studies on Cd and relevant minerals in Mae Sot contaminated area, such as fractionation and leach ability of Cd in agricultural soils and sediments, there were no study on sorption/desorption of Cd in this area, neither column experiment to investigate migration of Cd in these contaminated soils. Batch experiments are commonly used to study sorption and desorption behavior of heavy metals in soil or another media. The procedure was to vary concentration of heavy metals in soil, or media, to gain sorption coefficient (Herbert, 1995; Disli, 2010). Somehow, only these applications are not adequate to assess the movement of Cd through soil. As comparing to batch experiment, column experiment is more realistic to stimulate the real condition. For example, Plassard et al. (2000) compared retention and distribution gained between batch and column experiments of Cd, Pb, and Zn. The result showed the smaller amount of those metals retained in soil from column experiment than those in batch experiment, which may cause by preferential flow that can be found only in column experiment.

One of the factor affecting on sorption/desorption of Cd and other toxic metals on soils is ionic strength (IS) (Loganathan et al., 2012). For negatively charge soil, increasing in ionic strength results in decreasing of Cd sorption, because ionic strength cause changes in electrostatic potential of the adsorption plane (Naidu et al., 1994). Wikiniyadhanee (2012) reported that increasing in ionic strength cause decreasing in adsorption of both kaolinite clay and sand. In the same way, study of Watcharamai and Saenton (2013) showed that higher ionic strength (0.1 M) resulted in higher leaching of heavy metals from contaminated soil of Mae Sot, but as mentioned before, there were no further study of the adsorption of Cd in soil from this area. Pore water velocity is another physical factor, which should be concerned since soil infiltration rate can be changed. In rainy season, the farmer needs to draw the water into their rice field, causing the water head increase; consequently, the velocity infiltration rate of water into soils should be higher than that in summer season. Also, the effects of pore water velocity on Cd mobility were investigated by Pang et al. (2002) and Tsang and Lo (2006). According to study of Pang et al. (2002), pore water velocity inversely related with retardation factor (R) due to higher adsorption in long retention time. Pore water velocity also affect non equilibrium parameter (Tsang and Lo, 2006), increasing in pore water velocity also enhance α and diminish f for the sorption which is rate limited.

Therefore, the systematic experiments were carried out to investigate the effect of ionic strength on adsorption/desorption of Cd on contaminated soils from Mae Sot district, Tak province using batch technique and column tests. Furthermore, to fulfill the limitation of batch experiment and get a better understanding of effect of preferential flow onto Cd movement, column experiments of contaminated soils were conducted under various water flow velocity and ionic strength. Finally, such effects onto Cd sorption/desorption and transport were evaluated by sorption isotherms for batch experiments and by the mathematical model, so-called HYDRUS-1D, for column tests to deeply explain the sorption/desorption and transport behavior.

1.2 Hypothesis

Difference in ionic strengths and pore water velocities may cause different sorption/desorption and transport behavior of Cd through the saturated contaminated soil.

1.3 Objective

To evaluate the sorption and movement of behavior of Cd due to different pore water velocities and ionic strengths of solution through contaminated agricultural soil in Mae Sot district, Tak province

1.4 Scope of Study

1. Cd-contaminated soil was selected from agricultural areas nearby Mae Tao creek, Mae sot district, Tak province, Thailand, with a wide range of hydraulic conductivity values.
2. Soil column experiments were conducted under a saturated condition.

CHAPTER2

LITERATURE REVIEW

2.1 Cadmium and its effect to human health

Cadmium is a heavy metal with atomic number of 48, discovered in 1817 by German Chemist, Friedrich Stromeyer (Nordberg, 2009). Release of Cd to the environment can cause by both natural and anthropogenic activities.

Natural sources: By volcanic activities, weathering of rocks, and transportation by river (WHO, 2010).

Anthropogenic source: Cd is used worldwide in both industrial and agricultural sectors; for examples, alloys, batteries, color pigments, anti-corrosion agents, as well as application of municipal sewage sludge and phosphate fertilizer (Järup, 2003).

Additionally, zinc mining is one of main human sources, releasing Cd contaminated into the environment, since Zn and Cd are geologically associated.

Human can expose to Cd by consuming contaminated food and water, smoking cigarettes, and inhalation of Cd contaminated air (WHO, 2010; Järup, 2003). Impacts of exposure to Cd can be dreadful. It can accumulate in kidney and cause irreversible renal tubular dysfunction, and may progress in renal damage, or even death. Cadmium also disturb calcium metabolism which causes skeletal damage, resulting in low bone density (osteoporosis) for long term low level exposure, as well as itai-itai disease, the combination of osteomalacia (bone softening) and osteoporosis, for long term high level exposure. Moreover, Cd is human carcinogen classified by IARC (1993), and possibly carcinogenic as classified by European Commission (Järup and Åkesson, 2009).

Since Cd is highly toxic, there are standards controlling Cd level in the environment. For instance, USEPA drinking water standard is 0.005 mg/l, European

Union standard for total Cd in soil was 1.0-3.0 mg/kg (depending on soil pH), and CCFAC ceiling for Cd concentration in rice grain was 0.2 mg/kg.

2.2 Cadmium contaminated in soil

Earth crust contains Cd for only 0.2 mg/kg, which can be determined as trace element (Traina, 1999 cited in Lindsay, 1979), and mostly found high concentration in sedimentary rocks. Cadmium can be found in the particular area where has potential Zn ores such sphalerite ($ZnCO_3$), as by product of Zn mining (Traina, 1999). The European Union standard for maximum concentration of Cd in sludge amendment in soil is 1.0-3.0 mg/kg, depending on soil pH. Not only concentration of Cd, but it is important to understand phases and behavior of Cd contaminated in soils, because bioavailable Cd leads to contaminate in plant and crops that human consume.

2.3 General information of the study area

Soil samples apply in this research were taken from catchments area of Mae Tao creek, located near Thai-Myanmar border, in Phrathat Pha Daeng and Mae Ku sub-district, Mae sot district, Tak province, Thailand.

2.3.1 Geography and Geology

Mae Sot district, Tak province, has the mountainous area at the eastern part, while the western part are colluvium and alluvial plain areas. Moei river at the west are Thailand-Myanmar natural border.

Potential source of zinc ores in Padang came from Huai Hin Fon Formation, which grouped Upper Triassic-Jurassic age rocks, located on Doi Padang. It is secondary deposits of zinc ores such as zinc silicate, carbonate and oxide, e.g. hemimotphite [$Zn_4Si_2O_7$ $(OH)_2.H2O$], smithsonite ($ZnCO_3$), hydrozincite [$2ZnCO_3.3Zn(OH)_2$], and loseyite [$Mn(Zn)_7(OH)_{10}(CO_3)_2$]. This formation consists of dark gray limestone and light gray bedded limestone with fossils of ammonites, brachiopods, and coral reefs, inter-bedded with calcareous shale, sandstone, and red lime-conglomerate. Orient NE-SW with dipping 50 degree to NW (Maneewong, 2005).

2.3.2 Hydrogeology and hydrology

In 2010, Pollution Control Department (PCD) investigated the flow pattern of groundwater in this area by collecting the elevated level of groundwater in 20 wells in 4 sub-district, Pa Wor, Mae Ku, Mae Tao, and Pra That Pa Daeng. The results showed that the groundwater flow from the mountainous catchment area at the east with piezometric head 240 meters (amsl) to the drainage area at Moei river basin at the west with piezometric head 200-240 meters (amsl). Two main watersheds in this area are Mae Tao and Mae Ku. The groundwater pH in those 20 wells ranged from 6.2 to 7.9 , total hardness as CaCO3 ranged from 91to1206 mg/L, while Cd concentration was less than 0.003 mg/L.

For hydrology, the main water resources are Mae Tao creek and Mae Ku creek. Mae Tao creek flows from east at Ban Mae Tao to west at Moei River with the length of approx. 33 km. Mae Ku creek originated at Ban Nong Num Kheao and distributed in to 3 small creeks at Ban Mae Ku Noea. All sub streams ended at Moei river as same as Mae Tao creek. Surface water samples from the creeks were collected from 20 stations on August 2010 and analyzed for pH, Cd and hardness. They found that water pH ranged from 7.2 to8.4, hardness ranged from 152 to330 mg/L, and Cd concentration was less than 0.001 mg/L (PCD, 2010).

2.3.3 Background of Cd and heavy metals contamination

Cadmium contamination around Mae Tao Creek, Mae sot district, Tak province, Thailand, was first reported during 1998-2003, under the IWMI-DOA collaborative project, when Dr. Robert Simmons, the researcher of International Water Management Institute (IWMI), and Dr. Pichit Pongsakul, from Department of Agriculture (DOA), detected the high level of cadmium contaminated in paddy field and rice grain. These facts led to numerous investigations on Cd and heavy metals polluted in Mae Tao Creeks and adjacent areas, especially studies of soil contamination.

Whereas the European Union standard of Cd level in soil allowed maximum level of Cd in soil for 1.0-3.0 mg/kg (predominate on soil pH), and Thailand soil's Cd background is 0.002-0.141 mg/kg (Simmons et.al, 2005 cited Pongsakul and

Attajarusit, 1999), all previous studies reported that in some paddy fields around Mae Tao and Mae Ku creeks, Cd levels were exceedingly higher than the EU standard, which is related to high Cd level in rice grain grown in those fields (Kosolsaksakul et al., 2014).

Simmons et al. (2005), observed the contamination in paddy fields and rice grains. For the preliminary investigation (1998-2000), the target area was located in Ban Pa Te, which is closed to the Zn mineralized area. Soil samples of 0-30 cm. depth from 154 fields and rice grains samples from 90 fields were collected and analyzed for Cd and Zn concentrations. The results showed that: (1) Cd concentration in soils ranged from 3.4 to 284 mg/kg, (2) Zinc concentration in soils ranged from 197 to 8036 mg/kg and strongly correlated to the Cd concentration, (3) In the rice grain, Cd concentration ranged from 0.1-4.4 mg/kg, which 95% of the samples exceeded the Codex Committee on Food Additives and Contaminants (CCFAC) standard of 0.2 mg/kg.

For the extensive study (2001-2002), soil samples from 334 fields and rice grain samples from 434 fields from the extended areas along the Mae Tao creek were collected. The outcome revealed that: (1) Concentration of Cd and Zn ranged from 0.5-218 mg/kg and 700-1718 mg/kg, respectively, and are positively correlated. (2) Rice grain Cd concentration ranged from <0.05 to 7.7 mg/kg, and 85% of them are higher than the CAFCC standard, (3) Fifteen soil profiles were investigated for Cd and Zn concentration, and more than 80% of Cd and Zn loading was on the upper soil of 0-30 cm, supporting that the presumption that contamination in paddy field near Mae Tao creek was caused by contaminated irrigation water from Mae Tao creek (Simmons et.al, 2005).

Following the study of Simmons et al. (2005), to access bioavailability of Cd and related metals in contaminated paddy fields around Mae Tao creek, Akkajit (2010) investigated the concentration and fractionation of six related metals, which were Cd, Cu, Fe, Mn, Pb, and Zn, using BCR sequential extraction. The relationship between bioavailable Cd and other factors such soil pH, organic matter, soil ORP, and associated metals concentration were determined using Principal Component Analysis (PCA).

Ranges of metals concentrations of Cd, Cu, Fe, Mn, Pb and Zn are: 0.73-172.7 mg/kg, 5.0-27.5 mg/kg, 3473-17963 mg/kg, 65.27-1222 mg/kg, 6.4-160.3 mg/kg, and 26.12-3,138 mg/kg, respectively, confirming that metals concentration are in the normal ranges, except for Cd and Zn. Bioavailability of metals was determined by BCR sequential extraction, the outcome showed that Cd, Mn and Zn contained with high BCR1 proportion (25-30%), which is exchangeable phase and ready for bioavailable form. Additionally, Cd, Mn, Zn, and Pb contributed of high amount of BCR2, which are reducible fractions. Briefly, Cd, Mn, Zn, and Pb contain more than 40% of exchangeable and reducible fraction (BCR1+2); on the other hand, Cu and Fe are associated with other phases. The Principal Component Analysis (PCA), showed a weak relationship between bioavailable Cd (BCR1) and soil properties (pH, OM, ORP), but strongly correlated to total Cd concentration, as well as to Zn, Pb, and both total and available metals.

Another study, Kosolsaksakul (2014), investigated Cd partitioning in soils and its association to plant uptake. Soil Cd concentration ranges form 2.5-87.6 mg/kg, which lower than concentrations reported by Simmons et.al (2005), because the area covered only Ban Mae Tao Mai, but didn't covered Ban Pa Te, which is closer to mining area (Kosolsalsakul, 2014). For vertical profile, Cd contamination was evident down to 40 cm depth. Soils was classified into 3 groups: low contamination (<10 mg kg^{-1}), medium contamination (10-50 mg/kg), and high contamination (>50 mg kg^{-1}). Soil samples were extracted using BCR and Tessier sequential extraction. The results indicated high amount of Cd in BCR1 partition (67% -84%), which can be distinguished by Tessier sequential extraction to easily soluble phase (T1) and carbonate or weak acid soluble phase (T2). The greater contaminated soil tends to have the larger T2 partition (around 45% in medium contaminated soil, and 70% in high contaminated soil).

Not only fractionations of heavy metals contaminated in this area were investigated, but also leaching behavior of these metals form soils. Watcharamai and Saenton (2013) studied leach ability of Cd, Zn, Pb, Fe, and Mn, from 39 soil samples taken from Mae Tao watershed. The experiment was conducted in various pHs (i.e., , 7, 10), ionic strengths (0.01 and 0.1 M), and times (1-28 days). The result showed that leaching of heavy metals was reached equilibrium within 1 day, and leaching was

particularly lower than 1 percent (Cd 0-1.378%, Zn 0.058-0.287‰, Pb 6.124-17.113%, Fe 0-0.154%, and Mn 0.422-9.310%). Higher ionic strength (0.1M) resulted in higher release of heavy metals than lower ionic strength (0.01M). On the other hand, it is unclear explanation about effect of pH on leaching of heavy metals.

From these researches (Simmons et al., 2005; Akkajit and Tongcumpou, 2010; Kosolsaksakul, 2014), there are evidence of Cd contamination in the paddy field, caused by irrigation contaminated water from Mae Tao Creek, which contaminated highest up to 80 mg kg^{-1} in Ban Mae Tao Mai, and up to 200 mg/kg in Ban Pa Te. Additionally, the sequential extraction, showed possibility of releasing of Cd due to its high exchangeable phase, up to 30% according to Akkajit and Tongcumpou (2010) and up to 80% according to Kosolsaksakul (2014).

2.4 Solute transport through soil

In order to understand the contaminant transport through soil and groundwater, it is essential to understand the basic concept of solute transport. Many study using tracer (e.g., Br^-, Cl^-, and ^3H_2O) to access the water mobility through soil. The following is a summary of those findings.

Padilla et al. (1999) studied the NaCl transport through homogeneous silica sand under various pore water velocity (0.033-0.213 ml/min) and water content from unsaturated condition (13 columns) to saturated condition (3 columns), and estimated the transport parameter using Convective-Dispersion equilibrium (CDE) model and Mobile-Immobile (MIM) model. The result showed that water content has strong inverse effect to the dispersion that lower water content lead to higher dispersion coefficient, because lower water content lead to smaller flow channel, flow path, and higher tortuosity. Water content also affects many hydraulic parameters estimated by MIM, lower water content results in the lower mobile water fraction (β), and mass transfer coefficient (α). For the effect of water velocity, the fitted dispersion coefficient increases with increasing pore water velocity, but not strong relationship (r^2=0.30) in this study. For β, it increases with increasing pore water velocity at high water content (>23%). Pore water velocity directly affects to α because high flow velocity enhances solute mixing.

Shukla et al. (2003) investigated the effect of pore water velocity and displacement length to the diffusion and dispersion. The experiment was conducted under saturated condition in two types of soil, loam soil and sandy loam soil, which is packed in an acrylic column with displacement length of 10, 20 and 30 cm. The parameter D (diffusion coefficient) was estimated using CDE model and parameter λ was fitted with or without molecular diffusion coefficient (D_0) using the relationship as follow: $D = \lambda v + D_0$. In this study, parameter λ was independent of pore water velocity and displacement length in both soils, and D has linear relationship with v_m for $v_m \geq$ 0.1 cm/h.

Another study on effect of pore water velocity on Cl^- transport was done by Zhou and Wang (2016), the experiment was conducted under saturated undisturbed soil columns with 4 different pore water velocities (3.34-8.35 cm/h) and two different pulse inputs (0.1 PV and 0.5 PV). The model parameter was estimated using CDE model and T-R model and discussed by data from large pulse input. Dispersivity (λ) showed in the article seemed to be increase with increasing velocity as fitted by CDE model, but for T-R model λ is one order of magnitude less than as obtained from CDE model and does not show clear relationship as the CDE model, therefore authors does not conclude the effect of velocity on λ in this article. For Peclet number (Pe), it decreases with increasing velocity (except for velocity 3.34 cm/h), and Pe also showed that the advective flow dominated in all columns. Moreover, as fitted by T-R model, with increasing velocity, the mobile-immobile partition coefficient (β) decreases and mass transfer coefficient (ω) increases.

Fashi (2015) mentioned the effect of soil texture on breakthrough curves (BTCs) shape. BTCs shape of sandy soil tend to be more symmetrical than those derived from loam or clayey soil (Gonzales and Ukrainczyk, 1999 cited in Fashi 2015). Soil texture also affect λ (Urisano and Gimmi, 2004; Mohammadi and Vanclooser, 2001 cited in Fashi, 2015), the finer texture (e.g. loam soil) has higher λ than coarser texture (e.g. sandy soil).

In conclusion, there are many factors studied whether they affect the solute transport, for examples, soil texture, water content, and pore water velocity. The water

content apparently affects the solute transport and solute transport parameters. Soil texture seemed to affect dispersivity in some studies, and not clearly affect in the study of Fashi (2015). Flow rate and pore water velocity are generally affect the solute transport because they affect mixing regime; somehow, there are complicate and has some ambiguous points on the explanation (Fashi, 2015).

2.5 Adsorption and desorption of Cd on soils

Sorption of Cd in soil can be divided into two major types (Christensen and Haung, 1999).

Non-specific sorption is the sorption which Cd ions bind to surface's negative charge site by electrostatic attraction (McBride, 1989). Cadmium ions bound with non-specific sorption are easily replaced by other cations. It is thus considerable as exchangeable Cd, which is bioavailable and easier to leach (Loganathan et al., 2012).

Specific sorption is the sorption which Cd ions chemically bound to both negative and neutral surface charge sites. Cadmium adsorbed in this way forms inner-sphere complexes; it is hence not easy for Cd ions to be removed (Loganathan et al., 2012).

In addition, not only sorption on soils, but Cd can form organic ligand complexes, or precipitate in soils in form of CdS, $Cd(OH)_2$, $CdCO_3$, and $Cd_3(PO_4)_2$ (Christensen and Huang, 1999; Loganathan et al., 2012).

2.6 Factors controlling sorption and desorption of Cd

Since sorption of Cd on soil is complex, there were extensive researches on various factors influencing Cd sorption and desorption onto soils. This part gives examples of widely known factors, which are soil components and solutions.

2.6.1 Soil components

1. Metal oxides: Metal oxides, especially oxides of iron (Fe) and manganese (Mn), can specifically adsorb Cd. One of the obvious effects of iron oxide to Cd and relevant metals adsorption was in the research of Diagboya et al. (2015). One

part of this study had comparison between primitive soil and treated soil, which iron oxide was removed. The soil samples were two tropical soils collected from the ecological zone of Nigeria. The result found that iron oxides increases retention and decreases desorption of Cd in the long run.

2. Calcium carbonate: Presence of calcium carbonates ($CaCO_3$) can improve Cd adsorption. Cd^{2+} ions can be replaced by Ca^{2+} ions and then form $CdCO_3$ by chemisorption process (Christensen, 1999 cited McBride, 1980), even at low pH (Christensen, 1999 cited Stipp et al., 1992). Zhao et al. (2014) also studied effect of calcium carbonates on Cd sorption on some purple paddy soils. As expected in soils with calcium carbonate, Cd adsorption were higher and desorption rates were lower, as well as proportion of exchangeable Cd was lower than that of same soils in which calcite were eliminated.

3.Organic Matter: As claimed by Christensen (1999), low molecular weight organic such as, acetate, fumate, maleate, and etc. can be a carrier of the solute Cd. In contrast, high molecular weight organic, such as humic acid, can cause higher retention of Cd. Study of Zhao et al. (2014), found that removal of organic matter results in lower Cd amount adsorbed on soils within 22 hours for batch experiment. Though, Diagboya et al. (2015), investigated effect of organic matter on sorption of heavy metals, including Cd, for a long period (1-90 days). Interestingly, elimination of organic matter reduce all heavy metals only for first seven days, but not for longer time (>7 days).

4. Biological colloid: Microorganisms can adsorb soluble Cd efficiently due to its large surface area. Many studies use bacteria to remediate the contaminated water (Christensen, 1999 cited Huang and Bollag, 1997).

2.6.2 Solution phase

1. pH

pH is one of dominant factors, manipulating Cd sorption. In general, increasing pH lead to increasing adsorption of Cd (Naidu et al., 1994).The reasons were given by Barrow (1984) that the increasing pH decreases electrostatic potential of surface charge to become more negative. Hence, Cd sorption, which primarily

sorb nonspecifically on negative charges, became more specific (Naidu et.al, 1994).

2. Ionic strength (IS)

Normally, increasing in ionic strength result in decreasing Cd sorption, and vice versa. This was confirmed by many researches. (Naidu et al., 1994), varied solution IS (NaNO3 0.01-1.5 mol/dm^3), and found that for soil with normal pH ranges (pH>PZC), Cd sorption decreased with increasing IS. The explanation of this phenomena were concluded by Loganathan (2011) that increasing IS result in: (1) Lower pH, which lower adsorption of Cd, (2) Competition between electrolyte's cation and Cd^{2+}sorption, (3) Lowering Cd^{2+} activity (4) formation of Cd ion pairs, such as $CdCl^+$, and (5) Changing in electrostatic potential in adsorption plane.

The result were similar with other IS solution. Wikiniyadhanee (2012), studied sorption of cadmium on sand, kaolinite colloid, and kaolinite facilitated transport, the ionic strength was varied using $CaCl_2$ (0.0 – 3.6 mM). As expected, sorption capacity of Cd on kaolinite colloid and sand decreased with increasing IS, also high IS enhance transport of Cd through sand column. For colloid facilitated transport, kaolinite colloid enhanced transport of Cd in extremely low pH, but disturbed Cd transport at high IS.

3.Background electrolyte

Cation (Ca^{2+}, Mg^{2+}, K^+, and Na^+): Different solution's cation can change heavy metal adsorption. For Cd, its sorption is increased with background cation in the order of: $Ca^{2+}<Mg^{2+}<K^+<Na^+$ (Loganathan et.al, 2011 cited Fotovat and Nadiu, 1998). Naidu et.al, 2004, investigated effect of two different type IS solutions ($Ca(NO_3)_2$ and $NaNO_3$), at IS 0.03 mole/dm^3, and found that sorption of soil in solution with Na^+ is 2-4 times higher than with $Ca(NO_3)_2$. One reason given were the differences in ion valency, higher valency ions attribute to less negative charge on the adsorption plane; hence, Cd sorption is reduced (Naidu et al., 1994 and Loganathan, 2011 cited Bowden et al., 1993).

Inorganic anion (NO_3^-, Cl^-, SO_4^{2-}, and PO_4^{3-}): Between NO_3^- and Cl^- Cadmium adsorption was much greater in $NO3^-$, due to forming of $CdCl^+$ complex in the presence of Cl^- which have lower potential to be adsorbed (Loganathan et al., 2012); on the other hand, Cl^- increases cadmium mobility. For SO_4^{2-}, which is likely to be found in saline soil, neither enhances nor reduces Cd sorption (Loganathan et al., 2012 cited Homann and Zasoski, 1984, and Naidu et al., 1994). The greatest adsorption of cadmium among four inorganic anions (NO_3^-, Cl^-, SO_4^{2-}, and PO_4^{3-}) was PO_4^{3-}.

4. Heavy metals (Zn, Cu, Pb, etc.)

Cadmium is usually associated with other heavy metals such as zinc, copper, and lead. Therefore, there were extended studies about influence of heavy metals including Cd, on each other's sorption behavior. Among these metals (Cd Zn, Cu, and Pb), Cd have the lowest affinity; hence, Cd sorption is reduced when these metals exist.

2.6.3 Pore water velocity

As mentioned in topic 2.4, solute transport is dependent on soil moisture, soil texture, and pore water velocity. In this research, we interested in the mobility of Cd in one type of soil under saturated condition; therefore, regardless to the soil water content and soil texture, we will review the investigation on effect of Cd transport as effect by pore water velocity.

According to the study of Bajracharya et al. (1996), effect of flow velocity to Cd adsorption on homogeneous sand column were observed. Thirteen columns were set with flow velocity ranged from 5-150 cm/h with initial pH 6.0 (initial Cd concentration 1.0 mg/l for 12 columns and 0.6 mg/l in 1 column). Adsorption coefficient was found to be fairly constant, in both equilibrium and non-equilibrium transport (K_d ranges~10-13 l/kg in 12 columns). In contrast, (Tsang and Lo, 2006) used column experiment to observe transport of Cd in 3 soils, flow velocities were varied form 6-82 cm/h. It was found that transport of Cd can be explained by the two site non-equilibrium model (TSM) and the effective dispersion equilibrium model. The results show that sorption rate coefficient (α) increase and fraction of instantaneous sorption decreases (f) with increasing pore water velocity, implies that the sorption is rate limited by physical

process. Also, Pang et al. (2002) investigated effect of pore water velocity on Cd, Zn and Pb non-equilibrium transport on alluvial gravel column with initial concentration of 4 mg/l and pore water velocity (*V*) ranging from 3-60 m/day and analyzed by Two Site Adsorption/Desorption Model. The result showed that pore water velocity (*V*) is not related with instantaneous fraction (*f*), inversely related with retardation factor (*R*), and positively correlate with sorption and desorption rate coefficient (k_1 and α, respectively). Retardation factor for 3-60 m/day pore water velocity were, 26-289 for Cd, 24-255 for Zn, and 322-6377 for Pb. From these researches, it can be concluded that sorption of Cd and heavy metals can either be affected, or not be affected by pore water velocity.

2.7 Ionic Strength (IS)

Ionic strength of solution can be measured from concentration of ionic charge (EPA, 2013). The calculation of IS can calculate by the equation below (Appelo and Postma, 2004; Aquion, 2014).

$$I=\frac{1}{2}\sum_{i=1}^{n} c_i z_i^2$$

When I is ionic strength (mole/l), c_i is molar concentration (mole/l), and z_i is ion charge. Ionic strength can also be calculated by total dissolve solids (TDS)

$$I=2.5\times10^{-5}TDS$$

Or by electronic conductivity (EC)

$$IS\ (mM)=\frac{EC\ (\mu S/cm)}{54.5}$$

In general, IS of natural water is about 1-5 mM, 1-20 mM and 700 mM for surface water, groundwater, and seawater respectively (Apello and Postma, 2004; Aquion, 2014). However, ionic strength of water resources can be impacted by human activities, which are agricultural activities (irrigation and fertilizer application), wastewater discharge, mining activity, applying road salt in winter (EPA, 2013). Additionally, Naidu et al. (1994), also referred that the IS of soil solution generally ranges from less

than 5 mM in tropic soil, to more than 100 mM in less weathered soil or soil near fertilizer granules.

2.8 Cd Speciation in the environment

Cadmium can chemically associate with organic and inorganic compounds in various forms, depending on the environmental conditions. Powell et al. (2011) reviewed the modelling of Cd speciation and the stability constants related to the thermodynamic data.

For the formation of Cd in fresh water in equilibrium with atmospheric CO_2, and with ionic strength of 1.5 mM, the speciation of Cd is shown in Figure 2.1 The dominant species in this system is Cd^{2+} for pH≤8.65, and $CdCO^3$ for pH≥8.65. Only $CdSO_4$ and $CdOH^+$ are found as minor species.

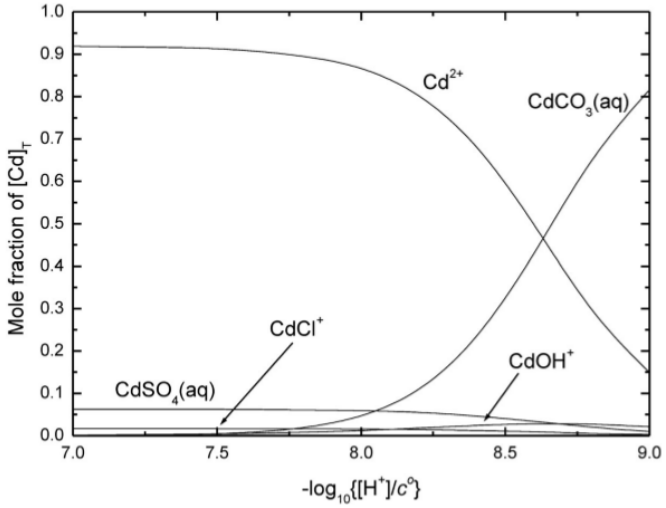

Figure 2.1: Cd speciation in fresh water system with air having a CO2 fugacity 370 µbar and ionic strength of 1.5 mM (Powell et al., 2011)

For saline of seawater system (ionic strength 670 mM), the formation of Cd species is different. For pH<8.5, mole fractions are invariant with pH, $CdCl_2$ is the greatest (44.8%), followed by $CdCl^+$, and $CdCl^{3-}$, while Cd^{2+} only compiles for 3%; $CdCO_3$ forms significantly for pH>9 (Figure 2.2). Note that this model includes the competing reaction of Ca^{2+} and Mg^{2+} with the inorganic anion.

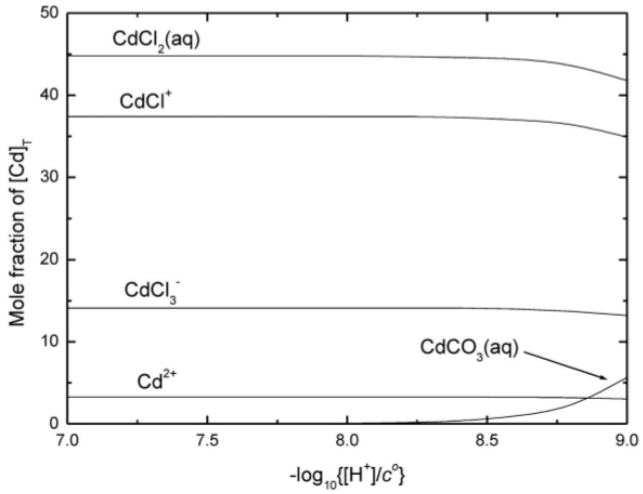

Figure 2.2: Cd speciation in saline water system with air having a CO_2 fugacity 316 µbar and ionic strength of 670 mM (Powell et al., 2011)

So, the Cd^{2+} is the dominant species for low ionic strength and neutral to weakly acidic condition, while $CdCl_2$ and $CdCl^+$ complexes are formed in neutral to weakly alkaline pH in a saline system.

2.9 Batch Experiment

Batch experiment is a common experiment used to express sorption behavior of contaminants in soil. Concept of this method is mixing exact amount of adsorbent (e.g. soil) with varied concentration of adsorbate solution (e.g. heavy metals), in same solid-solution ratio (Dişli, 2010). Outcome of the batch experiment, aside from sorption isotherm, are factors effecting sorption behavior of substance and media. Soil and heavy metals, for example, were conducted by many batch experiments, and found out that main factor controlling heavy metals sorption in soil were soil properties, pH, ionic strength (IS), metal oxides etc. In addition, batch experiment can be used to determine equilibrium time by varying contact time.

2.10 Column Experiment

Many researches used column experiment in order to estimate model parameter explaining mobility of heavy metal in soil (Dişli, 2010; Bajracharya et.al, 1996; Allen et.al, 1995; Seuntjens et.al, 2001). Soil column is a block of soil integrates with tool

collecting effluent, and it is able to control or measure flow rate (Lewis and Sjöstrom, 2010). The advantages of column experiment as comparing to batch experiment are that column experiment include the effect of flow velocity, therefore adsorption obtained from column appears to be more realistic (Bajracharya et al., 1996; Disli, 2010).

2.11 Flow Interruption

Flow interruption is a method developed to define the sorption mechanism in the miscible displacement experiment (column experiment) whether is equilibrium or non-equilibrium process. The concept of this method is explained by Brusseau et al. (1989), the process is to inject the steady flow rate of the solution containing interested substance into saturated sand column to gain Breakthrough Curve, then stop the flow at some point of BTCs (recommend at C/C_0=0.2-0.8) for some period of time (4-5 pore volume), then start the flow again and collect the solution for 5-10 pore volume. For the sorbing solute with rate limited sorption, during the flow interruption period, the sorption (or desorption) proceeds, therefore it decreases the adsorbate concentration during the adsorption process (front limb of BTCs), and enhance adsorbate concentration during the desorption process (back limb of BTCs) (Brusseau et al. (1989) and Brusseau et al. (1997)). But for the equilibrium sorption, flow interruption will show no effect to the BTCs.

CHAPTER3

METHODOLOGY

3.1 Data Preparation and Field Observation

3.1.1 Data Preparation

Prior to collecting the samples, data were collected and processed by ARC GIS program in order to select appropriate sampling point. The source of data was explained in the Table 3.1

Table 3.1: Data types and sources of data

Data	Type	Source
Topographic Map	Raster	Royal Thai Survey Department (2006)
Soil type	Shapefile	Land Development Department
Cadmium Contamination Map	Shapefile	Modified from Tongcumpou (2014)
Stream	Shapefile	Land Development Department

3.1.2 Field Observation and Soil Preparation

The study area is located around floodplain area of Mae Tao and Mae Ku creek, Mae Sot district, Tak province Thailand. Soil samples were collected from 18 sampling point from paddy field and other agricultural field, ten sampling points were selected from contaminated area according to Tongcumpou, 2014 and soil map. The samples taken from the field were separated in to 2 types;

a) Bulk soil sample

Surface soil samples were collected from the field. For each sampling location, the soil was collected 15 cm depth from 5 different points, approximately 10 meters apart, and then thoroughly mixed together to obtain composite soil samples at each specific location.

b) Soil core sample

The surface soil was excavated and soil samples were collected in duplicate at 15 cm depth using aluminum soil cores with a total volume of 100 cm^3.

3.2 Soil preparation and analysis

3.2.1 Soil Preparation

Soil samples were oven-dried at 60 ºC, grinded by a mortar, sieved through 2mm sieve. Only grain size under 2 mm were kept for further experiments.

3.2.2 Cadmium and Heavy metals concentration in soils

Microwave digestion were selected in order to digest soil sample which are prepared from section 3.1.1 following EPA method 3051A, which is a method for extraction of heavy metal in soil, but not complete decomposition. For this method, 5 grams of soil were digested by 9 ml HNO_3 and 3 ml HCl and put into the microwave digestion machine. Ramp temperature was set 175 ºC for 5.5 minutes, and hold for 4.5 minutes. After that, left samples in the machine for 30 minute. The samples were brought out and let them cooled down outside the microwave machine for 30 minutes, and filtrate with Whatman filter paper No.5, kept under 4 ºC and measure extracted heavy metals with ICP-AES.

3.2.3 Physico-chemical properties of soils

Bulk Density

Bulk density of soil were determined using soil core sample. First the soil sample with core were measured, and then soil cores were used for hydraulic conductivity measurement. Later, soil sample and core were oven-dried at 105 ºC for 3 days. Measured dry weight of soil and core, and bulk density were calculated using the following equation:

$$\text{Bulk Density} = \frac{(\text{Weight of dry soil and core -Core weight })}{\text{Soil core volume (100 cm3)}}$$

Equation 3.1: Calculation of soil's bulk density

Hydraulic conductivity

The measurement of soil hydraulic conductivity will be conducted at Department of Agriculture, Ministry of Agriculture and Cooperative. Prior to the experiment, the soil core samples were immersed in water and left until they fully saturated, approx.1 week. Then soils covered with tube were set with each soil core, and filled distilled water through the top of the soil core, with 10 cm height of falling water in triplicate. For the soil with low hydraulic conductivity that taken more than 1 hour to lower 10 cm distilled water, the time was record only once, and for samples which water head barely change (less than 5 cm in 1 hour) the height changed was recorded only once after 1 hour passed. For the experimental condition used conducted at Department of Agriculture, hydraulic conductivity can be calculated by following equation:

$$K_{20} = 0.30122 \times \log\frac{h_1}{h_2} \times \left(\frac{\mu_t}{t}\right) \times 36{,}000$$

Equation 3.2: Calculation of hydraulic conductivity at 20°C

When h_1 and h_2 refer to initial and final height of water in the tube, μ_t is water viscosity, t is time taken for head falling. K_{20} is hydraulic conductivity at 20° C which can calculated to seepage velocity, or pore water velocity (V_s) by dividing hydraulic conductivity velocity soil's porosity.

PZC

Point of Zero Charge (PZC) of soil were adapted from 5 grams of soil, which were mixed with the NaCl 0.01 M solution with initial pH of 1-12, adjusted by 0.1 M NaOH and 0.1 M HCl, in the 40-ml vial. After agitated for 1 hour, final pH was measured, created graph of initial pH and final pH, the point which initial pH equal to final pH is the PZC.

Soil pH

Soil pH was determined followed by Land Development Department (2010). Twenty grams of soil was added into 20 ml of distilled water (1:1 w/w) in the 60 ml PE bottle, stir regularly for 30 minutes and left for 30 minutes until soil is settled. Determine pH of the water above the soil by pH meter and pH value was recorded.

Soil EC

According to Land Development Department (2010), EC was determined using soil and water ratio of 1:5. Four grams of soil was mixed with 20 ml distilled water in 30 ml PE bottle, shaken or stirred 4-5 times in 30 minutes. After leaving samples settled for 30 minutes, EC was measured by EC probe and then EC value was recorded.

Other properties

The analytical method of soil properties are shown in table 3.2

Table 3.2: Soil properties and analytical method

Parameter	Method/ Instrument	Reference/ Place
Soil texture	Pipette Analysis	Land Development Department (2000)
CEC (Cation Exchange Capacity)	Ammonium acetate pH 7.0 method	Land Development Department (2000)
Soil Organic Matter	Walkley an Black Method	Land Development Department (2000)
Soil Mineral Composition	XRD	Department of Geology, Chulalongkorn University
Soil Chemical Composition	XRF	Department of Geology, Chulalongkorn University

3.3 Batch Experiments

Batch experiment was used in order to investigate adsorption isotherms and desorption of cadmium of highly contaminated soils affected by ionic strength. The application is explained in following diagram.

Adsorption Experiment
Each 20 ml of solute with Cd concentration of 0, 2.5, 5, 7.5, 10, 15, and 20 ppm, and varied IS (1, 10, and 100 mM $CaCl_2$), are mixed with 1.0 g of soil sample in polyethylene bottle

↓

pH of mixtures is kept constant at 7.0±0.2 using Nitric acid, and shake 200 rpm for 24 hours

↓

Supernatants are filtrate through Whatman #42 filter paper
and solutions are analyzed for Cd by ICP-OES

↓

Desorption Experiment
Soil left from previous adsorption experiment were re-suspended in
20 ml solution with same IS as the adsorption experiment
(1, 10, and 100 mM $CaCl_2$),

↓

pH of mixtures is kept constant at 7.0±0.2 using Nitric acid,
and shake 200 rpm for 24 hours

↓

Supernatants are filtrate through Whatman #42 filter paper
and solutions are analyzed for Cd by ICP-OES

3.4 Column experiments

Prior to column experiment, the selected soil is oven dried at 60°C, grinded and sieved through 2 mm sieve. Column used is Acrylic column with diameter 2.5 mm and 8 cm length. Soil packing in column was packed using “wet packing technique”. Piston pump is used to control influent flow at desire pore water velocity. Effluent will be collected by fractional collector (Figure3.1). There were two part of column experiments;

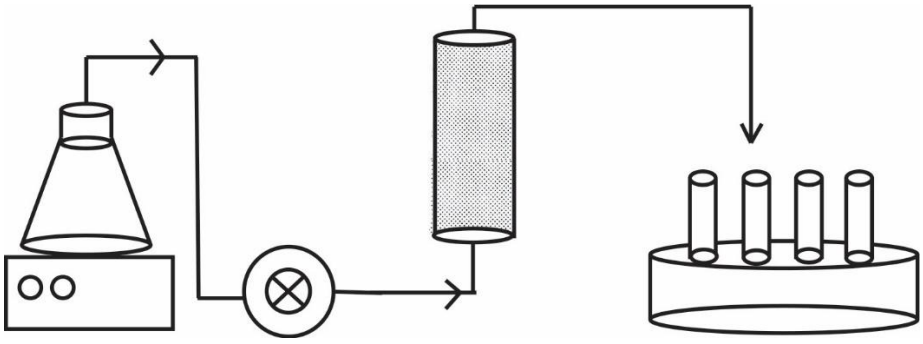

Figure 3.1: Schematic figure of saturated soil column

3.4.1 Tracer Test

Two columns of different pore water velocity (2 and 9 cm/hr) of wet packed soil, prepared as mentioned, are used for tracer experiment. After flushing with DI water for 2-3 pore volume, 10 mg/L of Bromide (Br^-) was used as an influent tracer and injected at the bottom end of the column. The effluent was collected at the top and determined by Ion Chromatography (IC). Breakthrough curves (BTCs) will be plotted between pore volume (V/V_0) and Br concentration (C/C_0).

3.4.2 Cadmium transport experiment

Six columns were done in this experiment under different in pore water velocity (2 and 9 cm/hr), and in ionic strength (1, 10, and 100 mM using $CaCl_2$). A concentration of influent is 10 mg/l Cd using $CdCl_2$ and pH will be adjusted to 7±0.2. The effluents will be collected until the Cd concentration were kept constant enough to create breakthrough curve, then flush the background solution until there are no Cd in the outflow (C/C_0<0.1). The flow interruption was done before the end of the experiment by stop flushing background solution for ~4 PV, then continue the flow for 5-10 PV and end the process. Effluents will be analyzed by Atomic Absorption Spectrophotometer (AAS). Breakthrough curves (BTCs) were plotted between pore volume (V/V_0) and cadmium concentration (C/C_0).

3.5 Data Analysis and Interpretation

3.5.1 Data Analysis for batch sorption experiments: Sorption isotherm

Sorption isotherms is a relationship between the concentration of the compound adsorbed on solid particles (Q), and concentration of compound remaining in the solute (C). Explain by function below (Limousin et al., 2007);

$$Q=f(C)$$

Equation 3.3: General function of sorption isotherm

Commonly, sorption isotherm can be used to explain factor controlling mobility and retention of substances on porous media (Foo and Hameed, 2010 cited Limousin et.al, 2007, and Allen et.al, 2004)

a) Langmuir sorption isotherm

Sorption model explained homogeneous adsorption, and no interaction between adsorbate on the surface site (Langmuir, 1916). Explain by equation 3.4;

$$Q_e = \frac{K_L C_e}{1+\eta C_e}$$

Equation 3.4a: Nonlinear form of Langmuir adsorption isotherm.

$$\frac{C_e}{Q_e} = \frac{1}{K_L} + \frac{\eta}{K_L} C_e$$

Equation 3.4b: Linear form of Langmuir adsorption isotherm.

When Q_e refer to amount of substance adsorbed on the media (mg/g); C_e refers to concentration of substance at equilibrium; K_L is Langmuir constant (l/g); b refers to Langmuir constant related to energy sorption (l/mg). Q_m refers to maximum sorption capacity (mg/g) (equal to K_L/m).

b) Freundlich sorption isotherm

Sorption model describing non-ideal adsorption, Freundlich model can be applied for multilayer adsorption, and heterogeneous surface. Explain by equation 3.5;

$$Q_e = K_F C_e^{1/n}$$

Equation 3.5a: Nonlinear form of Freundlich adsorption isotherm.

$$\log Q_e = \log K_f + \frac{1}{n} \log C_e$$

Equation 3.5b: Linear form of Freundlich adsorption isotherm

When Q_e refer to amount of substance adsorbed on the media (mg/g); C_e refers to concentration of substance at equilibrium; n refer to Freunldlich equation exponent; and K_F refers to Freundlich constant.

c) Linear sorption isotherm

When Freundlich exponent (1/n) =1, the sorption become linear isotherm. Explain by equation 3.6

$$Q_e = K_d C_e$$

Equation 3.6: Linear adsorption isotherm

When Q_e refer to amount of substance adsorbed on the media (mg/g); C_e refers to concentration of substance at equilibrium; and K_d refers to Linear constant.

3.5.2 Data Analysis for column experiment

a) CXTFIT

For tracer experiment, the CXTFIT program is commonly used to estimate the transport parameter for 1-dimensional solute transport with steady flow (Toride et al., 1999). There were two model used in this study

a.1) Equilibrium Transport: Convection-Dispersion Equation (CDE)

In general, the solute transport with steady state flow in homogeneous soil is express as

$$R\frac{\partial c}{\partial t} = D\frac{\partial^2 c}{\partial z^2} - v\frac{\partial c}{\partial z} - \mu c + \gamma(z)$$

Equation 3.7a: Convection-Dispersion Equation

When c is resident concentration; D is the dispersion coefficient (L^2T^{-1}); z is distance (L); t is time (T). R is retardation factor; μ is first-order decay coefficient; γ is zero-order production term.

The equation can be derived in to dimensionless form as

$$R\frac{\partial C_r}{\partial T} = \frac{1}{P}\frac{\partial^2 C_r}{\partial Z^2} - \frac{\partial C_r}{\partial Z} - \mu^E C_r + \gamma^E(Z)$$

Equation 3.7b: Dimensionless form of Convection-Dispersion Equation

Note that for conservative tracer such as Br^- used in this study, retardation factor (R) is 1, and the degradation and production can be neglected, as equation follow.

$$\frac{\partial C_r}{\partial T} = \frac{1}{P}\frac{\partial^2 C_r}{\partial Z^2} - \frac{\partial C_r}{\partial Z}$$

Equation 3.7c: Reduced form of Convection-Dispersion Equation for non-reactive solute

When C_r is reduced volume average concentration (c/c_0); T is dimensionless time ($\frac{vt}{L}$); Z is dimensionless distance ($\frac{z}{L}$) ; P is peclet number ($\frac{vL}{D}$); μ^E is first-order decay coefficient; γ^E is zero-order production coefficient; L is column length (L); v is velocity (L/T); and C_0 is characteristic concentration.

a.2) Physical non equilibrium transport: Two Region Model (T-R model)

Assuming that there are two solute phases, mobile phase that solute is flowing and immobile phase which solute is inactive. The dimensionless equation can be express as;

$$\beta R\frac{\partial C_m}{\partial T} = \frac{1}{P}\frac{\partial^2 C_m}{\partial Z^2} - \frac{\partial C_m}{\partial Z} - \omega(C_m - C_{im}) - \mu_m C_m + \gamma_m(Z)$$

$$(1-\beta)R\frac{\partial C_{im}}{\partial T} = \omega(C_m - C_{im}) - \mu_{im} C + \gamma_{im}(z)$$

Equation 3.8a and 3.8b: Dimensionless form of two region model

Also, note that for non-reactive solute, R=1 and neglect the degradation, the equation can be derived as;

$$\beta\frac{\partial C_m}{\partial t} = \frac{1}{P}\frac{\partial^2 C_m}{\partial z^2} - \frac{\partial C_m}{\partial z} - \omega(C_m - C_{im})$$

$$(1-\beta)\frac{\partial c_2}{\partial t} = \omega(C_1 - C_2)$$

Equation 3.9a and 3.9b: Reduced form of Two Region model for non-reactive solute

When C_1 is average concentration of mobile phase (c_m/c_0), C_1 is average concentration of immobile phase (c_{im}/c_0), subscribed m and im refer to mobile site and immobile site respectively. β is partitioning coefficient of the mobile site; and ω is dimensionless mass transfer coefficient. P in this model calculated from mobile phase ($\frac{v_m L}{D_m}$).

b) HYDRUS-1D

HYDRUS-1D is computer software; it is commonly used for 1 dimensional simulation of water, heat, and solute transport in saturated media (Šimůnek and Genuchten, 2008). For this report, Hydrus 1D is used to stimulate Cd transport using data obtained from column experiment.

Equilibrium Transport: Advection dispersion equation

Advection-Dispersion equation is used for describing uniform transport of solutes. Assumed that solute is adsorbed instantaneously on the porous media. Explain by equation 3.5.5

$$\frac{\partial \theta c}{\partial t} + \rho \frac{\partial s}{\partial t} = \frac{\partial}{\partial z}\left(\theta D \frac{\partial c}{\partial z}\right) - \frac{\partial qc}{\partial z} - \phi$$

Equation 3.10: advection dispersion equation

When c is effluent concentration (mg/l); θ is volumetric water content (dm^3/dm^3); s is sorbed concentration (mg/kg); t is time (d); ρ is soil bulk density (kg/l); D is dispersion coefficient (dm^2/d); z is distance (dm); q is a volumetric water flux density (dm/d) evaluated by Darcy–Buckingham law; ϕ is a sink-source term ($mg/(dm^3 \cdot d)$)

Chemical non-Equilibrium Transport: Two Site Model (TSM)

Two Site Model can describe chemical non-equilibrium transport of solutes. Assume that there are two types of solutes; first type is instantaneously adsorbed on to surface sites, and second part is kinetically adsorbed (adsorption changes by time).

$$\frac{\partial \theta c}{\partial t}+\rho \frac{\partial s^{e}}{\partial t}+\rho \frac{\partial s^{k}}{\partial t}=\frac{\partial}{\partial z}\left(\theta D \frac{\partial c}{\partial z}\right)-\frac{\partial qc}{\partial z}-\phi$$

Equation 3.11a: Solute transport in the system

$$s^{e}= f_{e}K_{d}c$$

Equation 3.11b: Sorbed concentration on the equilibrium sorption sites

$$s_{e}^{k}=(1-f_{e})K_{d}c$$

Equation 3.11c: Sorbed concentration on the kinetic sorption sites

$$\rho \frac{\partial s^{k}}{\partial t}=\alpha_{k}\rho\left(s_{e}^{k}-s^{k}\right)-\phi_{k}$$

Equation 3.11e: Mass balance of the kinetic sorption sites

When s^{e} is adsorbed solute concentration on type-1 sites (equilibrium sites), assumed to be instantaneous (mg/kg); s^{k} is adsorbed solute concentration on type-2 sites (kinetic sites), assumed to be 1st order kinetic rate (mg/kg); s_{e}^{k} is sorbed concentration that would be reached at equilibrium with the liquid-phase concentration (mg/kg); f_{e} is fraction of exchange site at equilibrium (-); K_{d} is distribution coefficient (l/kg)α_{k} is first order rate constant (per day); $\phi_{k}$is a sink–source terms at the kinetic sorption sites (mg/(l·d))

Note that the models that considered to be fitted well with the data for this study is the model with $R^{2}>0.95$ and root mean square error (RMSE) <0.05 for Cd transport experiment or mean square error (MSE) <0.25 for bromide transport experiment. The calculation of each coefficient can be described as follows (Iowa State, 2004).

$$R^{2}=1-\frac{SS_{E}}{SS_{T}}=1-\frac{\sum (y_{i}-\hat{y}_{i})^{2}}{\sum\left(y_{i}-\bar{y}_{i}\right)^{2}} \quad MSE = \frac{1}{n}\sum_{i=1}^{n}\left(y_{i}-\hat{y}_{i}\right)^{2}$$

$$\mathrm{RMSE} = \sqrt{\mathrm{MSE}}$$

When SS_E stands for sum square error, SS_T stands for sum square total, n is number of data, y_i stands for observed data or experimental data $\hat{y}_i$ stands for predict data, and $\bar{y}_i$ stands for mean of the data.

CHAPTER4

RESULTS AND DISCUSSION

4.1 Soil Sampling and Soil Selection

Eighteen soils samples, both bulk soil samples and soil core samples, were collected from the agricultural area nearby Mae Tao creek and Mae Ku Creek, based on zoning map generated by National Research Center for Environmental and Hazadous Waste Management as submitted to Padaeng Industry Ltd.(2005) (Reported in Akkajit and Tongcumpou,2010; and Tongcumpou, 2014). The sampling sites is shown in Figure 4.1 Red dots refer to highly Cd contaminated soils (>30 mg/kg), yellow dots refer to intermediately contaminated soil (3-30 mg/kg), Green dots refer to low or not contaminated soil (<3 mg/kg).

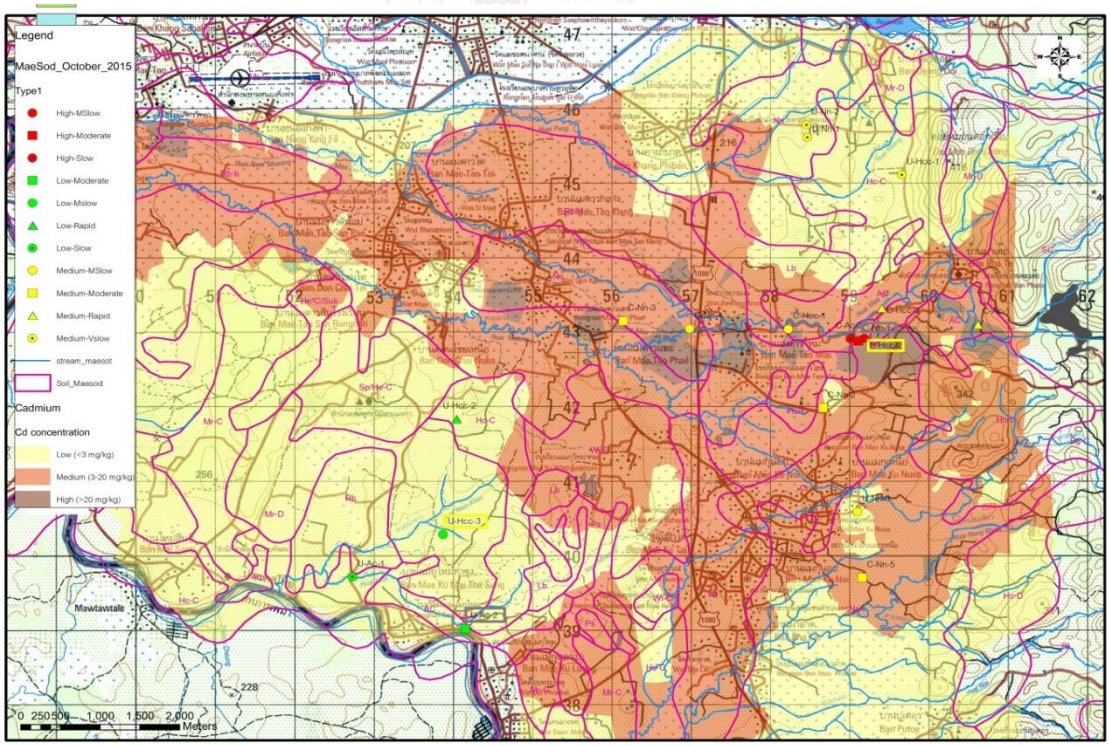

Figure 4.1: Soil sampling points around Mae Tao and Mae Ku creeks with 3 classes of Cd level in soils from low (green dots), medium (yellow dots), and high (red dots)

4.2 Soils and Selected soil properties

4.2.1 Properties of all soil samples collected

Prior to selecting one soil sample for further experiments, all collected soil samples were analyzed for 3 soil properties as follows: cadmium and zinc composition, bulk density and hydraulic conductivity. Summary of the results are shows in Table 4.1

Table 4.1: Summary of properties of the soil samples collected from agricultural areas nearby Mae Tao and Mae Ku creeks

Properties	Ranges
Cadmium	0.71-62.04 mg/kg
Zinc	<100-2342 mg/kg
Bulk Density	1.21-1.76 g/cm^3
Hydraulic conductivity (K)	0.001-7.766 cm/h

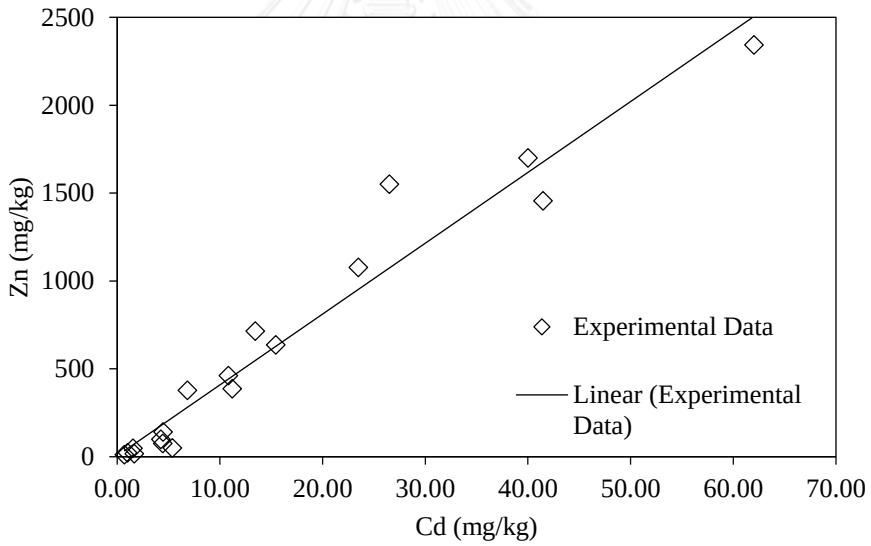

Figure 4.2: Relationship between Cd and Zn content in soils from Mae Tao and Mae Ku creeks

Cd content in the soils ranges from 0.71-62.04 mg/kg. Some of them were still considered to be contaminated by Cd according to European Union standard. Figure 4.2 shows the relationship between Cd and Zn content in soils (only 11 soil samples with Zn>100 mg/kg). Interestingly, Cd and Zn content in the soils were significantly correlated with $R^2 = 0.933$, the strong relationship between Cd and Zn also reported by

Simmons et al. (2005). From this study, the equation shows that Zn is approximately 37 times higher than Cd, and the background zinc level is approximately 115 mg/kg.

4.2.2 Physico-Chemical properties of the soil selected

The soil that appropriate for the batch and column experiments, should be the Cd-contaminated soils, which can potentially transport through groundwater. Thus, the selected soil should be intermediately or highly contaminated by Cd with a high hydraulic conductivity. The soil was selected according to above criteria was C-Ac-3 (See Appendix A).

The soil was collected from cut bank close to Mae Tao creek, located near agricultural field. The soil was intermediately contaminated with 26.5 mg/kg Cd and1550 mg/kg Zn, respectively. Hydraulic conductivity of soil ranged from 11.25 to38.40 cm/h which is relatively high among all soil samples. Bulk density was about 1.31 g/cm^3 After the soil was selected, physico-chemical properties of the soil were analyzed and reported as follows.

a. Particle Size

Particle size of selected soil was analyzed by Land Development Department (LDD) using the pipette method (Gee and Or, 2002). The soil composes of 64.5% sand, 23.2% silt, and 12.3% clay, classified as a sandy loam soil by USDA classification system.

b. Soil pH and electric conductivity

Soil pH was found approx. 7.8, considered as a slightly alkaline soil and soil electric conductivity is approx. 125.3 μS/cm.

c. Organic Matter

The soil organic matter analyzed by Land Development Department (LDD) was reported about 2.61%, identified as an intermediately high organic matter content (LDD, 2002).

d. Cation Exchange Capacity (CEC)

Cation exchange capacity of the soil is about 9.21 cmol/kg.

e. Point of Zero Charge (PZC)

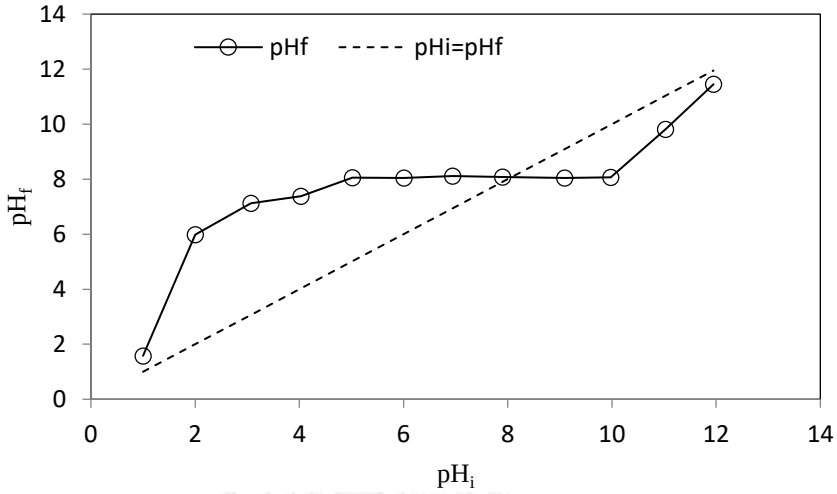

Figure 4.3: Point of zero charge of the selected soil

From Figure 4.3, PZC of the soil is about 8.0, which is a little bit higher than soil pH of 7.8, inferring that the soil has net positive charge (Naidu et al., 1994).

f. Mineral Composition

Minerals compositions of selected soil analyzed by XRD are shows in Figure 4.4. The soil composes of quartz, calcite, dolomite and clay mineral (Illite and Kaolinite). Quartz is found to have the highest peak among all minerals; on the other words, quartz is the major composition of the selected soil.

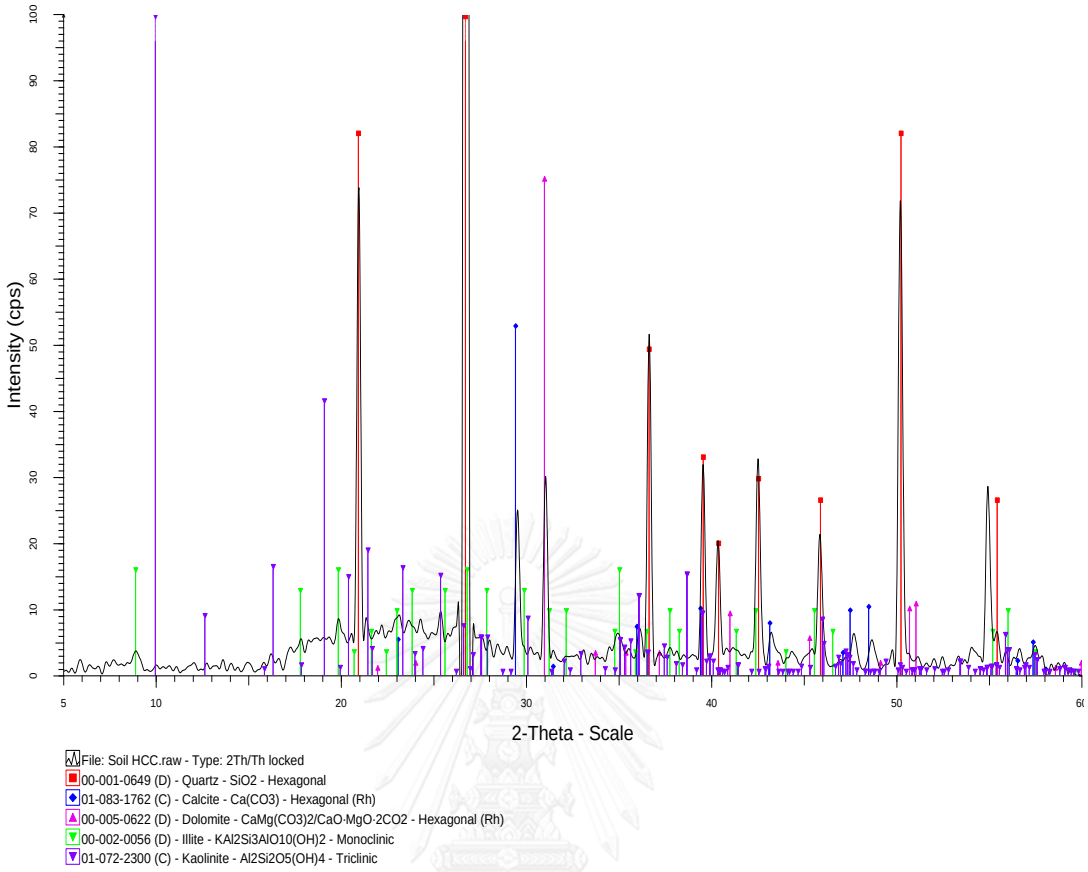

Figure 4.4: X-Ray diffraction pattern of the selected soil from Mae Tao area

g. Chemical Composition

The composition of selected soil was analyzed by XRF at the Scientific and Technological Research Equipment Centre, Chulalongkorn University. The chemical composition are shows in Table 4.2 as follows.

Table 4.2: Chemical composition of the selected soil

Constituents	Quantity (%)	Constituents	Quantity (%)
SiO_2	67.6%	MgO	0.840%
Al_2O_3	7.47%	TiO_2	0.353%
CaO	4.84%	ZnO	0.189%
Fe_2O_3	2.57%	Na_2O	0.120%
K_2O	1.19%	Loss on ignition	14.8%

4.3 Batch sorption and desorption experiments

4.3.1 Batch sorption experiments

Batch sorption experiments were done in order to observe the effect of IS on Cd sorption behavior on the contaminated soil, collected from Mae Tao creek area, under various IS at pH 7.0 (± 0.2).

The observed data shown in Figures 4.5a, 4.5b and 4.5c revealed that the increasing amount of initial Cd concentrations (from 0 to 20 ppm), resulted in increasing amount of Cd sorbed on the soil. Also, the increasing of IS results in decreasing of sorption capacity of Cd on the soil, which related to the study of , Naidu et al. (1994) and Wikiniyadhanee (2012). Because the higher IS, cation of the electrolyte (Ca, in this case) compete with Cd sorption on the soil, the adsorption of Cd decreases (Loganathan et al. 2010), and at high IS, Cd may form higher $CdCl^{+}$ complex fraction instead of Cd^{2+}. The lowest IS (1 mM) has highest adsorption coefficient for those three isotherm (k_d, k_l, k_f), follow by medium IS (10 mM), and the highest IS (100 mM) have lowest adsorption coefficient with one order of magnitude less than IS 1 and 10 mM (k_d, k_l, k_f) (see Table 4.3).

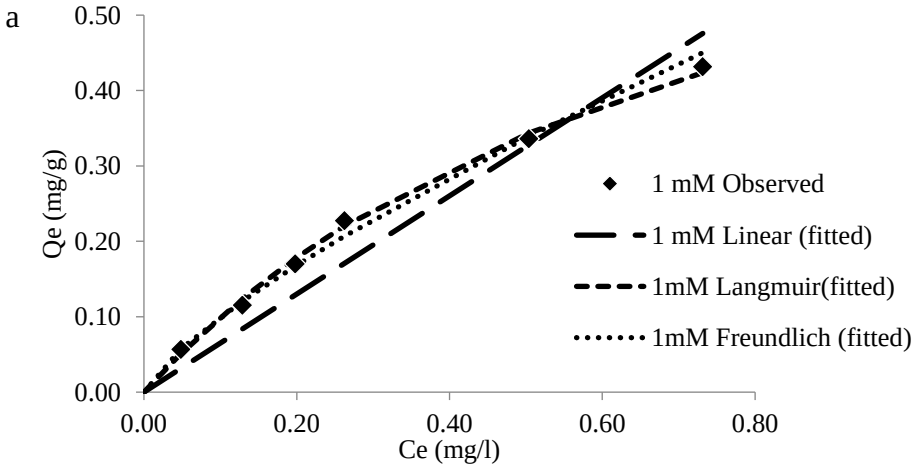

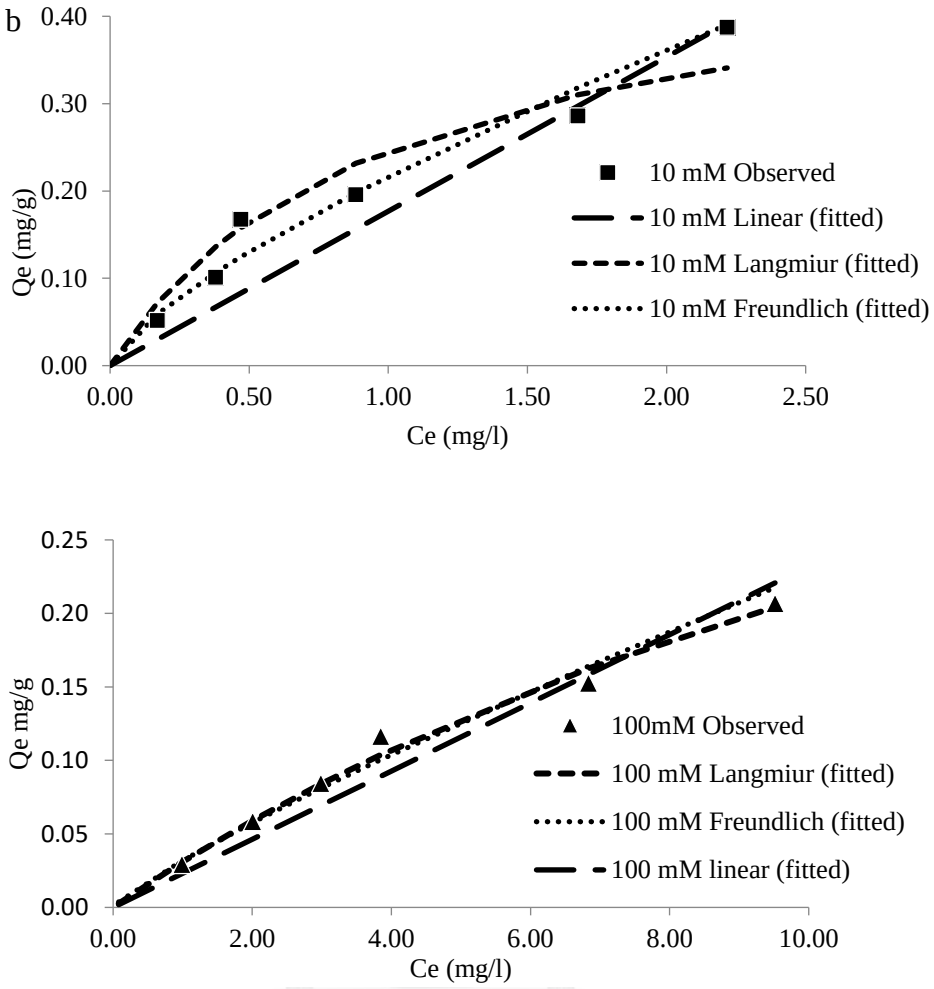

Figure 4.5: Observed and fitted data of Cd adsorption on the selected soil from Mae Tao area at IS 1 mM(a), 10 mM (b), and100 mM (c)

For the adsorption isotherm, after fitted the experimental result of the adsorption of Cd on the soil at IS 1, 10, and 100 mM with Linear, Langmuir, and Freundlich Isotherms, as shown in Figure 4.5a, 4.5b, and 4.5c for IS 1, 10 and 100 Mm, respectively. The results showed that at all IS conditions, Cd sorption is well explained by Freundlich Isotherm with R^2 0.995, 0.932 and 0.985 for IS 1, 10 and 100 mM, respectively (Table 4.3), indicating that Cd adsorbed on the selected soil by multilayer adsorption (Limousin et al., 2007). Therefore, the parameter for Freundlich isotherm will be mainly used to consider and discuss for the column experiment in the section 4.4, also the modelling of the Cd transport will explain by using Freundlich isotherm. Unless the Freundlich model doesn't well describe the Cd transport, the Langmuir model, will be applied.

Table 4.3: Parameters of Linear, Langmuir and Freundlich Isotherms for Cd on the selected soil form Mae Tao

IS mM	Linear Isotherm		Langmuir Isotherm				Freundlich Isotherm		
	K_d (l/g)	R^2	K_l (l/g)	η (l/mg)	Q_m (mg/g)	R^2	K_f (l/g)	1/n	R^2
1	0.6504	0.938	1.1217	1.2798	0.8765	0.955	0.5707	0.7584	0.995
10	0.1767	0.881	0.3409	0.4904	0.6952	0.844	0.2171	0.7363	0.932
100	0.0232	0.956	0.0327	0.0549	0.5957	0.846	0.0319	0.8523	0.985

4.3.2 Batch desorption experiments

Desorption of Cd on selected is significantly related to adsorbed amount of Cd from adsorption experiment. Increasing in adsorbed Cd in the adsorption experiment related to increasing of desorbed amount of Cd in the desorption experiment. This is shown in Figure 4.6, the R^2 for IS 1, 10 and 100 mM is 0.9259, 0.9689, and 0.9864, respectively. Moreover, desorped Cd amount is generally inversed with adsorbed Cd and desorption tends to increase with increasing IS. This is confirmed by the results in Table 4.4, that at lowest IS (1mM), soil has the highest Cd adsorption (96.72-98.32%) and the lowest desorption (1.65-2.90%), as well as at highest IS (100 mM), Cd has the lowest adsorption (52.36-59.74%), and highest desorption (36.11-43.90%).

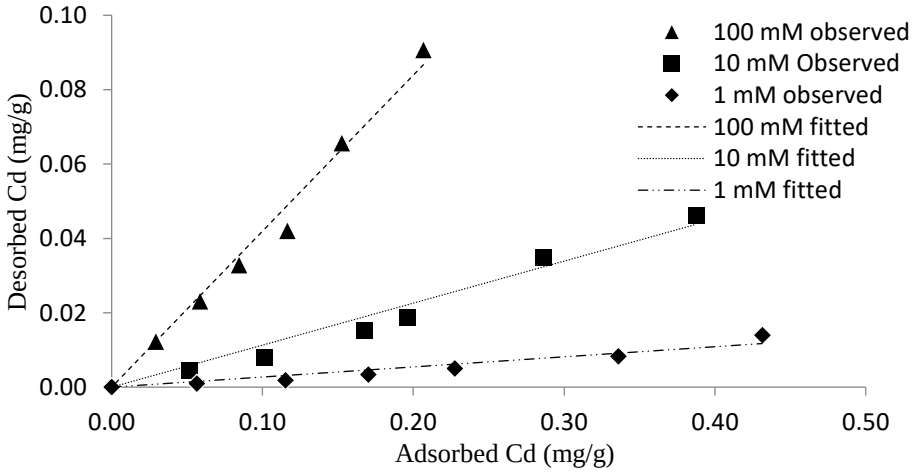

Figure 4.6: Desorbed Cd on the selected soil as compared to adsorbed Cd on the selected soil for IS 1, 10 and 100 mM at pH 7.0

Table 4.4: Percentage of Cd adsorption and desorption of the selected soil for IS 1, 10 and 100 mM at pH 7.0

Initial Concentration	Adsorption (%)			Desorption (%)		
	1 mM	10 mM	100 mM	1 mM	10 mM	100 mM
2.5	98.32	93.86	59.74	1.65	8.58	42.24
5	97.81	93.07	59.53	1.55	7.93	39.61
7.5	97.73	94.75	58.80	1.99	9.05	39.01
10	97.74	91.81	60.41	2.19	9.58	36.11
15	97.09	89.54	52.87	2.98	12.23	43.08
20	96.72	89.84	52.36	2.90	11.92	43.90

4.4 Column Experiments: Experimantal data and modelings

There were total 8 column experiments, which was packed by the wet-packing method. Pore water velocity was calculated from the average flow velocity after the experiment was completely set up. The properties of each column are shown in Table 4.5. The maximum Darcy's velocity of the soil was 3.84 cm/h, which can be calculated to pore water velocity of 9.14 cm/h (by divided by soil porosity). Thus, the high pore water velocity (K_s) in this research was approx. 9.0 cm/h, while low pore water velocity was approx. 2.0 cm/h.

Table 4.5: Properties of the packed soil columns in the column experiments

Column no.	Approx. K_s (cm/h)	Column length (cm)	Diameter (cm)	ρ (g/cm^3)	θ	Flow Rate (cm^3/h)	IS (mM)	pH
Tracer								
1	2.0	8.0	2.5	1.34	0.471	5.08	-	-
2	9.0	8.0	2.5	1.26	0.420	21.78	-	-
Cd (Lowflow)								
3	2.0	8.0	2.5	1.31	0.458	4.58	100	7.0±0.2
4	2.0	8.0	2.5	1.30	0.446	4.88	10	7.0±0.2
5	2.0	8.0	2.5	1.30	0.484	4.43	1	7.0±0.2
Cd (High flow)								
6	9.0	8.0	2.5	1.26	0.420	18.96	100	7.0±0.2
7	9.0	8.0	2.5	1.29	0.458	17.40	10	7.0±0.2
8	9.0	8.0	2.5	1.30	0.484	17.90	1	7.0±0.2

4.4.1 Tracer Experiments

The observed data of tracer experiment (using ~10 ppm Br^- ion) for low PV and high PV is shown in Figures 4.7 and 4.8 respectively. Then, the experimental data from both columns were retrenched and fitted by CDE model and T-R model using CXTFIT, all parameter used and gained from models is shown in Table 4.6

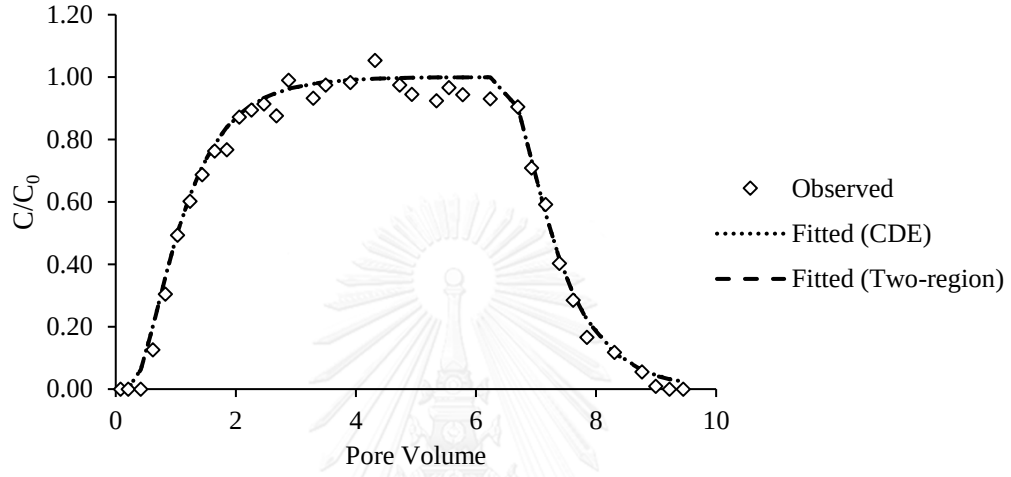

Figure 4.7: Observed data and fitted data by CDE and T-R models of bromide at low PV of Column no.1

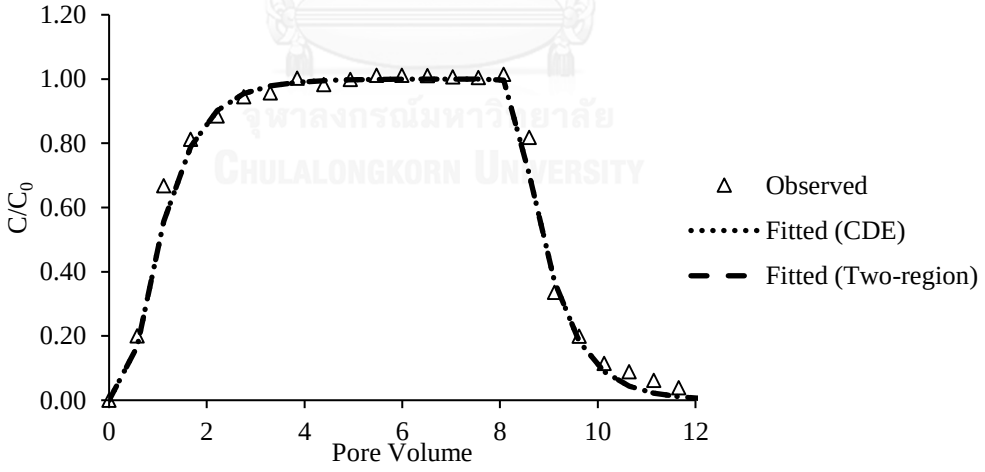

Figure 4.8: Observed data and fitted data of bromide by CDE and T-R models of bromide at high PV of Column no.2

Table 4.6: Estimated parameters from CXTFIT program for tracer experiments, fitted by CDE and T-R models

Column no.	V_s	CDE				T-R model					
		D	λ	P	R^2	D	λ	β	ω	P	R^2
	(cm/h)	cm^2/h	cm	(-)		cm^2/h	cm	(-)	(-)	(-)	
1	2.20	3.81	1.73	4.62	0.9890	3.76	1.71	1.000	100	4.68	0.9890
2	10.56	18.3	1.73	4.62	0.9904	18.3	1.73	0.999	0.517	4.62	0.9911

As shown in Figure 4.7, the results from the low PV column (Column no.1) can be fitted by both CDE and T-R models well with R^2 of 0.989. The breakthrough curve shape appeared to be symmetrical, indicating that equilibrium condition occurs in the column. Parameter D obtained from CDE and T-R models were very close (3.81 and 3.76 cm^2/h, respectively), The equilibrium partition in Two-region model (β) is 1.0, and ω is 100, confirming that the transport of the Br^- ions in the column is completely equilibrium (Toride et al. 1999), and can be well described by CDE model.

For the high velocity column (Column2), it was fitted by both CDE and T-R models well (R^2>0.99), as shown in Figure 4.8. The breakthrough curve appeared to be symmetrical. Parameter D gained from CDE and T-R models is equal (18.3 cm^2/hour). However, parameters estimated from T-R model showed the immobile (non-equilibrium) phase since β is 0.999 and ω is only 0.517. As mentioned, it may be concluded that Br^- (or water) appeared to be stagnant in a small portion of the soil column.

When comparing parameters estimated from Column nos. 1 and 2, increasing in pore water velocity results in greater dispersion coefficient because the dispersion coefficient (D) is the function of flow velocity ($D = \lambda v$) while dispersivity (λ) are equal in both velocities (~1.73 cm) since λ is dependent on travelling distance (or column length), water content, and soil texture (Padilla et al.,1999; Fashi et al., 2015), but independent on pore water velocity (Shukla et al., 2003).

For higher pore water velocity, β seemed to be decreased, which is agree with the study of Zhou (2016), suggesting that the higher pore water velocity makes the flow more restrict to preferential flow path. However, all column experiments were done by

pumping the effluent upward to prevent preferential flow path, so preferential flow would be a small part, which could be negligible. In addition, although only column no.2 can be explained by the non-equilibrium model, but it seemed to be for a very small stagnant part; thus, physical non-equilibrium parameters (β and ω) can be ignored in this study.

As mentioned above, even though there were some physical non-equilibrium showing in in the Cd column experiments, we assumed that the transport in all columns is described by the physical equilibrium. Since the tracer transport with low K_S could be well explained by CDE model, and the the tracer transport with high K_s showed only small non-equilibrium sites that can be neglected in T-R model, and still good fitted by CDE model. Therefore, parameter λ obtained from CDE model in both columns were used to predict Cd transport in the next section (section 4.4.2). Furthermore, Peclet number (Pe) ranges from 4.62-4.68, suggesting that the solute transport through these column is dominated by both diffusion and advection (Huysmans and Dassargues, 2004).

4.4.2 Cadmium transport experiments under various IS and pore water velocities

The effluent was periodically collected from each column and then analyzed for Cd by AAS. The breakthrough curves (BTCs) of Cd was gained by plotting between concentration (C/C0) and time in dimensionless form (C/C_0 v.s. PV). As there is a large number of data points for each column, some of the data points were eliminated and the latter were applied with HYDRUS-1D to access the transport parameters. The BTCs (Figures 4.8a-4.14a), fitted data from HYDRUS-1D (Figure 4.8b-4.14b) and the parameters obtained from the inverse solution of transport model (Table 4.7) are shown and discussed below. The colored line represents the best fitted model (with highest R^2 and lowest RMSE)

A. Observed and fitted Cd data of each soil column

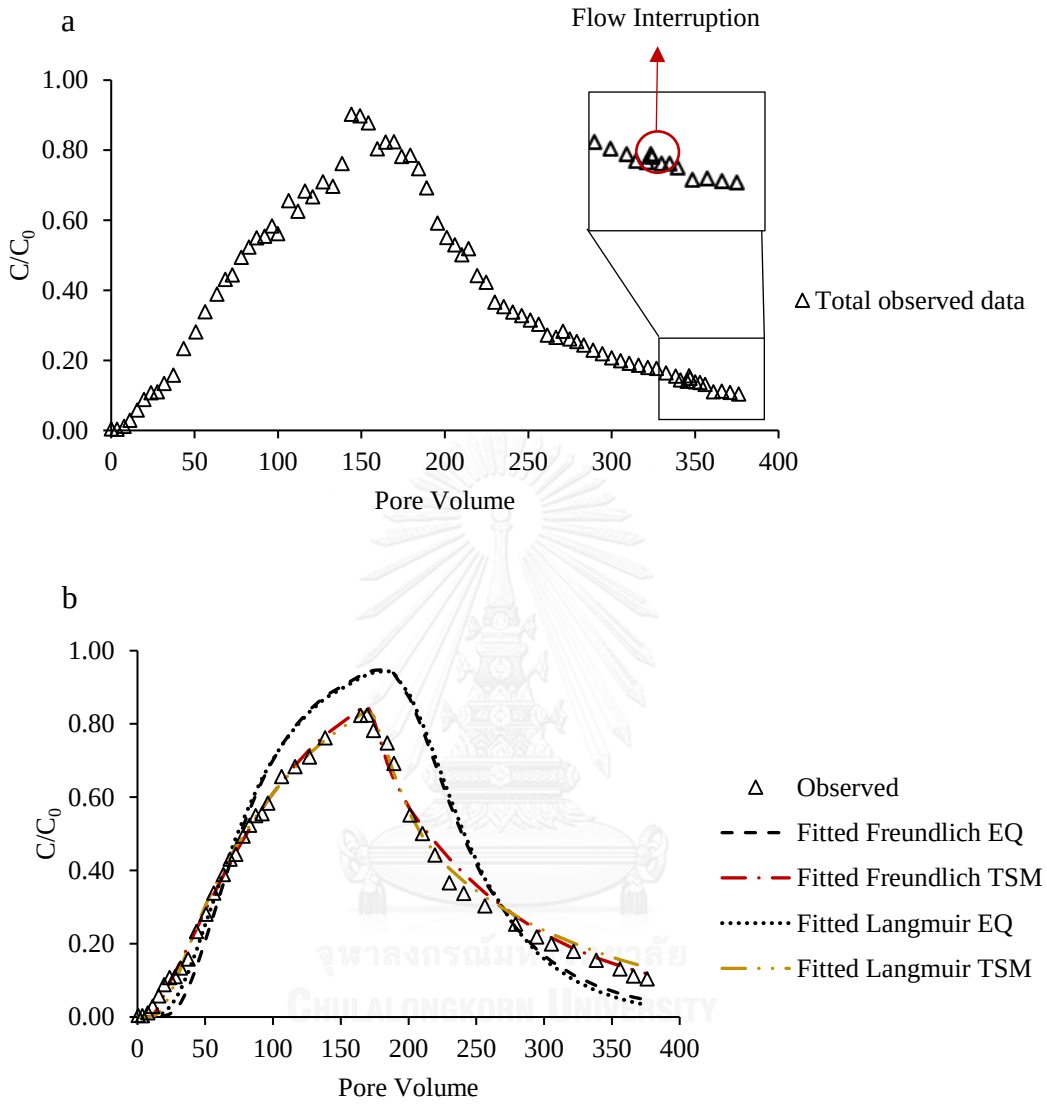

Figure 4.9: (a) Observed data of Column 3 and (b) fitted curves from different models of Column no.3 under low pore water velocity (2.0 cm/h) and high IS (100 mM)

For column no.3, the rising limb of BTC sharply increased and reached C/C_0=0.8 within approx. 160 PVs (~600 hours), but it took a longer time (200 PVs) to leach Cd out to reach C/C_0=0.1. The red circle showed the flow interruption result. Slightly increased Cd concentration in the effluent after the flow interruption and a nonsymmetrical shape of the BTC, were evidences to indicate the non-equilibrium condition occurring during Cd mobility.

The fitted EQ models (both Freundlich and Langmuir) took a longer time for Cd to start leaching from the column as compared to the observed data, reach the peak (at C/C_0=1) slower, while the desorption part was gone more quickly and have a short tailing. While both Freundlich and Langmiur TSM models can explain the observed data well with R^2 of 0.9917 for both models.

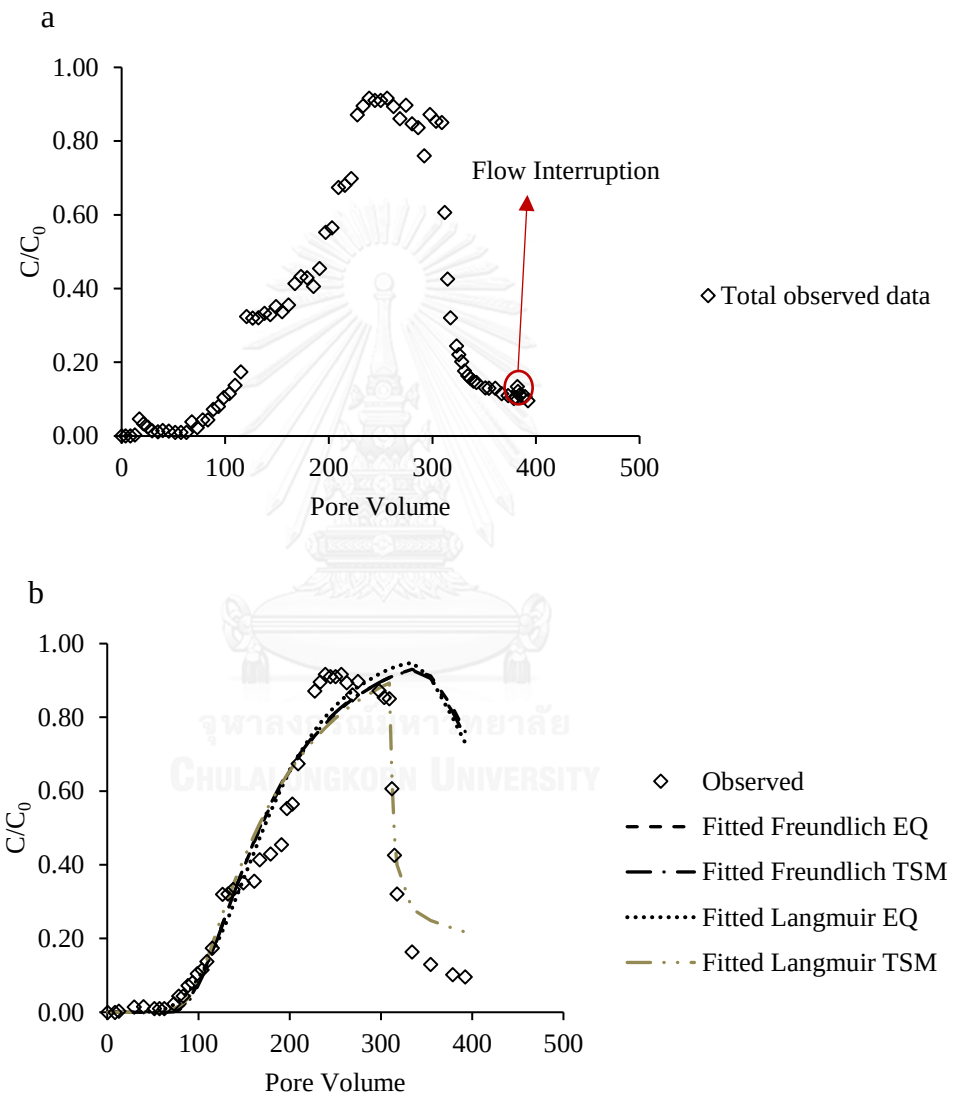

Figure 4.10: (a) Observed data and (b) fitted curves from different models of Column no.4 under low pore water velocity (2.0 cm/h) and medium IS (10 mM)

For Column no.4, the rising limb of BTC slightly increased to reach plateau (C/C_0~0.95) after 230 PVs, while the desorption part was drastically decreased with a short tailing from the plateau to C/C_0=0.1. This irregular BTC shape made it was hard

to fit with any equilibrium models and even with the Freundlich TSM model. Those models can only predict the front (increasing part) of BTC, but unable to fit with the desorption of the BTC at all. Only Langmuir TSM model can fit and explain observed Cd data migrating through column no. 4. In addition, the red circle in Figure 4.10a also shows non-equilibrium transport of Cd, which is agree with the well-fitted curve of the Langmuir TSM model.

For Column no.5, under low IS and low pore water velocity, the breakthrough time (at $C/C_0>0$) took a longest time (~300 PVs or 1300 hours). So, Cd was injected until C/C0 ~ 0.2 (~ 550 pore volume), then the background solution was injected in to the column to leach Cd sorbed out from the soil column. However, Cd concentration was slightly dropped a bit to $C/C_0=0.15$ and no further reduction observed within 200 PVs of the desorption part. The red circle in Figure 4.11a shows non-equilibrium transport of Cd.

The fluctuation of Cd concentration during PVs 300 to 450 is showed in Figure 4.4.5a; however, the fluctuation here doesn't go above C/Co=0.1. Thus, most of the sampling data here was discarded before modelling process.

The data were fitted well with both TSM models, but the trend of Langmuir TSM model was the most similar to the observed data with the highest R^2 of 0.9792. Neither of equilibrium models could explain the long tailing of this BTC.

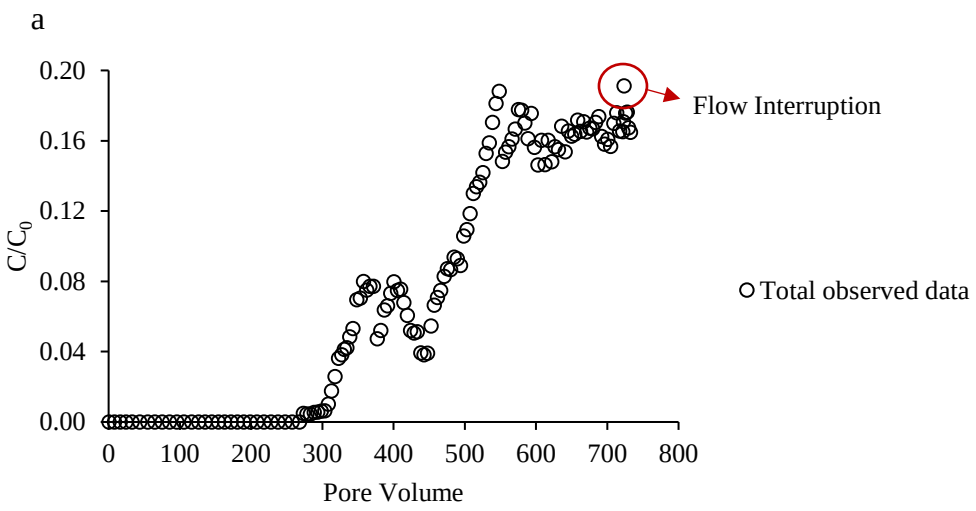

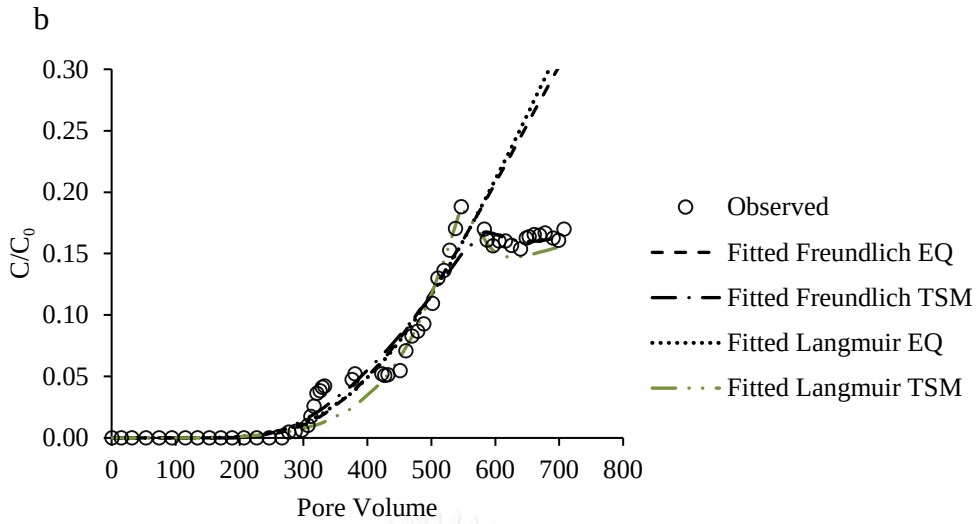

Figure 4.11: (a) Observed data and (b) Fitted curves from different models of Column no.5 under low pore water velocity (2.0 cm/h) and low IS (1 mM)

For Column no.6, the rising limb of BTC sharply increased and reached C/C_0=0.95 within approx. 100 PVs (~100 hours), which is the fastest among the others. The BTC showed tailing phenomenon on the declining limb, and red circle in Figure 4.12a shows a slightly increase of Cd after flow interruption; therefore the Cd transport under high flow (9.0 cm/h) and high IS (100 mM) was considered as a non-equilibrium transport.

Both Langmuir and Freundlich EQ models fitted the observed data with R^2>0.95, but still could not well fit the tailing of the BTC, as compared with the TSM models. The Freundlich TSM model was the best-fitted model for this column with R^2 of 0.9784), followed by the Langmuir TSM model (R^2=0.9760).

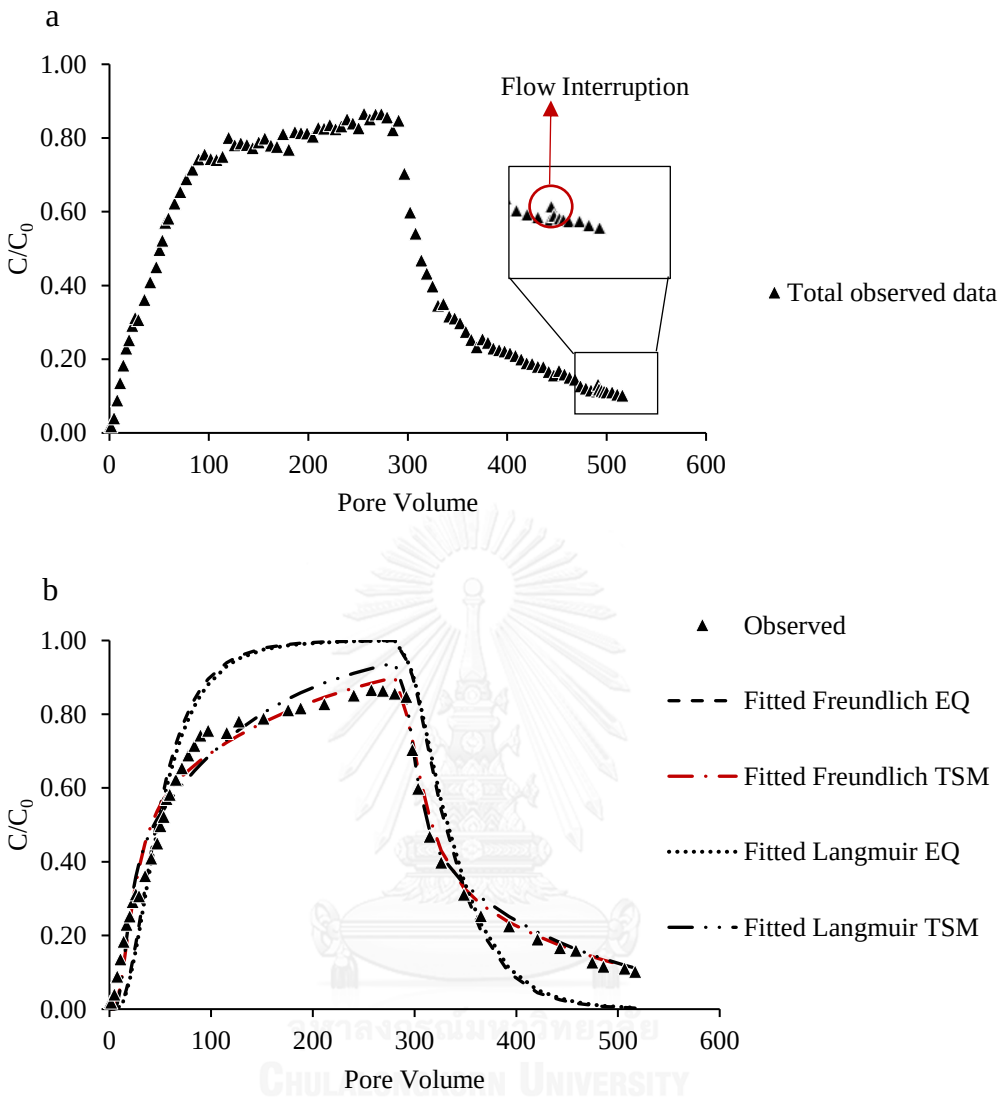

Figure 4.12: (a) Observed data and (b) Fitted curves from different models of Column no.6 under high pore water velocity (9.0 cm/h) and high IS (100 mM)

For column no.7, as the effluent flow dropped significantly after 250 PVs, the background solution was injected to leach Cd out of the soil column and needed to stop within 350 PVs without making complete BTCs and flow interruption.

As same as most of other columns, both equilibrium models can explain only the rising limb of the observed BTC, but unable to predict the decreasing limb (desorption part). Both TSM models still fitted well with the experimental data, but the Langmuir TSM showed slightly higher R^2 (0.9672) than Freundlich TSM model (0.9655).

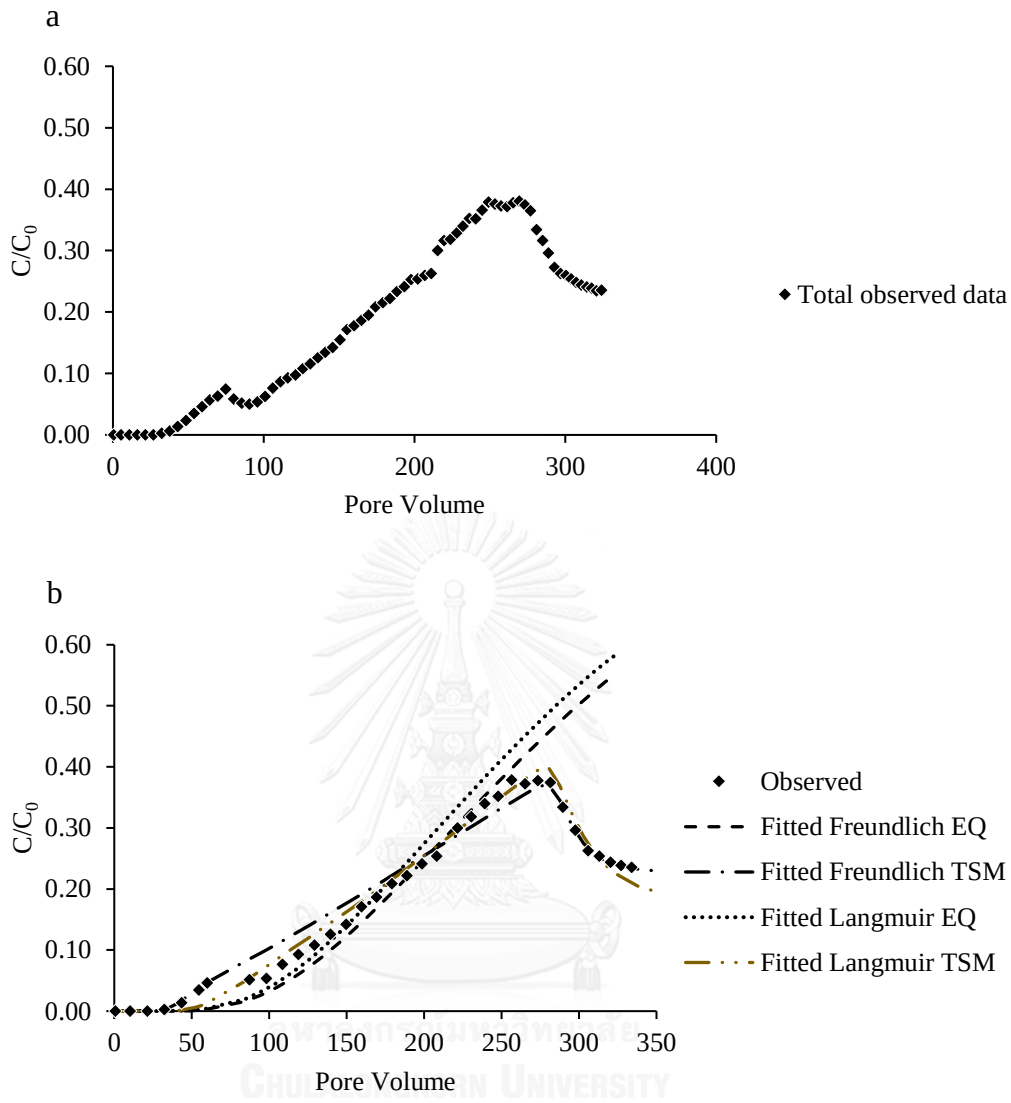

Figure 4.13: (a) Observed data and (b) Fitted curves from different models of Column no.7 under high pore water velocity (9.0 cm/h) and medium IS (10 mM)

The last column (Column no.8), Cd was injected to column approx. 500 PVs (~530 hours) to reach C/C_0 = 0.5, and was flushed Cd sorbed out by background solution until C/C_0~0.1. The trend of the decreasing limb shows tailing phenomenon. The flow interruption in Figure 4.14a (red circle) shows a bit increasing of Cd, indicating non-equilibrium transport of Cd in Column no.8.

Similarly, the only model that can well fit Cd transport was the Langmuir TSM model, while both EQ models, as same as other columns, cannot predict the Cd desorption limb. The Freundlich TSM model cannot fit observed data well both the

rising and decreasing limbs. As mentioned, the Langmuir TSM model is the best model, explaining Cd migration under high flow (9.0 cm/h) and low IS (1 mM).

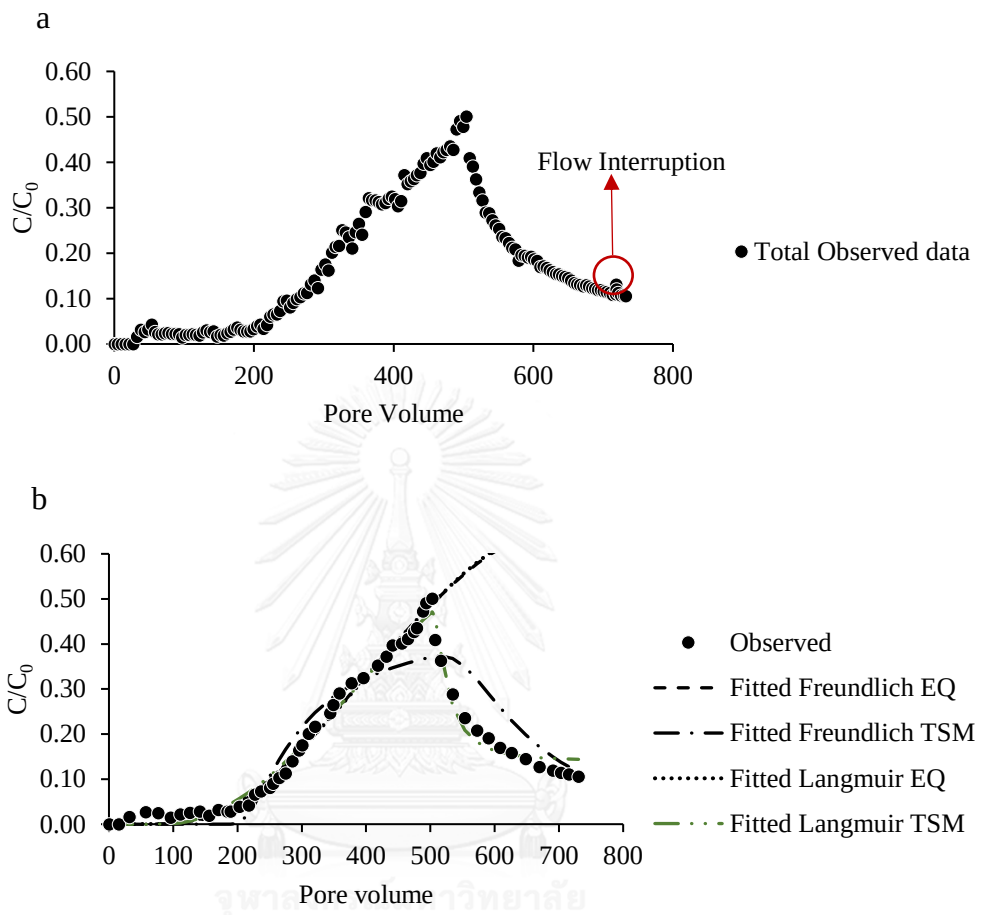

Figure 4.14: (a) Observed data and (b) Fitted curves from different models of Column no.8 under high pore water velocity (9.0 cm/h) and low IS (1 mM)

Table 4.7: Parameters of Cd transport through various IS and pore water velocities as fitted by the Langmuir TSM model

Column	IS (mM)	K_L (l/g)	η (l/mg)	Q_{max} (mg/g)	*f* (-)	α ($hour^{-1}$)	R^2	RMSE
Cd Low flow								
3	100	0.173	0.089	1.956	0.3762	0.0055	0.9917	0.0144
4	10	2.254	1.576	1.430	0.1611	0.0033	0.9506	0.0333
5	1	4.229	0.711	5.950	0.1593	0.0014	0.9792	0.0218
Cd High flow								
6	100	0.107	0.064	1.660	0.2298	0.0150	0.9760	0.0268
7	10	1.304	0.347	3.756	0.1572	0.0050	0.9672	0.0330
8	1	4.033	0.774	5.208	0.1437	0.0030	0.9822	0.0182

The conclusion regarding model results, based on R^2 and RMSE, the Langmuir two site model (TSM) is the appropriate model that can fitted observed BTCs from all columns with high R^2 (R^2>0.95) and low RMSE (<0.05), the fitted parameters gained from the Langmuir TSM model are represented in Table 4.7 and discussed in the next two consecutive sub-sections (B and C). Besides, other fitted parameters gained from EQ models and Freundlich TSM model are shown in Appendix E.

B. Effect of IS on Cd transport

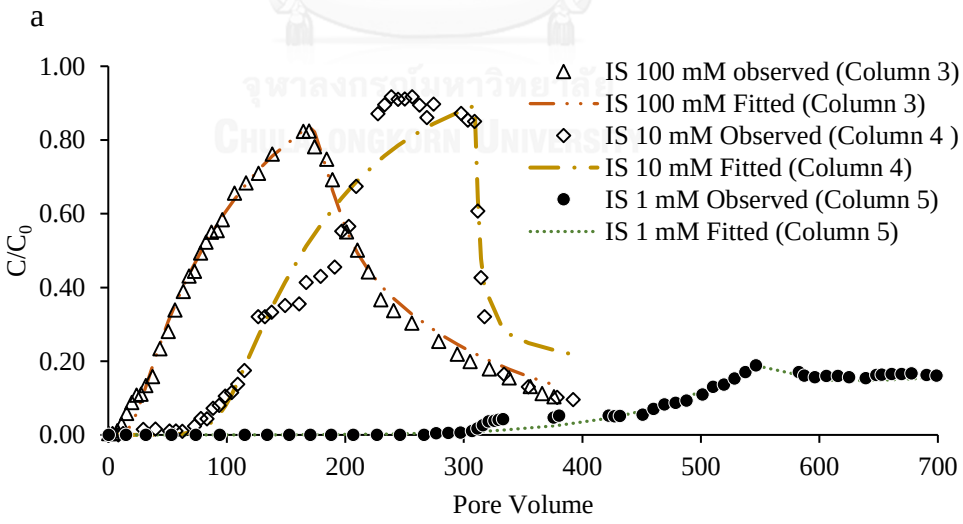

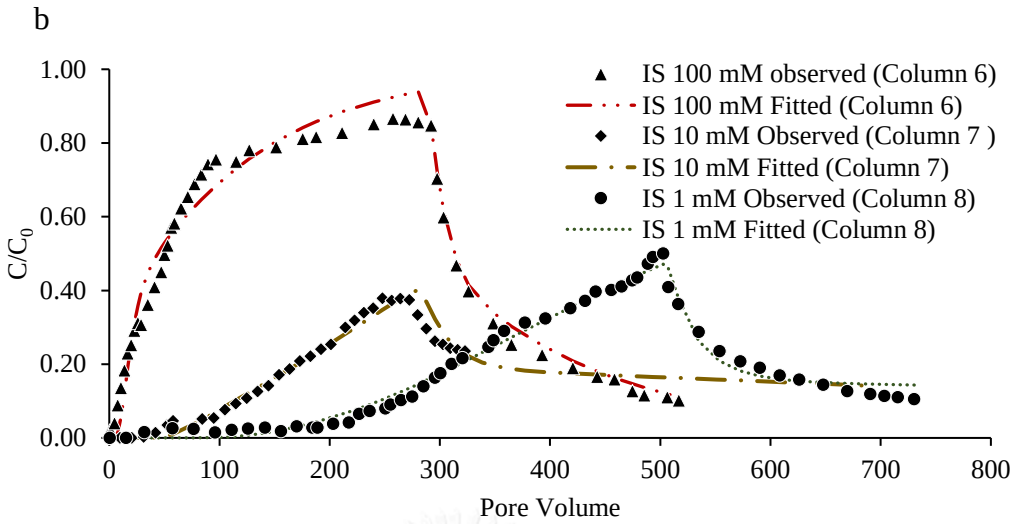

Figure 4.15: Effect of IS on Cd transport for (a) low pore water velocity columns and (b) high pore water velocity columns

IS exhibited similar effects on the Cd transport in both columns for low and high pore water velocity. Cd transport at the highest IS background (100 mM, in this case) tended to increase most sharply and reach plateau with the lowest PVs (Figure 4.15). On the other hand, the lowest IS column (1 mM) gradually increased and took a longest time to reach the same C/C_0 as compared to other higher IS columns (10 and 100 mM). Briefly, increasing IS significantly enhances Cd transport, this phenomenon can be reasonably explained by the competition between Ca^{2+} and Cd^{2+}, that decreases Cd^{2+} sorption onto the soil media (Wikiniyadhanee et al., 2015).

The parameters gained from the Langmuir TSM model would be described in details as follows. Increasing in IS resulted in decreasing of Langmuir coefficient (K_L), higher equilibrium fraction (f), and higher first order rate coefficient (α). Similarly, sorption coefficient (K_d, K_f) tended to be lower with increasing IS gained from Cd miscible displacement experiments as explained in Wikiniyadhanee et al. (2015), which was explained in their batch sorption experiments. Interestingly, K_L obtained from batch sorption experiment was about 3-4 times lower than those obtained from column experiments; anyhow, since the column transport experiment can be affected by other factors that don't presence in batch sorption experiments, such as flow rate, preferential flow path, transport distance, etc. Thus, K_L obtained from column experiments would be more reliable. Additionally, IS appeared to affect Cd sorption most between a range

of IS from 10 to 100 mM since the K_L for IS 100 mM was at least one order of magnitude lower than that of IS 10 mM, while K_L for IS 10 mM was not greater than 4 times of that for 1 mM. This effect is similar in both batch and column experiments. The higher equilibrium fraction (*f*) due to the higher IS can be explained by a similar phenomenon as Chotpantarat et al. (2012) found. For competitive sorption of metals transport, increasing of metals concentration (Pb^{2+}, Zn^{2+}, Mn^{2+}, and Ni^{2+}), with diffusion process is dominate *f* increases because of the ion competition for the instantaneous sorption sites; as a results, sorption mechanism becomes more equilibrium. In this research, similarly, higher IS (Ca^{2+}) caused the instantaneous sorption of the Cd^{2+} more than the lower IS; therefore, the fraction (*f*) of larger IS is higher than those of lower IS. Furthermore, the Peclet number for the low flow column and the high flow column were 6.45 and 3.98, respectively. Thus, the diffusion process should be dominated as same as Chotpantrarat et al. (2012) found. The first order rate coefficient (α) also increased with increasing IS, there were evidences of increasing in α with increasing secondary metals on sorption of Pb (Chotpantarat et al., 2012) and Cd (Serrano et al., 2005) . So, we can conclude that presence of other cations (higher IS) can affect the rate limiting stage of Cd^{2+} onto this contaminated soil as well. Since, at the high IS, Ca^{2+} competes with Cd, therefore, Q_{max} of Cd for the highest IS (1.956 and 1.660 mg/g for low and high flow columns, respectively) sorbed on the sorption site was lower than those for the lowest IS (5.950 and 5.208 mg/g for low and high flow, respectively).

C. Effect of flow velocity on Cd transport

The pore water velocity also effects Cd transport for both high and low IS columns (Figures 4.16a and 4.16b). The high pore water velocity (9 cm/h) resulted in the steeper curves both rising and declining BTCs. Moreover, for the medium IS (10 mM) columns, the initial breakthrough time ($C/C_0>0$) of Cd for high pore water velocity came faster than the that of the low pore water velocity, but the slope of the rising limb was more gradual since effluent flow appeared to be not constant and dropped significantly after 250 PVs (Figure 4.16b). Therefore, we should consider the effect of pore water velocity only for the high and low IS columns.

The parameters obtained from the Langmuir TSM model (Table 4.7) showed that pore water has an inverse relationship with K_L, and f, and positively relates with α for each same IS columns. Also, with higher retention time in the low pore water velocity, Cd are more accessible to diffuse to the sorption site thus caused. f increases, as reported in the studies of Kookana et al., (1993) and Tsang and Lo (2006). The explanation was that diffusion process is dominant in such system, suggesting that sorption was responsible for the rate-limited process; hence, the increasing velocity can enhance α (Tsang and Lo, 2006). The maximum sorption capacity, Q_{max}, appeared to be decreased as increasing the pore water velocity because Cd has a lower contact time for sorption, which is in lined with the results of lower equilibrium sorption sites (f), decreasing from 0.1593 to 0.1437 and 0.3762 to 0.2298 for 1 mM and 100 mM, respectively.

In brief, the pore water velocity causes lower adsorption sites because under the higher velocity the sorption process appeared to be more non-equilibrium condition, due to less contact time for Cd interacting with the soil.

C. Effect of flow velocity on Cd transport

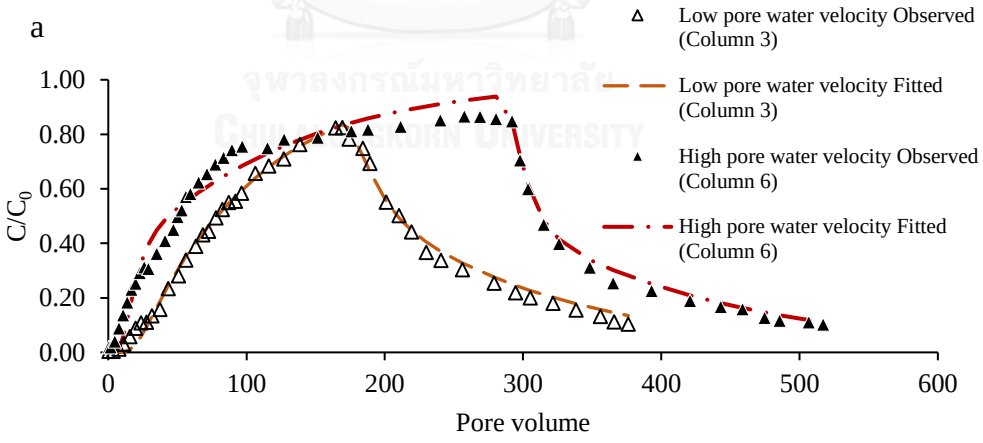

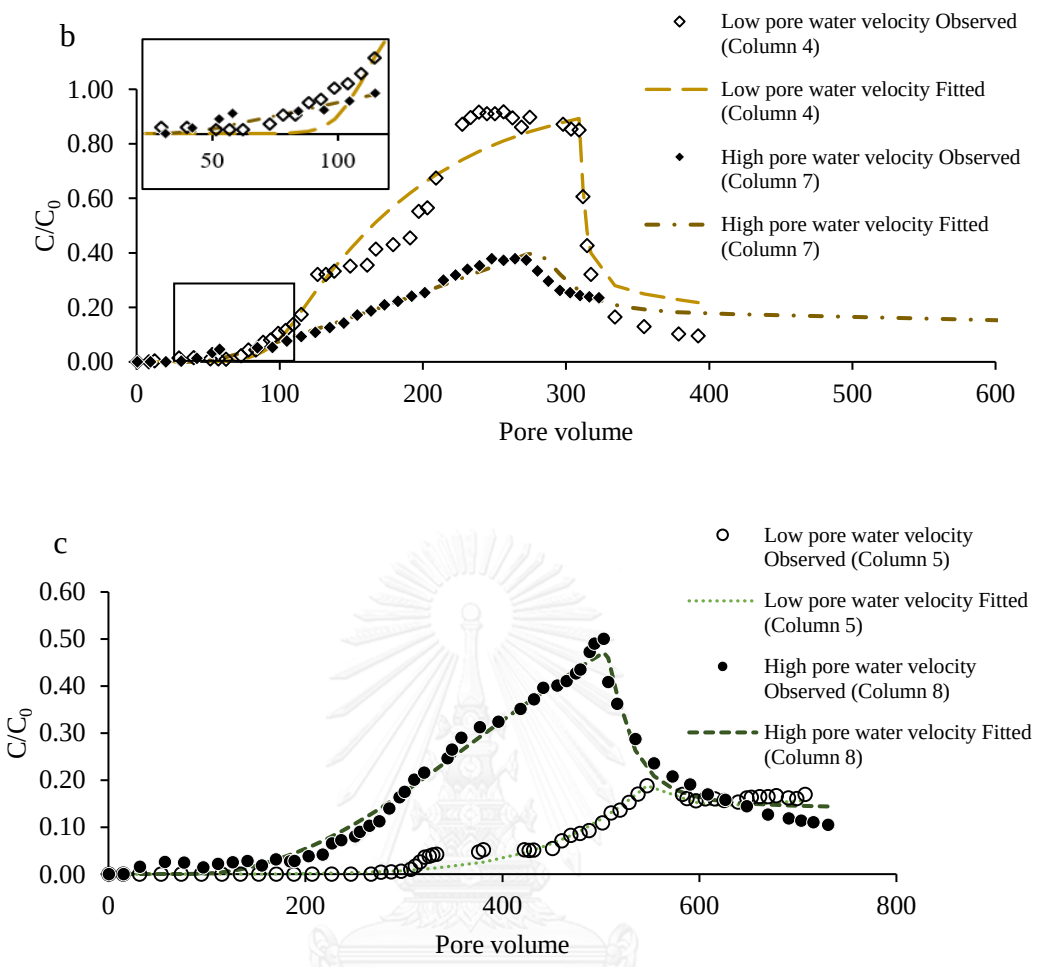

Figure 4.16: Effect of pore water velocity on Cd transport for IS 100 mM (a), 10 mM (b) and 1 mM (c)

CHAPTER 5

CONCLUSIONS AND RECOMMENDATIONS

5.1 Conclusion

The study of Cd sorption-desorption and transport on the soil collected from area near Mae Tao, creek, Mae Sot District, Tak Province, could be summarized as follows.

5.1.1 Properties of Soils and selected Soil from Mae Sot

There is some part of the Mae Sot still contaminated with Cd (0.71-62.04 mg/kg) according to European Union standard (>3 mg/kg). The selected soil is sandy loam, majorly compose with quartz, and some of calcite, dolomite, and clay mineral, and have intermediately high organic matter content. Cd content is 26.5 mg/kg. Soil pH (7.8) smaller than soil PZC (8.0), therefore the soil is considered to have net positive charge.

5.1.2 Batch sorption and desorption experiment

The batch adsorption experiment showed the decreasing of Cd adsorption with increasing Ionic Strength, agree with other researches (Naidu et al., 1994; Loganathan et al., 2011; Wikiniyadhanee, 2012). The adsorption isotherm of Cd is well fitted with Freundlich isotherm for all IS condition. Increasing in IS results in lower sorption coefficient (K_d, K_l, K_f), especially for IS 100 mM, all sorption coefficient is one order of magnitude lower than those of IS 10 mM.

For the desorption experiment, the higher IS leaded to higher desorption of Cd from the selected soil. The reasons for these results were, as the increasing IS, Ca^{2+}, competes with Cd^{2+} to adsorbed on the negative site of the soil; therefore, the sorption of Cd^{2+} decrease, and vice versa.

5.1.3 Effect of the pore water velocity on Tracer transport

From the bromide tracer experiments, for both the low pore water velocity (2.0 cm/h) and the high pore water velocity (9.0 cm/h), the BTCs seemed to be

symmetrical, and fitted both CDE and TR (using CXTFIT) models well. Dispersivity (D) increases with increasing velocity, while dispersivity (λ) is fairly constant. The column with low pore water velocity showed to be perfectly physical equilibrium with β=1.00 and ω=100. The column with high pore water velocity showed slightly physical nonequilibrium with β=0.99, but since the equilibrium partition is close to 1, and the results also fitted CDE model well; therefore, the transport is assumed to be physical equilibrium.

5.1.4 Effect of IS on Cd transport

The effect of IS on Cd transport apparently displayed in this research. For the comparable pore water velocity, BTCs of Cd for the higher IS tended to have steeper uptrend slope and hit the plateau faster. This results was agree with results of the batch sorption experiment, showing lower $K_{d,}$ K_l and K_f under higher IS. Equilibrium fraction site (f) and first order rate coefficient (α) also were greater with increasing IS because of ion competition where the diffusion process is dominant.

5.1.5 Effect of pore water velocity on Cd transport

Transport parameters i.e., K_l and f is inversely correlated with velocity, while α is positively correlated. This results may be related to the less contact time of Cd to the soil in higher pore water velocity so that Cd are more chemically non-equilibrium (lower f) and higher sorption rate due to the physical process (α). Hence Cd leaching under the higher pore water velocity is faster than that of the lower one.

5.2 Recommendations

1. The parameters obtained from this research can be applied to predict the Cd movement through the soil, and its potential to contaminate the groundwater supply in the study area.

2. There are more factors affecting Cd transport that should be concerned in further study in this area, for examples, pH, organic matter content, and soil types. In addition, co-transport of Cd with other metals such as Zn and Cu would be recommended.

3. As there are many soil types in the study area, in order to make the result become more realistic and practical, the adsorption parameters from various soils should be examined and stochastic modelling may be done considering real subsurface and soil distribution in the area.

4. The column experiments take very long time (2-12 weeks) and some of columns does not reach plateau because the soil has high efficiency to adsorb Cd; therefore, other technique (e.g. flow through cell), is implemented in further study

REFERENCES

Akkajit, P. and C. Tongcumpou (2010). Fractionation of metals in cadmium contaminated soil: and effect on bioavailable cadmium. Geoderma 156(3–4): 126-132.

Appelo, C.A.J. and Postma, D. (2004). Geochemistry Groundwater and Pollution, Second Edition. CRC Press : 124.

Aquion (2014). Activity & Ionic Strength. Retrieved 15 February 2016, from http://www.aqion.de/site/69.

Bajracharya, K., Y. T. Tran and D. A. Barry (1996). Cadmium adsorption at different pore water velocities. Geoderma 73(3–4): 197-216.

Brusseau, M. L., Q. Hu and R. Srivastava (1997). Using flow interruption to identify factors causing nonideal contaminant transport. Journal of Contaminant Hydrology 24(3): 205-219.

Brusseau, M. L., P. S. C. Rao, R. E. Jessup and J. M. Davidson (1989). Flow interruption: A method for investigating sorption nonequilibrium. Journal of Contaminant Hydrology 4(3): 223-240.

Christensen, T. H. and P. M. Haung (1999). Solid Phase Cadmium and the Reactions of Aqueous Cadmium with Soil Surfaces. Cadmium in Soils and Plants. M. J. McLaughlin and B. R. Singh. Dordrecht, Springer Netherlands: 65-96.

Chotpantarat, S., S. K. Ong, C. Sutthirat and K. Osathaphan (2011). Competitive sorption and transport of Pb2+, Ni2+, Mn2+, and Zn2+ in lateritic soil columns. Journal of Hazardous Materials 190(1–3): 391-396.

Diagboya, P. N., B. I. Olu-Owolabi and K. O. Adebowale (2015). Effects of time, soil organic matter, and iron oxides on the relative retention and redistribution of lead, cadmium, and copper on soils. Environmental Science and Pollution Research 22(13): 10331-10339.

Dişli, E. (2010). Batch and column experiments to support heavy metals (Cu, Zn and Mn) in alluvial sediments. Chinese Journal of Geochemistry 29(4): 365-374.

EPA (2013). "Ionic Strength." Retrieved 15 February, 2016, from http://www3.epa.gov/ caddis/ssr_ion_int.html.

Fashi, F.H. (2015). A review of solute transport modelling in soils and hydrodynamic dispersivity. International soil science congress conference. Sochi, Russia.(Conference Paper)

Huysmans, M. and A. Dassargues (2005). Review of the use of Péclet numbers to determine the relative importance of advection and diffusion in low permeability environments. Hydrogeology Journal 13(5): 895-904.

Iowa State (2004). Coefficient of Determination. Retrieved December 1, 2016, from http://www.public.iastate.edu/~alicia/stat328/Regression%20inference-part3.pdf

Järup, L. (2003). Hazards of heavy metal contamination. British Medical Bulletin 68(1): 167-182.

Järup, L. and A. Åkesson (2009). Current status of cadmium as an environmental health problem. Toxicology and Applied Pharmacology 238(3): 201-208.

Kanjanaprasert, N. 1986. Studies of diagnostic importance in soil development and potential of alfisol and inceptisol soil around Mae Klong basin. (Doctoral of science), Kasetsart University. Bangkok

Kookana, R.S., Schuller, R.D., Aylmore, L.A.G. (1993). Simulation of simazine transport through soil columns using time-dependent sorption data measured under flow conditions. Journal of Contaminant Hydrology. 14: 93–115.

Kosolsaksakul, P., J. G. Farmer, I. W. Oliver and M. C. Graham (2014). Geochemical associations and availability of cadmium (Cd) in a paddy field system, northwestern Thailand. Environmental Pollution 187: 153-161.

Land Development Department (2002). Land use of Thailand in 2002 [In thai]

Land Development Derartment (2010). Procedure Manual of Soil chemical Analysis process (In thai)

Langmuir, I. (1916). The Constitution and Fundamental Properties of Solids and Liquids. Part I. Solids. Journal of the American Chemical Society 38(11): 2221-2295.

Lewis, J. and J. Sjöstrom (2010). Optimizing the experimental design of soil columns in saturated and unsaturated transport experiments. Journal of Contaminant Hydrology 115(1–4): 1-13.

Limousin, G., et al. (2007). Sorption isotherms: A review on physical bases, modeling and measurement. Applied Geochemistry 22(2): 249-275.

Loganathan, P., S. Vigneswaran, J. Kandasamy and R. Naidu (2012). Cadmium Sorption and Desorption in Soils: A Review. Critical Reviews in Environmental Science and Technology 42(5): 489-533.

Maneewong, P. (2005). Cadmium distribution in stream sediment and suspended solid along Huai Mae Tao and Huai Mae Ku, Mae Sot district, Tak province, Chulalongkorn University. Master of Science.

McBride, M. B. (1989). Reactions Controlling Heavy Metal Solubility in Soils. Advances in Soil Science. B. A. Stewart. New York, NY, Springer New York: 1-56.

Naidu, R., N. S. Bolan, R. S. Kookana and K. G. Tiller (1994). Ionic-strength and pH effects on the sorption of cadmium and the surface charge of soils. European Journal of Soil Science 45(4): 419-429.

Nkedi-Kizza, P., P. S. C. Rao and A. G. Hornsby (1987). Influence of organic cosolvents on leaching of hydrophobic organic chemicals through soils. Environmental Science & Technology 21(11): 1107-1111.

Nordberg, G. F. (2009). Historical perspectives on cadmium toxicology. Toxicol Appl Pharmacol 238(3): 192-200.

O'Neal, A.M., 1952. A Key of Evaluating Soil Permeability by means of certain field clues. Soil Science Society of America Journal. 16: 321-315

Padilla, I. Y., T. C. J. Yeh and M. H. Conklin (1999). The effect of water content on solute transport in unsaturated porous media. Water Resources Research 35(11): 3303-3313.

Pang, L., M. Close, D. Schneider and G. Stanton (2002). Effect of pore-water velocity on chemical nonequilibrium transport of Cd, Zn, and Pb in alluvial gravel columns. Journal of Contaminant Hydrology 57(3–4): 241-258.

Plassard, F., T. Winiarski and M. Petit-Ramel (2000). Retention and distribution of three heavy metals in a carbonated soil: comparison between batch and unsaturated column studies. Journal of Contaminant Hydrology 42(2–4): 99-111.

Pollution Control Department. 2004, November. Soil Quality Standards for Habitat and Agriculture. Accessed 15 March 2014, from http://www.pcd.go.th/info_serv/en_reg_std_soil01.html

Pollution Control Department, 2010. Document of the observation project on distribution and source of cadmium contamination in Mae Tao basin, Mae Sot district, Tak province. Bangkok (In Thai)

Serrano, S., F. Garrido, C. G. Campbell and M. T. García-González (2005). Competitive sorption of cadmium and lead in acid soils of Central Spain. Geoderma 124(1–2): 91-104.

Shukla, M. K., T. R. Ellsworth, R. J. Hudson and D. R. Nielsen (2003). Effect of Water Flux on Solute Velocity and Dispersion. Soil Science Society of America Journal 67(2): 449-457.

Simmons, R. W., P. Pongsakul, D. Saiyasitpanich and S. Klinphoklap (2005). Elevated Levels of Cadmium and Zinc in Paddy Soils and Elevated Levels of Cadmium in Rice Grain Downstream of a Zinc Mineralized Area in Thailand: Implications for Public Health. Environmental Geochemistry and Health 27(5): 501-511.

Šimůnek, J. and M. T. v. Genuchten (2008). Modeling Nonequilibrium Flow and Transport Processes Using HYDRUS. Vadose Zone Journal 7(2).

Tongcumpou, C. (2014). Overview the Issue of Cd Contamination in Mae Sot, Tak province.

Traina, S. J. (1999). The Environmental Chemistry of Cadmium. Cadmium in Soils and Plants. M. J. McLaughlin and B. R. Singh. Dordrecht, Springer Netherlands: 11-37.

Tsang, D. and I. Lo (2006). Influence of Pore-Water Velocity on Transport Behavior of Cadmium: Equilibrium versus Nonequilibrium. Practice Periodical of Hazardous, Toxic, and Radioactive Waste Management 10(3): 162-170.

Watcharamai, T. and S. Saenton (2013). Leaching of Heavy Metals from Mae Tao Watershed's Agricultural Soils, Mae Sot District, Tak Province. International Graduate Research Conference, Chiang Mai University, Thailand.

WHO (2010). Exposure to Cadmium: A Major Pubilc Health Concenrn. Geneva, World Health Organization.

Wikiniyadhanee, R. (2012). Impacts of Ionic Strength on Facilitated Transport of Cd by Kaolinite Colloid in Saturated Sand Column, Chulalongkorn University. Master of Science.

Wikiniyadhanee, R., S. Chotpantarat and S. K. Ong (2015). Effects of kaolinite colloids on Cd2 + transport through saturated sand under varying ionic strength conditions: Column experiments and modeling approaches. Journal of Contaminant Hydrology 182: 146-156.

Zhou, B. and Q. Wang (2016). Effect of pore water velocities and solute input methods on chloride transport in the undisturbed soil columns of Loess Plateau. Applied Water Science: 1-8.

APPENDICIES

Appendix A

Properties of soils collected from Mae Tao area

Table A-1: Data of all soil samples collected from agricultural area near Mae Tao and Mae Ku creeks.

Station	UTM-X	UTM-Y	Landuse	ρ (g/cm3)	K_s (mm/hr)	Cd (mg/kg)	SD (±mg/kg)	Zn (mg/kg)	SD (±mg/kg)
C-Ac-1	460603	1843105	Mae Tao point bar soil	1.24	7.04	13.45	2.84	716.00	54.82
C-Ac-2	458995	1842919	Rice Field	1.55	0.09	41.47	3.71	1456.55	61.61
C-Ac-3	459394	1843324	Cut bank area	1.31	23.67	26.52	2.11	1550.95	152.47
C-Hcc-1	458213	1843045	Sugar Cane Field	1.60	0.21	6.86	0.59	377.95	116.21
C-Hcc-2	459172	1842923	Rice Field	1.50	1.69	62.04	6.08	2342.72	65.11
C-Nn-1	459094	1842885	Rice Field	1.47	2.52	40.01	1.29	1701.02	17.46
C-Nn-2	458650	1841985	Cassava Field	1.58	0.20	4.49	0.29	142.11	11.06
C-Nn-3	456137	1843154	Paddy Field	1.24	1.52	23.50	3.01	1077.03	32.70
C-Nn-4	456972	1843049	Abandoned paddy field	1.42	1.04	15.47	0.54	636.29	12.39
C-Nn-5	459145	1839709	Sugar Cane Field	1.53	3.19	10.85	0.55	461.81	25.58
U-Ac-1	452727	1839721	Agricultural Field	1.67	0.09	1.53	0.05	<100	-
U-Ac-2	454148	1839026	Rice and Beans Field	1.63	2.30	1.01	0.02	<100	-
U-Hcc-1	459643	1845119	Agricultural Field	1.76	0.04	4.27	0.21	<100	-
U-Hcc-2	454038	1841835	Agricultural Field	1.67	58.64	1.68	0.10	<100	-
U-Hcc-3	453866	1840287	Cassava Field	1.70	0.91	0.71	0.08	<100	-
U-Nn-1	458454	1845622	Agricultural Field	1.50	0.02	5.39	0.23	<100	-
U-Nn-2	458444	1845788	Agricultural Field	1.50	0.04	4.45	0.18	<100	-
U-Nn-3	459084	1840592	Agricultural Field	1.69	0.33	11.21	0.87	386.86	1.10

Appendix B

Batch sorption and desorption experimental data

Table B-1: Experimental and fitted data of Cd amount adsorbed on the soil at IS 1mM, 10 mM and 100 mM

Solution IS (mM)	Ce (mg/l)	Qe (observed) (mg/g)	SD (observed) (mg/g)	Linear Q_e (fitted) (mg/g)	Langmuir Q_e (fitted) (mg/g)	Freundlich Q_e (fitted) (mg/g)
1	nd	nd	nd	0.0000	0.0000	0.0000
	0.0483	0.0565	0.0003	0.0314	0.0510	0.0573
	0.1289	0.1153	0.0004	0.0838	0.1241	0.1206
	0.1980	0.1701	0.0004	0.1287	0.1772	0.1671
	0.2626	0.2274	0.0013	0.1707	0.2204	0.2070
	0.5040	0.3360	0.0010	0.3277	0.3437	0.3394
	0.7315	0.4314	0.0018	0.4756	0.4238	0.4502
10	nd	nd	nd	0.0020	0.0058	0.0083
	0.1587	0.0522	0.0006	0.0280	0.0719	0.0589
	0.3389	0.1019	0.0013	0.0599	0.1359	0.1063
	0.5444	0.1663	0.0012	0.0962	0.1582	0.1246
	0.7986	0.1969	0.0015	0.1411	0.2318	0.1981
	1.8921	0.2822	0.0041	0.3343	0.3101	0.3183
	2.2220	0.3916	0.0037	0.3926	0.3409	0.3903
100	0.0799	-0.0016	0.0000	0.0019	0.0026	0.0037
	0.9917	0.0293	0.0004	0.0230	0.0308	0.0317
	2.0067	0.0585	0.0007	0.0466	0.0591	0.0578
	2.9898	0.0844	0.0030	0.0694	0.0840	0.0811
	3.8474	0.1164	0.0059	0.0893	0.1039	0.1006
	6.8325	0.1526	0.0063	0.1585	0.1625	0.1641
	9.5154	0.2067	0.0028	0.2208	0.2044	0.2176

Table B-2: Experimental data of Cd adsorption and desorption on the soil at IS 1mM, 10 mM and 100 mM

Solution IS (mM)	Initial Conc. (mg/l)	Qe desorbed (mg/g)	SD ± (mg/g)	Qe adsorbed (mg/g)	% Desorb
1	2.91	0.0009	4.5E-05	0.0565	1.65
	5.92	0.0018	3.4E-04	0.1153	1.55
	8.81	0.0034	2.3E-04	0.1701	1.99
	11.73	0.0050	2.4E-04	0.2274	2.19
	17.52	0.0083	3.9E-04	0.3360	2.98
	22.48	0.0139	2.6E-03	0.4314	2.90
10	2.77	0.0044	8.8E-05	0.0522	8.27
	5.47	0.0080	1.0E-03	0.1019	6.47
	8.97	0.0152	1.9E-03	0.1663	9.04
	10.78	0.0188	1.4E-03	0.1969	10.39
	16.08	0.0350	1.2E-03	0.2822	11.99
	21.82	0.0462	3.4E-03	0.3916	12.95
100	2.4635	0.0124	3.2E-04	0.0293	42.24
	4.9587	0.0232	1.1E-03	0.0585	39.61
	7.2575	0.0329	9.3E-04	0.0844	39.01
	9.719	0.0421	2.5E-03	0.1164	36.11
	14.496	0.0657	1.3E-03	0.1526	43.08
	19.972	0.0907	1.4E-03	0.2067	43.90

Appendix C

Tracer transport experimental and fitted data

Table C-1: Experimental and Fitted data of Column1 (Tracer transport with low pore water velocity)

Time (hour)	Observed (ppm)	Fitted CDE (ppm)	Fitted T-R (ppm)	Dimensionless form			
				PV	C/C0 Observed	C/C0 CDE	C/C0 TRM
0.30	0.0000	0.0000	0.0000	0.08	0.0000	0.0000	0.0000
0.77	0.0000	0.0260	0.0247	0.21	0.0000	0.0024	0.0023
1.51	0.0000	0.6961	0.6847	0.42	0.0000	0.0637	0.0626
2.26	1.3798	2.2130	2.2001	0.62	0.1262	0.2025	0.2013
3.01	3.3278	3.9406	3.9353	0.83	0.3045	0.3605	0.3600
3.76	5.3956	5.5044	5.5086	1.03	0.4937	0.5036	0.5040
4.50	6.5830	6.7910	6.8027	1.24	0.6023	0.6213	0.6224
5.25	7.5155	7.8022	7.8185	1.44	0.6876	0.7138	0.7153
6.00	8.3382	8.5783	8.5967	1.65	0.7629	0.7848	0.7865
6.75	8.3826	9.1663	9.1851	1.85	0.7669	0.8386	0.8404
7.49	9.5303	9.6086	9.6265	2.06	0.8719	0.8791	0.8807
8.24	9.7741	9.9402	9.9565	2.26	0.8942	0.9094	0.9109
8.99	9.9938	10.1882	10.2027	2.47	0.9143	0.9321	0.9335
9.74	9.5751	10.3736	10.3861	2.68	0.8760	0.9491	0.9502
10.48	10.8142	10.5123	10.5229	2.88	0.9894	0.9618	0.9628
11.98	10.1925	10.6937	10.7010	3.29	0.9325	0.9784	0.9790
12.73	10.6478	10.7519	10.7579	3.50	0.9742	0.9837	0.9843
14.22	10.7387	10.8285	10.8322	3.91	0.9825	0.9907	0.9911
15.72	11.5172	10.8718	10.8740	4.32	1.0537	0.9947	0.9949
17.21	10.6473	10.8965	10.8976	4.73	0.9741	0.9969	0.9970
17.96	10.3306	10.9045	10.9052	4.94	0.9452	0.9977	0.9977

Time (hour)	Observed (ppm)	Fitted CDE (ppm)	Fitted T-R (ppm)	Dimensionless form			
				PV	C/C0 Observed	C/C0 CDE	C/C0 TRM
19.45	10.1030	10.9152	10.9153	5.35	0.9243	0.9986	0.9987
20.20	10.5598	10.9187	10.9185	5.55	0.9661	0.9990	0.9989
21.04	10.3092	10.9219	10.9213	5.78	0.9432	0.9993	0.9992
22.71	10.1638	10.9256	10.9247	6.24	0.9299	0.9996	0.9995
24.38	9.8845	9.8502	9.8625	6.70	0.9043	0.9012	0.9023
25.22	7.7408	8.0060	8.0154	6.93	0.7082	0.7325	0.7333
26.05	6.4688	6.1327	6.1318	7.16	0.5918	0.5611	0.5610
26.89	4.3993	4.5616	4.5511	7.39	0.4025	0.4173	0.4164
27.73	3.1149	3.3432	3.3266	7.62	0.2850	0.3059	0.3044
28.56	1.8100	2.4321	2.4126	7.85	0.1656	0.2225	0.2207
30.23	1.2921	1.2765	1.2576	8.31	0.1182	0.1168	0.1151
31.91	0.6009	0.6694	0.6545	8.77	0.0550	0.0612	0.0599
32.74	0.0993	0.4855	0.4727	9.00	0.0091	0.0444	0.0432
33.58	0.0000	0.3526	0.3418	9.23	0.0000	0.0323	0.0313
34.41	0.0000	0.2565	0.2475	9.46	0.0000	0.0235	0.0226

Table C-2: Experimental and Fitted data of Column2 (Tracer transport with high pore water velocity)

Time (hour)	Observed (ppm)	Fitted CDE (ppm)	Fitted T-R (ppm)	Dimensionless form			
				PV	C/C0 Observed	C/C0 CDE	C/C0 TRM
0.10	0.0000	0.0000	0.0000	0.00	0.0000	0.0000	0.0000
0.44	1.9065	1.5921	1.5930	0.58	0.2007	0.1676	0.1677
0.85	6.3390	5.2932	5.2934	1.12	0.6673	0.5572	0.5572
1.26	7.7195	7.5029	7.5027	1.67	0.8126	0.7898	0.7898
1.68	8.4047	8.5710	8.5708	2.21	0.8847	0.9022	0.9022
2.09	8.9798	9.0673	9.0670	2.76	0.9452	0.9545	0.9544
2.50	9.0884	9.2969	9.2966	3.30	0.9567	0.9786	0.9786
2.92	9.5285	9.4039	9.4035	3.85	1.0030	0.9899	0.9898
3.33	9.3315	9.4541	9.4535	4.39	0.9823	0.9952	0.9951
3.74	9.4897	9.4779	9.4772	4.94	0.9989	0.9977	0.9976
4.15	9.6069	9.4891	9.4883	5.47	1.0112	0.9989	0.9988
4.54	9.6146	9.4946	9.4936	5.99	1.0121	0.9994	0.9993
4.94	9.6002	9.4973	9.4963	6.52	1.0105	0.9997	0.9996
5.33	9.5628	9.4986	9.4976	7.04	1.0066	0.9999	0.9997
5.72	9.5399	9.4993	9.4983	7.56	1.0042	0.9999	0.9998
6.12	9.6345	9.4667	9.4655	8.08	1.0142	0.9965	0.9964
6.51	7.7726	6.6717	6.6699	8.60	0.8182	0.7023	0.7021
6.90	3.1946	3.4947	3.4937	9.12	0.3363	0.3679	0.3678
7.29	1.8941	1.7297	1.7289	9.62	0.1994	0.1821	0.1820
7.68	1.0897	0.8462	0.8455	10.13	0.1147	0.0891	0.0890
8.06	0.8413	0.4150	0.4142	10.64	0.0886	0.0437	0.0436

Time (hour)	Observed (ppm)	Fitted CDE (ppm)	Fitted T-R (ppm)	Dimensionless form			
				PV	C/C0 Observed	C/C0 CDE	C/C0 TRM
8.45	0.5898	0.2048	0.2041	11.15	0.0621	0.0216	0.0215
8.83	0.3702	0.1019	0.1013	11.66	0.0390	0.0107	0.0107
9.22	0.2778	0.0511	0.0506	12.17	0.0292	0.0054	0.0053

Appendix D

Cd transport experimental and fitted data

Table D-1: Experimental and Fitted data of Column3 (Cd transport with low pore water velocity, IS 100 mM)

Time (hour)	Observed (ppm)	F-EQ (ppm)	F-TSM (ppm)	L-EQ (ppm)	L-TSM (ppm)	Dimensionless form					
						PV	C/C_0 Observed	C/C_0 F-EQ	C/C_0 F-TSM	C/C_0 L-EQ	C/C_0 L-TSM
2.00	0.04	0.00	0.00	0.00	0.00	0.51	0.0040	0.0000	0.0000	0.0000	0.0000
14.02	0.03	0.00	0.00	0.00	0.00	3.57	0.0034	0.0000	0.0000	0.0000	0.0000
30.39	0.10	0.00	0.00	0.00	0.00	7.73	0.0113	0.0000	0.0000	0.0000	0.0001
44.25	0.25	0.00	0.02	0.01	0.02	11.26	0.0289	0.0000	0.0024	0.0007	0.0019
61.09	0.51	0.00	0.25	0.04	0.10	15.54	0.0581	0.0003	0.0282	0.0042	0.0109
77.46	0.77	0.02	0.54	0.11	0.27	19.71	0.0878	0.0023	0.0614	0.0126	0.0306
93.40	0.95	0.07	0.81	0.24	0.52	23.77	0.1076	0.0080	0.0925	0.0269	0.0593
108.75	0.97	0.17	1.07	0.41	0.82	27.67	0.1100	0.0192	0.1215	0.0469	0.0934
124.34	1.18	0.33	1.33	0.65	1.16	31.64	0.1338	0.0378	0.1509	0.0735	0.1315
146.54	1.39	0.68	1.70	1.07	1.65	37.29	0.1578	0.0778	0.1933	0.1212	0.1871
170.89	2.05	1.19	2.11	1.60	2.16	43.48	0.2335	0.1354	0.2401	0.1818	0.2457
199.27	2.47	1.89	2.59	2.28	2.71	50.71	0.2807	0.2149	0.2945	0.2591	0.3081
220.89	2.98	2.46	2.95	2.81	3.10	56.21	0.3386	0.2795	0.3352	0.3192	0.3519
248.94	3.42	3.20	3.40	3.48	3.55	63.34	0.3890	0.3634	0.3866	0.3959	0.4035
268.35	3.79	3.69	3.70	3.93	3.84	68.28	0.4311	0.4195	0.4209	0.4467	0.4362
285.58	3.90	4.11	3.96	4.31	4.08	72.67	0.4436	0.4671	0.4503	0.4897	0.4639
306.23	4.34	4.58	4.26	4.74	4.36	77.92	0.4936	0.5207	0.4844	0.5382	0.4952
324.62	4.60	4.97	4.52	5.09	4.59	82.60	0.5231	0.5652	0.5134	0.5785	0.5218
342.72	4.84	5.33	4.76	5.42	4.81	87.21	0.5496	0.6058	0.5408	0.6155	0.5468
361.28	4.88	5.67	5.00	5.73	5.03	91.93	0.5545	0.6441	0.5677	0.6506	0.5712

Time (hour)	Observed (ppm)	F-EQ (ppm)	F-TSM (ppm)	L-EQ (ppm)	L-TSM (ppm)	Dimensionless form					
						PV	C/C_0 Observed	C/C_0 F-EQ	C/C_0 F-TSM	C/C_0 L-EQ	C/C_0 L-TSM
378.41	5.14	5.96	5.20	5.99	5.22	96.29	0.5839	0.6767	0.5915	0.6806	0.5928
418.19	5.77	6.53	5.66	6.52	5.63	106.41	0.6558	0.7420	0.6427	0.7414	0.6396
456.51	6.02	6.98	6.04	6.95	5.98	116.16	0.6836	0.7932	0.6867	0.7897	0.6798
498.61	6.24	7.38	6.42	7.33	6.33	126.87	0.7094	0.8383	0.7296	0.8329	0.7193
544.02	6.70	7.71	6.78	7.66	6.66	138.43	0.7616	0.8761	0.7699	0.8699	0.7568
646.75	7.25	8.21	7.41	8.15	7.26	164.57	0.8233	0.9326	0.8415	0.9265	0.8255
665.83	7.25	8.27	7.50	8.22	7.36	169.42	0.8244	0.9399	0.8522	0.9340	0.8362
684.39	6.88	8.33	7.17	8.28	7.23	174.14	0.7818	0.9460	0.8145	0.9404	0.8219
724.01	6.58	8.35	6.10	8.32	6.34	184.23	0.7476	0.9484	0.6927	0.9453	0.7199
743.34	6.09	8.25	5.70	8.25	5.84	189.14	0.6923	0.9379	0.6473	0.9378	0.6638
790.28	4.85	7.64	4.99	7.73	4.88	201.09	0.5510	0.8684	0.5675	0.8783	0.5542
826.26	4.41	6.91	4.58	7.05	4.34	210.24	0.5010	0.7854	0.5200	0.8016	0.4934
861.96	3.89	6.10	4.20	6.27	3.94	219.33	0.4420	0.6931	0.4778	0.7124	0.4475
903.88	3.22	5.16	3.81	5.32	3.57	229.99	0.3664	0.5859	0.4327	0.6047	0.4052
945.80	2.97	4.30	3.45	4.43	3.26	240.66	0.3374	0.4883	0.3919	0.5038	0.3703
1007.10	2.67	3.25	2.98	3.32	2.88	256.26	0.3032	0.3694	0.3389	0.3774	0.3273
1096.34	2.23	2.15	2.42	2.13	2.43	278.97	0.2533	0.2444	0.2749	0.2418	0.2757
1157.25	1.93	1.62	2.10	1.55	2.16	294.47	0.2189	0.1846	0.2388	0.1767	0.2458
1200.00	1.75	1.34	1.91	1.24	2.00	305.34	0.1991	0.1520	0.2165	0.1414	0.2269
1263.86	1.58	1.01	1.65	0.89	1.77	321.59	0.1793	0.1143	0.1874	0.1011	0.2014
1329.80	1.36	0.75	1.43	0.63	1.57	338.37	0.1548	0.0857	0.1620	0.0714	0.1782
1399.04	1.16	0.56	1.23	0.44	1.38	355.99	0.1314	0.0639	0.1395	0.0495	0.1568

Time (hour)	Observed (ppm)	F-EQ (ppm)	F-TSM (ppm)	L-EQ (ppm)	L-TSM (ppm)	Dimensionless form					
						PV	C/C_0 Observed	C/C_0 F-EQ	C/C_0 F-TSM	C/C_0 L-EQ	C/C_0 L-TSM
1438.27	0.99	0.48	1.13	0.35	1.28	365.97	0.1121	0.0542	0.1284	0.0402	0.1459
1478.01	0.91	0.41	1.04	0.29	1.19	376.08	0.1037	0.0460	0.1182	0.0326	0.1355

* F-EQ = Freundlich Equilibrium model; F-TSM = Freundlich Two Site Model;
L-EQ = Langmuir Equilibrium model; L-TSM = Langmuir Two Site Model

Table D-2: Experimental and Fitted data of Column4 (Cd transport with low pore water velocity, IS 10 mM)

Time (hour)	Observed (ppm)	F-EQ (ppm)	F-TSM (ppm)	L-EQ (ppm)	L-TSM (ppm)	Dimensionless form					
						PV	C/C_0 Observed	C/C_0 F-EQ	C/C_0 F-TSM	C/C_0 L-EQ	C/C_0 L-TSM
2.00	0.00	0.00	0.00	0.00	0.00	0.56	0.0000	0.0000	0.0000	0.0000	0.0000
30.45	0.00	0.00	0.00	0.00	0.00	8.49	0.0000	0.0000	0.0000	0.0000	0.0000
45.20	0.03	0.00	0.00	0.00	0.00	12.60	0.0032	0.0000	0.0000	0.0000	0.0000
105.74	0.13	0.00	0.00	0.00	0.00	29.49	0.0147	0.0000	0.0000	0.0000	0.0000
142.54	0.14	0.00	0.00	0.00	0.00	39.75	0.0154	0.0000	0.0000	0.0004	0.0000
184.96	0.10	0.00	0.00	0.02	0.01	51.58	0.0105	0.0000	0.0000	0.0026	0.0006
204.83	0.09	0.00	0.00	0.05	0.01	57.12	0.0105	0.0000	0.0000	0.0051	0.0016
223.68	0.09	0.00	0.00	0.08	0.03	62.38	0.0101	0.0000	0.0000	0.0087	0.0032
261.39	0.21	0.03	0.01	0.19	0.09	72.89	0.0231	0.0030	0.0015	0.0209	0.0099
280.24	0.40	0.08	0.05	0.27	0.15	78.15	0.0442	0.0086	0.0057	0.0298	0.0161
298.85	0.40	0.17	0.13	0.37	0.23	83.34	0.0437	0.0183	0.0142	0.0409	0.0250
317.29	0.66	0.30	0.25	0.49	0.34	88.48	0.0723	0.0325	0.0273	0.0542	0.0377
335.40	0.73	0.46	0.41	0.63	0.50	93.53	0.0801	0.0508	0.0450	0.0696	0.0548
354.26	0.95	0.67	0.62	0.80	0.71	98.79	0.1050	0.0741	0.0680	0.0880	0.0785
373.11	1.04	0.92	0.86	0.99	0.98	104.05	0.1150	0.1010	0.0951	0.1087	0.1083
392.08	1.25	1.19	1.14	1.20	1.30	109.34	0.1376	0.1310	0.1256	0.1320	0.1433
412.47	1.58	1.50	1.46	1.45	1.67	115.02	0.1743	0.1659	0.1613	0.1594	0.1843
453.45	2.91	2.18	2.16	2.00	2.43	126.45	0.3204	0.2404	0.2379	0.2210	0.2675
473.95	2.91	2.53	2.51	2.31	2.78	132.17	0.3208	0.2787	0.2772	0.2545	0.3070
494.72	3.02	2.88	2.87	2.63	3.13	137.96	0.3330	0.3172	0.3168	0.2898	0.3453

Time (hour)	Observed (ppm)	F-EQ (ppm)	F-TSM (ppm)	L-EQ (ppm)	L-TSM (ppm)	Dimensionless form					
						PV	C/C_0 Observed	C/C_0 F-EQ	C/C_0 F-TSM	C/C_0 L-EQ	C/C_0 L-TSM
534.72	3.18	3.53	3.55	3.26	3.76	149.11	0.3511	0.3892	0.3909	0.3599	0.4141
577.35	3.22	4.19	4.22	3.95	4.36	161.00	0.3554	0.4615	0.4650	0.4351	0.4806
599.37	3.75	4.51	4.54	4.29	4.65	167.14	0.4137	0.4967	0.5007	0.4731	0.5123
642.41	3.90	5.08	5.12	4.93	5.16	179.14	0.4300	0.5597	0.5649	0.5441	0.5692
685.03	4.13	5.58	5.63	5.52	5.62	191.03	0.4551	0.6156	0.6210	0.6088	0.6196
706.54	5.01	5.82	5.87	5.80	5.83	197.03	0.5527	0.6415	0.6469	0.6390	0.6429
727.96	5.13	6.04	6.09	6.05	6.03	203.00	0.5651	0.6657	0.6710	0.6674	0.6647
750.09	6.12	6.25	6.30	6.30	6.22	209.17	0.6743	0.6891	0.6942	0.6949	0.6860
815.85	7.90	6.80	6.85	6.94	6.73	227.51	0.8713	0.7502	0.7549	0.7649	0.7417
836.34	8.13	6.95	6.99	7.11	6.87	233.22	0.8959	0.7668	0.7712	0.7835	0.7570
856.99	8.32	7.10	7.13	7.26	7.00	238.98	0.9168	0.7825	0.7865	0.8009	0.7716
877.24	8.26	7.23	7.26	7.41	7.12	244.63	0.9106	0.7969	0.8006	0.8168	0.7851
897.32	8.26	7.35	7.38	7.54	7.23	250.23	0.9107	0.8103	0.8136	0.8313	0.7976
919.45	8.32	7.47	7.50	7.67	7.35	256.40	0.9170	0.8240	0.8269	0.8461	0.8107
941.58	8.11	7.59	7.61	7.80	7.46	262.57	0.8945	0.8367	0.8392	0.8596	0.8229
963.71	7.81	7.70	7.72	7.91	7.57	268.74	0.8610	0.8486	0.8507	0.8719	0.8343
984.86	8.14	7.79	7.81	8.01	7.66	274.64	0.8974	0.8591	0.8608	0.8828	0.8445
1067.89	7.91	8.11	8.11	8.32	7.97	297.79	0.8720	0.8940	0.8942	0.9176	0.8791
1087.97	7.75	8.17	8.17	8.38	8.04	303.39	0.8542	0.9011	0.9009	0.9244	0.8862
1108.05	7.72	8.23	8.23	8.44	8.10	308.99	0.8506	0.9077	0.9072	0.9305	0.8929
1118.09	5.50	8.26	8.26	8.47	5.82	311.79	0.6068	0.9109	0.9103	0.9336	0.6419
1128.14	3.87	8.29	8.28	8.49	4.34	314.60	0.4264	0.9140	0.9132	0.9364	0.4781

Time (hour)	Observed (ppm)	F-EQ (ppm)	F-TSM (ppm)	L-EQ (ppm)	L-TSM (ppm)	Dimensionless form					
						PV	C/C_0 Observed	C/C_0 F-EQ	C/C_0 F-TSM	C/C_0 L-EQ	C/C_0 L-TSM
1138.38	2.91	8.32	8.31	8.52	3.63	317.45	0.3209	0.9171	0.9161	0.9393	0.3997
1197.81	1.49	8.44	8.42	8.60	2.54	334.02	0.1641	0.9302	0.9283	0.9483	0.2800
1271.04	1.18	8.27	8.22	8.23	2.26	354.45	0.1300	0.9123	0.9058	0.9072	0.2493
1358.11	0.92	7.49	7.39	7.24	2.07	378.73	0.1018	0.8262	0.8144	0.7982	0.2280
1406.78	0.87	6.90	6.78	6.63	1.98	392.30	0.0958	0.7613	0.7476	0.7306	0.2180

Table D-3: Experimental and Fitted data of Column5 (Cd transport with low pore water velocity, IS 1 mM)

Time (hour)	Observed (ppm)	F-EQ (ppm)	F-TSM (ppm)	L-EQ (ppm)	L-TSM (ppm)	Dimensionless form					
						PV	C/C_0 Observed	C/C_0 F-EQ	C/C_0 F-TSM	C/C_0 L-EQ	C/C_0 L-TSM
2.00	0.00	0.00	0.00	0.00	0.00	0.47	0.0000	0.0000	0.0000	0.0000	0.0000
64.14	0.00	0.00	0.00	0.00	0.00	14.94	0.0000	0.0000	0.0000	0.0000	0.0000
135.82	0.00	0.00	0.00	0.00	0.00	31.65	0.0000	0.0000	0.0000	0.0000	0.0000
228.85	0.00	0.00	0.00	0.00	0.00	53.33	0.0000	0.0000	0.0000	0.0000	0.0000
317.36	0.00	0.00	0.00	0.00	0.00	73.95	0.0000	0.0000	0.0000	0.0000	0.0000
404.38	0.00	0.00	0.00	0.00	0.00	94.23	0.0000	0.0000	0.0000	0.0000	0.0000
494.15	0.00	0.00	0.00	0.00	0.00	115.15	0.0000	0.0000	0.0000	0.0000	0.0001
575.53	0.00	0.00	0.00	0.00	0.00	134.11	0.0000	0.0000	0.0000	0.0000	0.0002
655.03	0.00	0.00	0.00	0.00	0.00	152.63	0.0000	0.0000	0.0000	0.0001	0.0003
731.75	0.00	0.00	0.00	0.00	0.01	170.51	0.0000	0.0001	0.0000	0.0003	0.0006
807.80	0.00	0.00	0.00	0.01	0.01	188.23	0.0000	0.0002	0.0000	0.0006	0.0009
886.82	0.00	0.01	0.00	0.01	0.01	206.65	0.0000	0.0006	0.0002	0.0012	0.0014
972.53	0.00	0.01	0.01	0.02	0.02	226.62	0.0000	0.0013	0.0013	0.0023	0.0022
1056.16	0.00	0.02	0.03	0.03	0.03	246.11	0.0000	0.0026	0.0034	0.0039	0.0031
1143.48	0.00	0.04	0.06	0.06	0.04	266.45	0.0000	0.0048	0.0066	0.0062	0.0045
1187.78	0.04	0.06	0.08	0.07	0.05	276.78	0.0046	0.0062	0.0087	0.0078	0.0053
1232.03	0.05	0.07	0.10	0.08	0.06	287.09	0.0054	0.0080	0.0110	0.0095	0.0063
1275.34	0.06	0.09	0.12	0.10	0.07	297.18	0.0063	0.0100	0.0136	0.0115	0.0074
1316.88	0.09	0.11	0.15	0.12	0.08	306.86	0.0102	0.0122	0.0164	0.0137	0.0087
1336.98	0.16	0.12	0.16	0.13	0.08	311.54	0.0176	0.0133	0.0178	0.0148	0.0093

Time (hour)	Observed (ppm)	F-EQ (ppm)	F-TSM (ppm)	L-EQ (ppm)	L-TSM (ppm)	Dimensionless form					
						PV	C/C_0 Observed	C/C_0 F-EQ	C/C_0 F-TSM	C/C_0 L-EQ	C/C_0 L-TSM
1357.07	0.23	0.13	0.17	0.14	0.09	316.22	0.0259	0.0146	0.0193	0.0160	0.0100
1377.85	0.32	0.14	0.18	0.15	0.10	321.06	0.0363	0.0159	0.0208	0.0173	0.0108
1398.17	0.34	0.15	0.20	0.16	0.10	325.80	0.0383	0.0173	0.0225	0.0186	0.0116
1413.75	0.37	0.16	0.21	0.17	0.11	329.43	0.0413	0.0184	0.0237	0.0197	0.0123
1429.55	0.38	0.17	0.22	0.18	0.12	333.11	0.0423	0.0196	0.0250	0.0208	0.0130
1612.46	0.42	0.33	0.38	0.33	0.21	375.73	0.0474	0.0367	0.0428	0.0368	0.0241
1633.01	0.46	0.35	0.40	0.35	0.23	380.52	0.0522	0.0390	0.0450	0.0390	0.0258
1812.49	0.46	0.55	0.59	0.54	0.40	422.34	0.0522	0.0623	0.0669	0.0610	0.0455
1832.81	0.45	0.58	0.62	0.57	0.43	427.08	0.0507	0.0652	0.0696	0.0638	0.0484
1853.13	0.46	0.60	0.64	0.59	0.46	431.81	0.0514	0.0683	0.0723	0.0668	0.0515
1934.87	0.48	0.72	0.74	0.70	0.58	450.86	0.0547	0.0811	0.0837	0.0792	0.0656
1974.59	0.63	0.78	0.79	0.76	0.65	460.12	0.0708	0.0877	0.0895	0.0857	0.0735
2014.32	0.73	0.84	0.85	0.82	0.73	469.37	0.0829	0.0945	0.0954	0.0924	0.0822
2054.06	0.77	0.90	0.90	0.88	0.81	478.63	0.0868	0.1015	0.1014	0.0993	0.0918
2094.25	0.82	0.96	0.95	0.94	0.91	488.00	0.0929	0.1088	0.1077	0.1066	0.1023
2151.83	0.97	1.06	1.03	1.04	1.05	501.42	0.1094	0.1196	0.1168	0.1175	0.1189
2190.21	1.15	1.12	1.09	1.11	1.16	510.36	0.1301	0.1270	0.1230	0.1250	0.1310
2229.05	1.21	1.19	1.15	1.18	1.28	519.41	0.1364	0.1346	0.1294	0.1328	0.1441
2267.89	1.35	1.26	1.20	1.25	1.40	528.46	0.1527	0.1423	0.1359	0.1408	0.1580
2306.72	1.51	1.33	1.26	1.32	1.53	537.51	0.1705	0.1502	0.1425	0.1490	0.1727
2345.56	1.67	1.40	1.32	1.39	1.67	546.56	0.1882	0.1582	0.1492	0.1574	0.1880
2500.90	1.51	1.69	1.48	1.71	1.44	582.76	0.1700	0.1912	0.1675	0.1926	0.1621

Time (hour)	Observed (ppm)	F-EQ (ppm)	F-TSM (ppm)	L-EQ (ppm)	L-TSM (ppm)	Dimensionless form					
						PV	C/C_0 Observed	C/C_0 F-EQ	C/C_0 F-TSM	C/C_0 L-EQ	C/C_0 L-TSM
2520.32	1.43	1.73	1.48	1.75	1.40	587.28	0.1612	0.1954	0.1675	0.1971	0.1583
2559.15	1.38	1.81	1.47	1.83	1.35	596.33	0.1563	0.2039	0.1664	0.2064	0.1527
2599.91	1.42	1.89	1.46	1.92	1.32	605.83	0.1602	0.2129	0.1646	0.2162	0.1492
2641.68	1.42	1.97	1.44	2.01	1.31	615.56	0.1602	0.2221	0.1627	0.2264	0.1474
2682.32	1.39	2.05	1.43	2.09	1.30	625.03	0.1567	0.2311	0.1613	0.2364	0.1469
2743.06	1.36	2.17	1.42	2.23	1.31	639.18	0.1536	0.2447	0.1600	0.2515	0.1474
2781.44	1.44	2.24	1.41	2.31	1.31	648.13	0.1626	0.2533	0.1597	0.2611	0.1483
2800.64	1.45	2.28	1.41	2.36	1.32	652.60	0.1637	0.2576	0.1597	0.2659	0.1488
2836.76	1.47	2.35	1.42	2.44	1.33	661.02	0.1654	0.2657	0.1599	0.2750	0.1499
2872.89	1.46	2.43	1.42	2.52	1.34	669.44	0.1651	0.2737	0.1603	0.2840	0.1511
2909.02	1.48	2.50	1.43	2.60	1.35	677.86	0.1668	0.2818	0.1610	0.2930	0.1523
2963.20	1.44	2.60	1.44	2.71	1.37	690.48	0.1625	0.2937	0.1621	0.3064	0.1541
2999.33	1.43	2.67	1.44	2.79	1.38	698.90	0.1609	0.3016	0.1630	0.3152	0.1553
3035.46	1.50	2.74	1.45	2.87	1.39	707.32	0.1699	0.3093	0.1639	0.3239	0.1565

Table D-4: Experimental and Fitted data of Column6 (Cd transport with high pore water velocity, IS 100 mM)

Time (hour)	Observed (ppm)	F-EQ (ppm)	F-TSM (ppm)	L-EQ (ppm)	L-TSM (ppm)	Dimensionless form					
						PV	C/C_0 Observed	C/C_0 F-EQ	C/C_0 F-TSM	C/C_0 L-EQ	C/C_0 L-TSM
0.50	0.17	0.00	0.00	0.00	0.00	0.57	0.0201	0.0000	0.0000	0.0000	0.0000
1.47	0.15	0.00	0.00	0.00	0.00	1.68	0.0184	0.0000	0.0000	0.0000	0.0000
4.10	0.34	0.00	0.02	0.00	0.01	4.71	0.0402	0.0001	0.0030	0.0001	0.0011
6.74	0.74	0.02	0.19	0.01	0.13	7.74	0.0884	0.0022	0.0229	0.0017	0.0153
9.38	1.13	0.08	0.53	0.07	0.47	10.77	0.1357	0.0101	0.0638	0.0083	0.0562
12.01	1.53	0.23	0.99	0.20	1.00	13.80	0.1835	0.0281	0.1188	0.0238	0.1198
14.65	1.92	0.46	1.48	0.40	1.60	16.83	0.2296	0.0551	0.1777	0.0477	0.1913
17.28	2.11	0.75	1.97	0.66	2.15	19.86	0.2523	0.0899	0.2359	0.0791	0.2572
19.92	2.43	1.10	2.42	0.98	2.61	22.89	0.2908	0.1316	0.2901	0.1173	0.3130
22.56	2.60	1.48	2.84	1.34	3.00	25.92	0.3118	0.1777	0.3396	0.1600	0.3590
25.19	2.56	1.90	3.19	1.73	3.30	28.95	0.3069	0.2272	0.3826	0.2066	0.3953
30.47	3.02	2.74	3.76	2.54	3.74	35.01	0.3614	0.3287	0.4505	0.3038	0.4485
35.74	3.41	3.55	4.17	3.32	4.06	41.07	0.4089	0.4248	0.4998	0.3978	0.4860
41.01	3.76	4.28	4.49	4.05	4.31	47.13	0.4499	0.5121	0.5378	0.4844	0.5157
43.65	4.15	4.62	4.63	4.39	4.42	50.16	0.4973	0.5533	0.5544	0.5256	0.5289
46.28	4.36	4.94	4.75	4.71	4.52	53.19	0.5217	0.5919	0.5691	0.5645	0.5415
48.92	4.77	5.24	4.86	5.02	4.62	56.22	0.5708	0.6279	0.5823	0.6009	0.5535
51.56	4.86	5.52	4.96	5.30	4.72	59.25	0.5818	0.6612	0.5941	0.6349	0.5650
56.83	5.20	6.00	5.13	5.79	4.90	65.31	0.6230	0.7180	0.6141	0.6935	0.5869
62.10	5.46	6.40	5.27	6.21	5.07	71.37	0.6543	0.7660	0.6315	0.7435	0.6076

Time (hour)	Observed (ppm)	F-EQ (ppm)	F-TSM (ppm)	L-EQ (ppm)	L-TSM (ppm)	Dimensionless form					
						PV	C/C_0 Observed	C/C_0 F-EQ	C/C_0 F-TSM	C/C_0 L-EQ	C/C_0 L-TSM
67.38	5.75	6.73	5.40	6.56	5.24	77.43	0.6887	0.8063	0.6471	0.7859	0.6273
72.65	5.97	7.01	5.52	6.86	5.39	83.48	0.7145	0.8399	0.6614	0.8216	0.6460
77.92	6.20	7.25	5.63	7.11	5.54	89.54	0.7425	0.8679	0.6747	0.8515	0.6638
84.36	6.31	7.47	5.76	7.36	5.72	96.95	0.7555	0.8952	0.6897	0.8811	0.6846
100.18	6.26	7.85	6.04	7.77	6.10	115.13	0.7492	0.9401	0.7232	0.9305	0.7305
110.73	6.52	8.00	6.20	7.94	6.33	127.24	0.7813	0.9582	0.7429	0.9508	0.7575
131.82	6.58	8.18	6.50	8.15	6.71	151.48	0.7883	0.9797	0.7781	0.9755	0.8041
152.91	6.77	8.26	6.75	8.24	7.03	175.72	0.8112	0.9891	0.8085	0.9866	0.8419
163.46	6.82	8.29	6.87	8.27	7.17	187.84	0.8168	0.9924	0.8222	0.9905	0.8581
183.97	6.91	8.32	7.06	8.31	7.39	211.41	0.8274	0.9960	0.8460	0.9948	0.8851
209.01	7.11	8.34	7.27	8.33	7.61	240.19	0.8509	0.9983	0.8711	0.9977	0.9114
224.04	7.23	8.34	7.38	8.34	7.72	257.46	0.8660	0.9990	0.8842	0.9986	0.9243
234.06	7.22	8.34	7.45	8.34	7.78	268.97	0.8646	0.9993	0.8921	0.9990	0.9317
244.08	7.15	8.35	7.51	8.34	7.84	280.48	0.8561	0.9995	0.8995	0.9993	0.9385
254.09	7.08	7.91	6.69	7.95	7.06	291.99	0.8475	0.9477	0.8015	0.9523	0.8453
259.10	5.88	7.55	6.09	7.62	6.02	297.75	0.7040	0.9039	0.7296	0.9122	0.7214
264.11	5.00	7.03	5.42	7.14	5.15	303.51	0.5985	0.8423	0.6494	0.8550	0.6167
274.05	3.91	5.75	4.34	5.92	4.04	314.93	0.4681	0.6887	0.5196	0.7085	0.4839
283.75	3.33	4.51	3.59	4.71	3.46	326.08	0.3982	0.5407	0.4304	0.5640	0.4145
303.16	2.60	2.73	2.74	2.91	2.84	348.37	0.3110	0.3268	0.3285	0.3485	0.3399
317.71	2.11	1.78	2.37	1.93	2.52	365.10	0.2532	0.2133	0.2844	0.2315	0.3021
341.96	1.88	0.82	1.96	0.92	2.09	392.97	0.2252	0.0987	0.2353	0.1105	0.2508

Time (hour)	Observed (ppm)	F-EQ (ppm)	F-TSM (ppm)	L-EQ (ppm)	L-TSM (ppm)	Dimensionless form					
						PV	C/C_0 Observed	C/C_0 F-EQ	C/C_0 F-TSM	C/C_0 L-EQ	C/C_0 L-TSM
366.19	1.58	0.37	1.65	0.43	1.74	420.81	0.1896	0.0447	0.1980	0.0515	0.2087
385.40	1.39	0.21	1.45	0.25	1.51	442.89	0.1664	0.0251	0.1731	0.0295	0.1805
399.10	1.33	0.13	1.31	0.16	1.36	458.63	0.1590	0.0161	0.1572	0.0192	0.1629
413.12	1.06	0.09	1.19	0.10	1.22	474.74	0.1267	0.0102	0.1424	0.0124	0.1466
422.61	0.97	0.06	1.11	0.08	1.14	485.65	0.1157	0.0073	0.1332	0.0090	0.1365
440.84	0.92	0.04	0.98	0.04	0.99	506.59	0.1106	0.0042	0.1172	0.0053	0.1191
449.91	0.85	0.03	0.92	0.03	0.93	517.01	0.1018	0.0031	0.1100	0.0039	0.1113

Table D-5: Experimental and Fitted data of Column7 (Cd transport with high pore water velocity, IS 10 mM)

Time (hour)	Observed (ppm)	F-EQ (ppm)	F-TSM (ppm)	L-EQ (ppm)	L-TSM (ppm)	Dimensionless form					
						PV	C/C_0 Observed	C/C_0 F-EQ	C/C_0 F-TSM	C/C_0 L-EQ	C/C_0 L-TSM
0.50	0.00	0.00	0.0	0.00	0.00	0.48	0.0000	0.0000	0.0000	0.0000	0.0000
10.10	0.00	0.00	0.0	0.00	0.00	9.77	0.0000	0.0000	0.0000	0.0000	0.0000
21.20	0.00	0.00	0.0	0.00	0.00	20.51	0.0000	0.0000	0.0000	0.0000	0.0000
32.31	0.02	0.00	0.0	0.00	0.00	31.24	0.0025	0.0000	0.0000	0.0001	0.0001
43.41	0.13	0.00	0.1	0.00	0.01	41.98	0.0137	0.0003	0.0142	0.0005	0.0013
54.51	0.33	0.01	0.3	0.02	0.06	52.72	0.0348	0.0014	0.0351	0.0019	0.0061
59.95	0.43	0.02	0.4	0.03	0.10	57.98	0.0461	0.0024	0.0439	0.0031	0.0105
87.16	0.48	0.15	0.8	0.19	0.46	84.30	0.0515	0.0160	0.0812	0.0198	0.0490
98.05	0.50	0.25	0.9	0.30	0.63	94.82	0.0537	0.0264	0.0957	0.0319	0.0675
108.52	0.72	0.37	1.0	0.44	0.80	104.95	0.0764	0.0389	0.1099	0.0464	0.0852
118.86	0.87	0.51	1.2	0.60	0.96	114.95	0.0927	0.0538	0.1243	0.0634	0.1024
129.14	1.02	0.67	1.3	0.78	1.12	124.90	0.1081	0.0708	0.1389	0.0826	0.1194
139.37	1.18	0.84	1.4	0.98	1.28	134.79	0.1259	0.0899	0.1536	0.1038	0.1363
149.61	1.34	1.04	1.6	1.19	1.44	144.69	0.1421	0.1107	0.1687	0.1268	0.1534
159.44	1.61	1.24	1.7	1.41	1.60	154.20	0.1713	0.1322	0.1833	0.1503	0.1701
169.24	1.76	1.46	1.9	1.64	1.76	163.68	0.1868	0.1548	0.1979	0.1748	0.1870
179.04	1.96	1.68	2.0	1.88	1.92	173.15	0.2087	0.1783	0.2127	0.2001	0.2043
188.83	2.09	1.90	2.1	2.13	2.09	182.62	0.2219	0.2026	0.2275	0.2261	0.2218
198.63	2.27	2.14	2.3	2.37	2.25	192.10	0.2411	0.2274	0.2424	0.2524	0.2397
208.04	2.38	2.36	2.4	2.61	2.42	201.20	0.2536	0.2515	0.2566	0.2779	0.2570

Time (hour)	Observed (ppm)	F-EQ (ppm)	F-TSM (ppm)	L-EQ (ppm)	L-TSM (ppm)	Dimensionless form					
						PV	C/C_0 Observed	C/C_0 F-EQ	C/C_0 F-TSM	C/C_0 L-EQ	C/C_0 L-TSM
221.57	2.82	2.69	2.6	2.96	2.65	214.28	0.3000	0.2865	0.2771	0.3144	0.2821
230.27	2.99	2.90	2.7	3.18	2.80	222.70	0.3186	0.3089	0.2902	0.3378	0.2984
238.98	3.20	3.11	2.9	3.39	2.96	231.12	0.3401	0.3313	0.3033	0.3610	0.3146
247.69	3.31	3.32	3.0	3.61	3.11	239.54	0.3520	0.3535	0.3163	0.3838	0.3309
256.40	3.56	3.53	3.1	3.82	3.26	247.96	0.3788	0.3755	0.3293	0.4064	0.3472
265.10	3.50	3.73	3.2	4.03	3.41	256.39	0.3725	0.3971	0.3421	0.4285	0.3633
273.32	3.55	3.92	3.3	4.22	3.56	264.33	0.3778	0.4173	0.3542	0.4489	0.3784
281.48	3.52	4.11	3.4	4.41	3.70	272.23	0.3743	0.4369	0.3660	0.4688	0.3933
289.42	3.14	4.28	3.5	4.58	3.76	279.90	0.3341	0.4556	0.3721	0.4877	0.4003
297.47	2.78	4.46	3.2	4.76	3.47	287.69	0.2962	0.4742	0.3452	0.5064	0.3691
305.77	2.47	4.63	2.9	4.94	3.03	295.71	0.2627	0.4929	0.3033	0.5251	0.3220
313.11	2.39	4.78	2.6	5.09	2.69	302.81	0.2539	0.5089	0.2748	0.5410	0.2866
320.18	2.29	4.92	2.42	5.22	2.45	309.65	0.2437	0.5238	0.2572	0.5558	0.2602
327.09	2.25	5.06	2.32	5.35	2.26	316.34	0.2388	0.5378	0.2465	0.5695	0.2407
333.84	2.21	5.18	2.26	5.47	2.13	322.86	0.2355	0.5508	0.2400	0.5821	0.2263
350.00	-	-	2.18	-	1.92	338.49	-	-	0.2321	-	0.2040
370.00	-	-	2.14	-	1.79	357.83	-	-	0.2275	-	0.1900
390.00	-	-	2.10	-	1.72	377.18	-	-	0.2239	-	0.1827
410.00	-	-	2.07	-	1.68	396.52	-	-	0.2202	-	0.1783
430.00	-	-	2.03	-	1.65	415.86	-	-	0.2164	-	0.1752
450.00	-	-	2.00	-	1.62	435.20	-	-	0.2125	-	0.1726
470.00	-	-	1.96	-	1.60	454.55	-	-	0.2085	-	0.1702

Time (hour)	Observed (ppm)	F-EQ (ppm)	F-TSM (ppm)	L-EQ (ppm)	L-TSM (ppm)	Dimensionless form					
						PV	C/C_0 Observed	C/C_0 F-EQ	C/C_0 F-TSM	C/C_0 L-EQ	C/C_0 L-TSM
490.00	-	-	1.92	-	1.58	473.89	-	-	0.2044	-	0.1678
510.00	-	-	1.88	-	1.56	493.23	-	-	0.2003	-	0.1655
530.00	-	-	1.84	-	1.53	512.57	-	-	0.1961	-	0.1632
550.00	-	-	1.80	-	1.51	531.91	-	-	0.1919	-	0.1608
570.00	-	-	1.76	-	1.49	551.26	-	-	0.1877	-	0.1585
590.00	-	-	1.73	-	1.47	570.60	-	-	0.1835	-	0.1561
610.00	-	-	1.69	-	1.45	589.94	-	-	0.1794	-	0.1538
630.00	-	-	1.65	-	1.42	609.28	-	-	0.1752	-	0.1514
650.00	-	-	1.61	-	1.40	628.63	-	-	0.1711	-	0.1491
670.00	-	-	1.57	-	1.38	647.97	-	-	0.1670	-	0.1468
690.00	-	-	1.53	-	1.36	667.31	-	-	0.1630	-	0.1444
710.00	-	-	1.50	-	1.34	686.65	-	-	0.1590	-	0.1421

Table D-6: Experimental and Fitted data of Column8 (Cd transport with high pore water velocity, IS 1 mM)

Time (hour)	Observed (ppm)	F-EQ (ppm)	F-TSM (ppm)	L-EQ (ppm)	L-TSM (ppm)	Dimensionless form					
						PV	C/C_0 Observed	C/C_0 F-EQ	C/C_0 F-TSM	C/C_0 L-EQ	C/C_0 L-TSM
0.50	0.00	0.00	0.00	0.00	0.00	0.47	0.0000	0.0000	0.0000	0.0000	0.0000
16.19	0.00	0.00	0.00	0.00	0.00	15.25	0.0000	0.0000	0.0000	0.0000	0.0000
33.76	0.15	0.00	0.00	0.00	0.00	31.81	0.0159	0.0000	0.0000	0.0000	0.0000
60.80	0.25	0.00	0.00	0.00	0.00	57.28	0.0264	0.0000	0.0000	0.0000	0.0000
81.40	0.23	0.00	0.00	0.00	0.00	76.68	0.0245	0.0001	0.0000	0.0003	0.0001
102.04	0.14	0.01	0.00	0.02	0.01	96.13	0.0145	0.0007	0.0000	0.0018	0.0008
117.94	0.21	0.02	0.00	0.04	0.03	111.11	0.0219	0.0021	0.0000	0.0038	0.0028
133.81	0.24	0.04	0.00	0.07	0.06	126.06	0.0255	0.0047	0.0000	0.0071	0.0068
149.92	0.27	0.08	0.00	0.11	0.12	141.23	0.0281	0.0089	0.0000	0.0119	0.0131
165.46	0.18	0.14	0.00	0.17	0.20	155.87	0.0185	0.0147	0.0000	0.0182	0.0211
180.52	0.30	0.21	0.00	0.25	0.29	170.06	0.0317	0.0220	0.0000	0.0259	0.0304
195.58	0.26	0.30	0.00	0.33	0.39	184.25	0.0277	0.0313	0.0000	0.0352	0.0411
200.60	0.27	0.33	0.00	0.37	0.43	188.98	0.0280	0.0346	0.0000	0.0385	0.0449
215.67	0.37	0.44	0.03	0.48	0.54	203.17	0.0388	0.0463	0.0026	0.0501	0.0571
230.73	0.40	0.57	0.23	0.60	0.67	217.36	0.0417	0.0599	0.0238	0.0634	0.0706
240.77	0.62	0.66	0.43	0.69	0.76	226.82	0.0655	0.0697	0.0455	0.0729	0.0804
250.81	0.69	0.76	0.66	0.79	0.86	236.28	0.0727	0.0803	0.0697	0.0832	0.0907
265.88	0.76	0.93	1.02	0.95	1.02	250.47	0.0803	0.0977	0.1069	0.1000	0.1073
270.90	0.86	0.99	1.13	1.01	1.08	255.20	0.0902	0.1036	0.1191	0.1057	0.1130
281.22	0.98	1.11	1.36	1.12	1.19	264.93	0.1030	0.1165	0.1429	0.1181	0.1254

Time (hour)	Observed (ppm)	F-EQ (ppm)	F-TSM (ppm)	L-EQ (ppm)	L-TSM (ppm)	Dimensionless form					
						PV	C/C_0 Observed	C/C_0 F-EQ	C/C_0 F-TSM	C/C_0 L-EQ	C/C_0 L-TSM
291.82	1.07	1.24	1.58	1.25	1.32	274.91	0.1125	0.1303	0.1659	0.1315	0.1386
302.75	1.33	1.38	1.78	1.39	1.45	285.21	0.1399	0.1451	0.1874	0.1459	0.1528
313.69	1.56	1.53	1.97	1.53	1.59	295.51	0.1639	0.1604	0.2071	0.1607	0.1674
319.16	1.67	1.60	2.06	1.60	1.66	300.66	0.1753	0.1682	0.2162	0.1683	0.1749
329.66	1.91	1.75	2.21	1.74	1.80	310.56	0.2011	0.1835	0.2326	0.1832	0.1895
340.26	2.06	1.89	2.35	1.89	1.94	320.55	0.2162	0.1992	0.2475	0.1986	0.2044
365.31	2.34	2.26	2.63	2.25	2.29	344.15	0.2464	0.2374	0.2770	0.2361	0.2405
370.26	2.52	2.33	2.68	2.32	2.36	348.81	0.2649	0.2450	0.2821	0.2436	0.2477
380.31	2.76	2.48	2.77	2.46	2.50	358.27	0.2905	0.2606	0.2915	0.2590	0.2624
400.39	2.97	2.77	2.93	2.76	2.77	377.19	0.3128	0.2918	0.3079	0.2900	0.2915
420.23	3.08	3.07	3.06	3.05	3.04	395.88	0.3243	0.3224	0.3216	0.3207	0.3201
444.18	3.34	3.41	3.19	3.40	3.37	418.45	0.3517	0.3589	0.3353	0.3574	0.3540
458.46	3.53	3.62	3.26	3.61	3.55	431.90	0.3717	0.3804	0.3424	0.3792	0.3738
468.50	3.77	3.76	3.30	3.75	3.68	441.36	0.3968	0.3954	0.3471	0.3943	0.3875
483.57	3.81	3.97	3.36	3.96	3.88	455.55	0.4010	0.4175	0.3534	0.4167	0.4077
493.61	3.91	4.11	3.40	4.10	4.00	465.01	0.4111	0.4320	0.3574	0.4315	0.4209
503.65	4.06	4.25	3.43	4.24	4.13	474.47	0.4270	0.4464	0.3612	0.4462	0.4339
508.67	4.14	4.31	3.45	4.31	4.19	479.20	0.4351	0.4535	0.3630	0.4534	0.4404
518.71	4.49	4.45	3.49	4.45	4.31	488.66	0.4725	0.4675	0.3665	0.4678	0.4531
523.74	4.67	4.51	3.50	4.52	4.37	493.39	0.4907	0.4745	0.3682	0.4749	0.4594
533.61	4.76	4.64	3.53	4.65	4.48	502.69	0.5006	0.4879	0.3711	0.4886	0.4711
538.46	3.89	4.70	3.54	4.71	4.37	507.27	0.4089	0.4945	0.3724	0.4954	0.4596

Time (hour)	Observed (ppm)	F-EQ (ppm)	F-TSM (ppm)	L-EQ (ppm)	L-TSM (ppm)	Dimensionless form					
						PV	C/C_0 Observed	C/C_0 F-EQ	C/C_0 F-TSM	C/C_0 L-EQ	C/C_0 L-TSM
548.17	3.45	4.82	3.55	4.84	3.62	516.41	0.3628	0.5073	0.3736	0.5086	0.3806
567.84	2.74	5.06	3.50	5.08	2.50	534.94	0.2878	0.5323	0.3680	0.5342	0.2628
587.92	2.24	5.29	3.32	5.31	1.99	553.86	0.2358	0.5563	0.3494	0.5588	0.2087
607.87	1.98	5.50	3.05	5.53	1.73	572.65	0.2080	0.5781	0.3210	0.5811	0.1819
626.83	1.81	5.67	2.75	5.70	1.60	590.52	0.1907	0.5966	0.2897	0.5998	0.1677
645.80	1.61	5.82	2.46	5.85	1.52	608.39	0.1697	0.6122	0.2588	0.6155	0.1593
664.77	1.50	5.94	2.19	5.97	1.47	626.26	0.1582	0.6246	0.2300	0.6277	0.1541
687.95	1.37	6.03	1.89	6.06	1.43	648.09	0.1445	0.6346	0.1984	0.6372	0.1502
710.82	1.21	6.08	1.63	6.10	1.40	669.64	0.1269	0.6393	0.1715	0.6412	0.1477
733.23	1.13	6.08	1.42	6.09	1.39	690.74	0.1188	0.6392	0.1493	0.6404	0.1460
746.61	1.09	6.06	1.31	6.07	1.38	703.36	0.1143	0.6376	0.1378	0.6382	0.1452
759.78	1.05	6.03	1.21	6.04	1.37	715.76	0.1108	0.6344	0.1276	0.6346	0.1445
775.43	1.00	5.98	1.11	5.98	1.37	730.50	0.1053	0.6288	0.1169	0.6284	0.1437

Appendix E

Fitted Parameter for Cd Transport

Table E-1: Fitted parameter for Freundlich Equilibrium model

Column	IS (mM)	K_F (l/g)	1/n (-)	R^2	RMSE
Cd Low K_s (2.0 cm/hour)					
3	100	0.081	0.8985	0.9456	0.0725
4	10	0.237	0.7765	0.5979	0.1098
5	1	0.930	0.9386	0.8918	0.0970
Cd High K_s (9.0 cm/hour)					
6	100	0.041	1.0000	0.9704	0.0675
7	10	0.262	1.0000	0.7267	0.1537
8	1	0.498	0.9591	0.3451	0.1936

Table E-2: Fitted parameter for Freundlch TSM model

Column	IS (mM)	K_F (l/g)	1/n (-)	*f* (-)	α ($hour^{-1}$)	R^2	RMSE
Cd Low K_s (2.0 cm/hour)							
3	100	0.019	0.6883	0.1880	8.71E-03	0.9917	0.0146
4	10	0.508	0.7613	0.4767	4.86E-09	0.6050	0.1089
5	1	2.172	0.5861	0.1524	1.06E-03	0.9728	0.0223
Cd High K_s (9.0 cm/hour)							
6	100	0.079	0.9984	0.2895	1.11E-02	0.9784	0.0216
7	10	0.804	0.6164	0.0950	6.15E-03	0.9655	0.0257
8	1	4.240	0.5236	0.1301	5.10E-04	0.8806	0.0470

Table E-3: Fitted parameter for Langmuir Equilibrium model

Column	IS (mM)	K_L (l/g)	Nu (l/mg)	R^2	RMSE
Cd Low K_s (2.0 cm/hour)					
3	100	0.066	3.20E-02	0.9452	0.0734
4	10	0.222	6.27E-02	0.6124	0.1093
5	1	0.973	3.63E-02	0.8781	0.1054
Cd High K_s (9.0 cm/hour)					
6	100	0.043	2.16E-05	0.9652	0.0673
7	10	0.254	3.97E-05	0.7425	0.1730
8	1	0.490	1.01E-02	0.3397	0.1944

VITA

Miss Athiya Waleeittikul was born in 14, June, 1992, in Bangkok. Homeland is Rangsit, Pathumthani. Studied junior high school and high school at Suankularb Wittayalai Rangsit school. And graduated with Bachelor Degree of Science from Department of Geology, Chulalongkorn University in April, 2014. With interesting in environmental science and management, she decided to continue to study postgraduate program in hazardous substances and environmental management.